Optimisation of mechanical activation of aluminium for an economical on-demand hydrogen production

Ertan Maqbool Siddiqui

A thesis submitted in partial fulfilment of requirement at
London South Bank University for the degree of
Doctor of Philosophy
in
Chemical, Process and Energy Engineering
This research programme was carried out with the financial collaboration of

Advance Material Group, School of Engineering,
London South Bank University

September 2017

Declaration

I declare that the thesis has been composed by myself with fabulous support of my supervisor. The thesis is submitted for examination in consideration of the award of a higher degree of Doctor of Philosophy in Chemical, Process and Energy Engineering. I would like to emphasise that it is my personal effort and that the work has not be submitted for any other degree or professional qualification. Furthermore, I took reasonable care to ensure that the work is original and to the best of my knowledge, does not breach copyright law and has not been taken from other sources except where such work has been cited and acknowledged within the text.

Dedication

I would like to dedicate

To my whole family especially, my parents Engr Dr Maqbool Siddiqui F.IChemE, Robina (Moni) Siddiqui, my siblings Sahib Nisa and Dr Khalid Siddiqui. To the director of studies Assoc. Prof. Anna-Karin Axelsson and my second supervisor Prof. John Zhou and my Sponsor iHOD USA CEO Mr Mark Collins ESQ and Chase Collins. For Trusting me from the start and keeping me smiling and motivated until the end. Lastly, this dedication would not be complete if I do not mention God Almighty. I am grateful to him for providing a dyslexic person ability and chance to reach this milestone.

Acknowledgements

I would like to express my special thanks and gratitude to director of studies Assoc. Prof. Anna-Karin Axelsson, for her dedication and encouragement. To my supervisors Professor John Zhou (*University of Technology, Sydney*) and Dr Donglin Zhao. I am thankful to Dr Claire Benson, Dr James Ingram, Dr Paul Battersby, Dr Nick Power (*Open University*) and for their assistance and guidance. Dr Sandra Dudley McEvoy, Prof. Hari Reehal, Prof. David Mba, Dr John Orrin, Prof. Charles Egbu for moral support. Mrs Louise Thompson (Campbell), Miss Titi Obdende for making sure I am financially stable during the time at School. John Speed and Mike Goring for making sure for my health and safety at the laboratory. Steve Johns, William Cheung, Charles Coster and Ken Unadat for their help in setting up equipment and making the rig. Prof. Matjaž Valant **(***University of Nova Gorica)* for analysis and all the analytical analysis. Furthermore, Dr Jeremey Balls for SEM Pictures, Dr Lorna Anguilano (*Brunel University*) for XRD analysis. Tara Singh Ghatauray, Hassan Zabihi, Perekaboere Ivy Sagbana, Dr Muhammad Thayab, Dr Rim Saada, Dr Isaac Adegboyega, Dr Mohammed Misbahu, Ridouan Chaouki, Antigoni Paspali, Victor Nnamdi Onyenkeadi, Aseel Abdul-Amir Al-Qutbi, Elaheh Hojaji Najafabadi, Zahra Echresh Zadeh, Omar Abo El-Azayem, Roxana O'Hara, Priyadarshi Sahu, Muhammed fayaz and Farzin Vajihi my PhD peers from whom I have learnt a lot from, out of some who have already graduated. My Brother, Dr Khalid Siddiqui (*Max Plank Institute*) for his proofreading. My friends, Themistokles Zafiropoulos, Shah Shams Hadi Shah, Syed Taseen Syed, Omer Shah, Valter Da Silva, M. Saad Zulfiqar, Shehroz Hiraj, Kanan Huseynov, Teny Pattery and Jonathan Charles for their support. I would also like to mention Dr Samuel Larkai one of the best lecturers I have the privilege to be a student of during my BEng (Hons) Chemical and Process Engineering. Most of all to my sponsor iHOD USA, for providing me with the golden opportunity to do this brilliant PhD project. Their financial support assisted me tremendously in finishing this project under four years' time. I have developed and enhanced my engineering understanding and during the process learnt new techniques. PhD has broadened my intellectual level, for that, I am thankful to iHOD USA and London South Bank University.

Contribution to knowledge

I would like to acknowledge the contribution of Professor Dr Matjaz Valant (Dean of School for Environmental Sciences and Head of Materials Research Laboratory at University of Nova Gorica Slovenia) for his support and especially for his services in providing us with all the metallic analysis including XRD, SEM and EDX during the research.

Abstract

Hydrogen gas, H_2 is generated when aluminium metal is reacted with water. Due to the protective oxide layer, the reaction does not take place at ambient conditions. Different activation schemes are possible however most are either expensive or not very practical for H_2 generation. This work attempted to address this issue of activation of aluminium particles by means of a reactive ball milling technique. A number of studies based on the activation (preparing it to react with water without the aid of any external heat or catalyst) of aluminium Al, by this method, was reported previously where the energy investment was substantial. This gap in knowledge motivated us to perform milling with a different approach. Milling protocols were identified and devised and presented a milling programme which aided in reducing the energy investment considerably. The motivation behind this work is to use the Al powder prepared by milling in a hydrogen generator connected to fuel cells for in situ generation. Due to the sensitive nature of fuel cell, it was necessary to produce hydrogen gas at a steady rate. It was found that the powder made up of a mixture of metal oxides and salt prepared in-house, provided an excellent base to achieve this. It was also seen that milling of the Al particles to 40 µm proved to perform the best for hydrogen production with yield reaching 85 % in 3 hrs reaction time using only 0.3 g of activated aluminium at ambient conditions. Reaction time can be improved by increasing milling time it would not be economically attractive. After reactive milling and reactions were examined/ inspected using SEM, EDX and XRD techniques for in-depth analysis of Al particle crystalline structure, morphology and size. Milling modifies the surface of the aluminium particles promoting hydrogen gas production. It was also noted that this reaction does not require any heat and that it can generate hydrogen gas at the ambient conditions. It was noticed that when the initial temperature of the solution is increased the reaction rate first improves up to 32 ^oC than it declines at 45 ^oC and beyond when larger Al particles are used. This work revealed that reaction requires agitation throughout the process in order to maintain a high yield of hydrogen. While this presented work used deionised water, it should be mentioned that other solvents (aqueous solutions) may be used for hydrogen production as shown in the research. However, the highest amount of yield was produced when deionised water and urea solution was used at 25 ^oC.

"If we had a hydrogen economy worldwide, every nation on earth could create its own energy source to support its economy and the threat of war over diminishing resources would just evaporate" - Dennis Weaver

Contents

List of abbreviations and symbols

%	Percentage
µm	Micrometre ($1x10^{-6}$)
µm	Microliter
λ	Wavelength
ΔH_r	Standard enthalpy of reaction
θ	Braggs angle
α- β- γ-$Al(OH)_3$	Alpha, Beta and Gamma aluminium hydroxides
Bpd	Barrel per day
bar	1 bar = 14.5038 PSI
BOC	BOC Group plc
^oC	Celsius
C_p	Heat capacity (°C· kg)
Cl^-	Chlorine ions
CSTR	Continuous flow stirred-tank reactor
EDX	Energy-Dispersive X-ray spectroscopy
FWHM	The full width at half maximum
g	Gram
g/ml	Gram per millilitre
GC	Gas chromatography
GFM	The gas mass flow meter
GJ	Gigajoule
GW	GigaWatts
H_2	Hydrogen
Hrs	Hours
ICP-MS	Inductively coupled plasma mass spectrometry
kg	Kilograms
K	Kelvin
kJ/mol	Kilojoules per mole
kWh	Kilowatts hours
Kwh/Nm^{-3}	Kilowatts hours /Normal Metres Cubed
kW	Kilowatts
kV	Kilovolts

L or l	Litre
LHNE	London Hydrogen Network Expansion
M	Molar
min	Minutes
MJ/kg	Megajoules per kilogram
Ml	Millilitre
Ml/s	Millilitre per second
Ml/g Al	Millilitre per gram aluminium
Mm	Millimetre
MO	Metal oxide
Mol/L	Molar concentration
M_w	Molecular weight
N/A	Not applicable
n	Number of moles / positive integer
OH^-	Hydroxide ion
OH^*	Ohio State in the United States of America
PC	Personal computer
PEM	Polymer electrolyte membrane electrolysis
PO	Potash
rpm	Revolutions per minute
sec	Second
R	Gas Constant
R_T	Retention time
SEM	Scanning electron microscope
Tonnes	1 tonnes = 1000 kg
TCD	Thermal conductivity detector
W	Watt
wt %	Weight percentage
XRD	X-ray Diffraction

List of tables

List of figures

Prior publication

J. Zhou, **E. Siddiqui**, H. Ngoa, W, Guo, Estimation of uncertainty in the sampling and analysis of polychlorinated biphenyls and polycyclic aromatic hydrocarbons from contaminated soil in Brighton, UK, J of Science of the Total Environment 497–498 (2014) 163–171.

Chapter 1 Introduction

The goal of this research work was to develop a cost-effective method for activating aluminium particles for an on-demand hydrogen production. This chapter presents the main outline for this thesis and provides justification for the importance of hydrogen as an energy carrier. It provides a brief overview of the current hydrogen technologies, energy economics and efficiencies. It also puts forward the rationale for developing on-demand energy sources aimed at off-the-grid usage. Finally, the aims and objectives of this research are presented, alongside the structure of the thesis.

1.1 Background

The current technologies used for generation of hydrogen consuming traditional fossil fuel routes produce adequate amount and might be satisfactory for the current purposes. They are, nevertheless, not clean for the environment as they have a large carbon footprint.

Increasing awareness of the climate change and growing energy demand has caused both political and economic debates on reviewing current technologies. This has led to a significant amount of research and development activities into alternative energy, which includes hydrogen production. A considerable part of today's energy is generated using fossil fuels in one way or another. Renewable energy alternatives are less polluting than fossil fuel nevertheless may still contribute to the environmental impact indirectly. Many ‘clean’ renewable energy technologies use fossil-derived energy in their production. Therefore, these clean technologies contribute to greenhouse gas emissions in their production, storage and during shipment. This is one example of why there has been a significant investment in the last decades in hydrogen for fuel cells development. These fuel cells do not contribute directly to pollution and their by-products are electric power and water.

Another advantage of hydrogen as a fuel is that it has a high energy content, in the order of MJ/kg (1 MJ/kg = 1 x 10^6 J/kg) compared to other fuel sources. Table 1-1 lists different fuel types and their energy contents in MJ/kg. One can see from the

Table 1-1, that hydrogen in the liquid state provides about 120 MJ/kg compared with liquefied natural gas (LPG) with 54.3 MJ/kg thus, making it a superior fuel.

Table 1-1: Energy contents of available fuels [1].

Fuel	Energy Content (MJ/kg)
Hydrogen	120
LPG (Liquefied natural gas)	54.4
Propane	49.6
Aviation gasoline	46.8
Automatic gasoline	46.4
Automatic diesel	45.4
Ethanol	29.6
Methanol	19.7
Coke (Made from coal)	27
Wood (Dry)	16.2
Bagasse	9.6

The industrial production of hydrogen gas began in 1912, but it has never been properly utilised as a commercial product due to health and safety concerns. Hydrogen started to gain popularity in the world of science and engineering, especially in the developing countries [2]. More recently, both policymakers and researchers are working hand-in-hand to create a unique energy system based on hydrogen. Currently, the energy market has started to show a profound interest in the production, transport and storage issues around the hydrogen economy [3]. The development of hydrogen for fuel is part of a complex system beyond the generation. The complexity includes transporting hydrogen from the production site to the delivery point. It is also challenging to store hydrogen because it requires an extensive pressure of 300 bar to be liquefied for shipment. All these aspects have a direct impact on hydrogen economics. As a consequence; many safety and feasibility studies around hydrogen generation have been launched all over the

world [4] along with the actual hydrogen generation technologies that do not depend on fossil fuels. Hydrogen can be used as either combustion fuel or as an energy carrier for fuel cells to produce electric power and heat [5]. Fuel cells convert the chemical energy from hydrogen into electricity through a chemical reaction together with oxygen. There are two types of the fuel cells which are widely used in various applications. They are proton exchange membrane fuel cell (PEM) and solid oxide fuel cells (SOFC) where the anodic and cathodic functionalities are quite different, refer to Figure 1-1. In a PEM, the anodic (for the hydrogen reaction) and cathodic (for the oxygen reaction) can be seen below:

$$\text{Anode reaction: } 2H_2 \rightarrow 4H^+ + 4e^- \quad (1.1)$$

$$\text{Cathode reaction: } O_2 + 4H + 4e^- \rightarrow 2H_2O \quad (1.2)$$

$$\text{Overall cell reaction: } 2H_2 + O_2 \rightarrow 2H_2O \quad (1.3)$$

In these type of fuel cells, the hydrogen produces H^+ ions that are transported through the membrane giving its name; a proton exchange fuel cell (PEM). PEM fuel cells can produce powers of between 0-500 kW with an estimate of 50 % efficiency using hydrogen fuel. The fuel cells where this research targets the on-demand hydrogen production up to 100 W [6]. Solid oxide fuel cells (SOFS) have a solid electrolyte, a nonporous metal oxide consisting of typically ZrO_2 treated with Y_2O_3 and O^{2-} ions are transported from the cathode to the anode (compare with transported H^+ in PEM), see Figure 1-1, temperatures of operation are typically higher at 800-1000 °C.

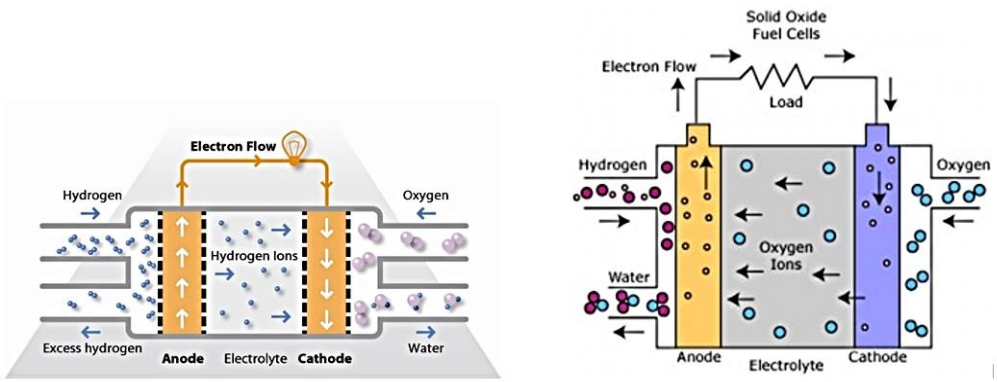

Figure 1-1: Principle of Proton membrane fuel cell (PEM) and solid oxide fuel cell (SOFC) using hydrogen gas as fuel when producing electric current [7]**.**

For SOFC, the anodic (where the hydrogen fuel is reacted) and cathodic reaction (where oxygen is reacted) can be described by:

Anode reaction: $2H_2 + 2O^- \rightarrow 2H_2O + 4e^-$ (1.4)

Cathode reaction: $O_2 + 4e^- \rightarrow 2O_2^-$ (1.5)

Overall cell reaction: $2H_2 + O_2 \rightarrow 2H_2O$ (1.6)

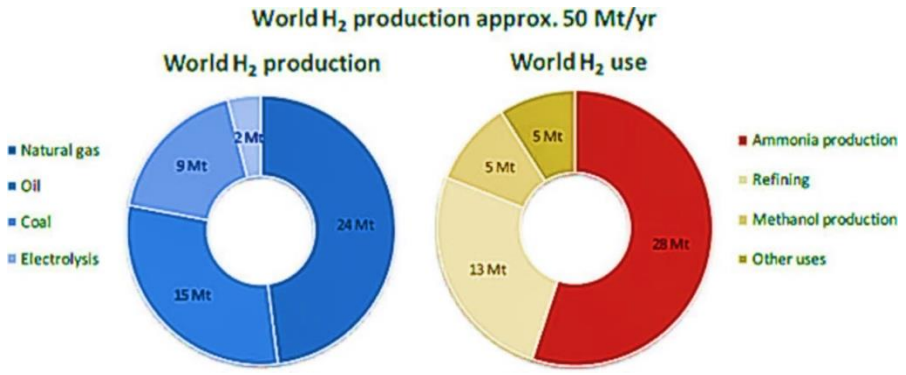

Figure 1-2: Estimated world hydrogen production and use 2008 where it is evident how electrolysis and steam reforming natural gases were the dominant technologies and hydrogen was dominantly produced for ammonia production [8]**.**

The fuel cell market is growing rapidly and it is estimated that the stationary fuel cell market will reach 50 GW (1 GW = 1 x 10^9 W) by 2020 [9] making this hydrogen generation research very timely. For this research, the hydrogen generation is aimed to be used mainly in an on-demand PEM configuration. Hydrogen for fuel cells is currently produced via three basic routes; biomass, fossil fuel (natural gas) and water as shown in see Figure 1-3.

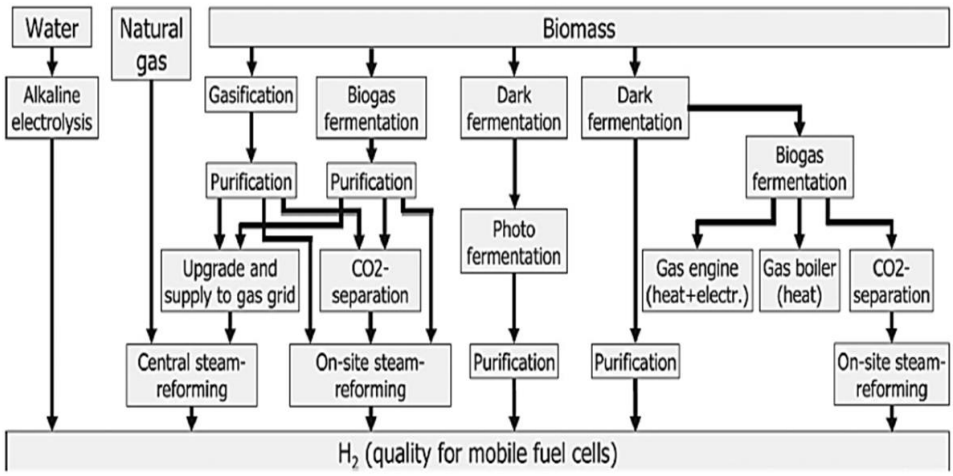

Figure 1-3: Different pathways for hydrogen gas production aimed at fuel cells [10]**.**

The demand for hydrogen is rapidly increasing and is forecasted to do so, Figure 1-2 and 1-4, which points to its wide acceptance as a safe alternative fuel. Currently, hydrogen production is reaching 50 million tonnes per year [11]. One of the leading continents for hydrogen production is North America as shown in Figure 1-4 [12] followed by Europe and Asia, where China is currently investing billions of dollars in hydrogen securing hydrogen as a future fuel. Despite an increased interest in hydrogen generation for the large scale aimed at commercial and power generation. The small-scale production is not widely available for individual consumers, which would help it to be adapted to the modern lifestyle, i.e. in cars.

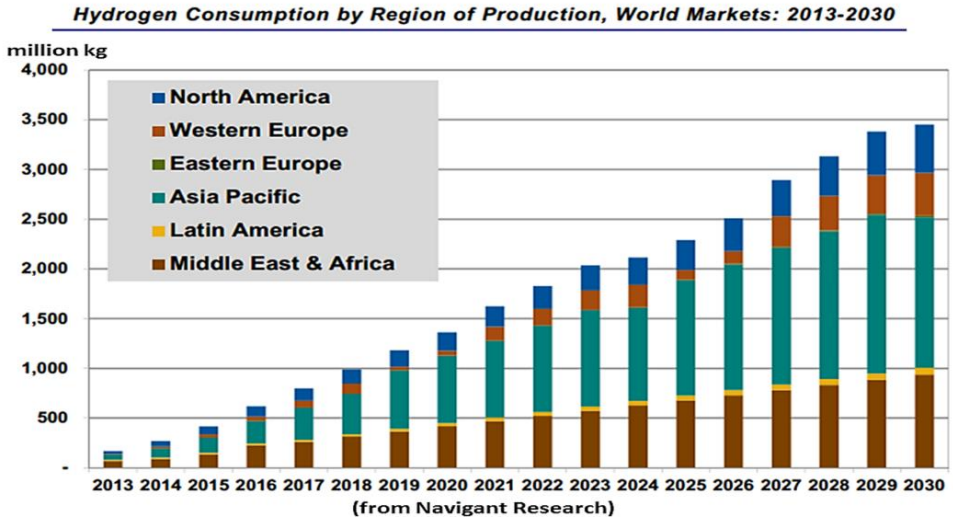

Figure 1-4: Predicted hydrogen demand future forecast [12]**.**

While hydrogen as a safe and clean fuel is gaining recognition, there is still cause for concern especially when one closely inspects the various current technologies that provide H_2 to customers. A few of them are discussed below:

Steam reforming is the group term for methods that are responsible for 95 % of the global hydrogen production today as shown in Figure 1-2 [11]. In this process, steam (gaseous water) reacts with methane at very high temperatures (700-1100 °C) in the presence of a metal-based catalyst (often nickel) as shown by the equation.

$$CH_4 + H_2O\ (\text{steam}) \rightleftharpoons CO + 3H_2\ (\text{gas}) \qquad (1.7)$$

As the reaction equation 1.7 shows, hydrogen gas is produced together with carbon monoxide. A few things should be mentioned about this process. Firstly, carbon monoxide is a toxic gas which not only is dangerous but also contributes to

atmospheric pollution. It is known to affect the climate indirectly by reacting with hydroxyl radicals (OH) that otherwise react with the greenhouse gases. Thus, by reducing the OH radical abundance in the atmosphere Carbon monoxide, CO production causes environmental issues. Secondly, to produce steam to react with methane (itself a greenhouse gas), large boilers (steam reformers) are needed which require fuel to operate.

Furthermore, these steam reformers are often based in close proximity of a refinery for access to steam and methane. In other words, they are not found near where the hydrogen fuel is to be consumed and as such hydrogen has to be transported in a suitable form to locations where it will eventually get used. To make it transportable, hydrogen gas is compressed and stored in high-pressure tanks, which not only cost additional energy and money but also the storage is hazardous. By just reflecting on the hydrogen generation itself, the hydrogen produced by steam reformation costs approximately three times more than the natural gas if comparing it by a unit of energy produced. Therefore, hydrogen economics needs to be evaluated as cost per 1 litre of H_2 in Section C and justified. Another hydrogen generation methodology worth mentioning is the electrolysis of water, where electric current is passed through water which causes it to decompose. As a result, O_2 is produced at the positive electrode (anode) and hydrogen is given off at the cathode (negative electrode) see Figure 1- 5.

In Figure 1-5, it can be seen how water reacts at the anode to form O_2 (gas) and, H^+ (protons). The released electrons flow through an external circuit and the hydrogen ions selectively move across the membrane to the cathode. At the cathode, the hydrogen ions combine with electrons from the external circuit to form hydrogen gas.

The anodic and cathodic reactions are:

$$\text{Anode reaction: } 2H_2O \rightarrow O_2 + 4H^+ + 4e^- \quad (1.8)$$

$$\text{Cathode reaction: } 4H^+ + 4e^- \rightarrow 2H_2 \quad (1.9)$$

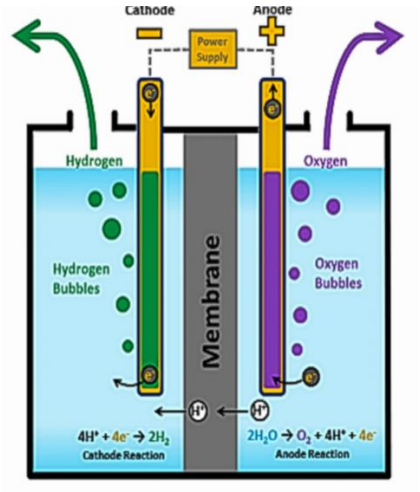

Figure 1-5: Working principle of Polymer Electrolyte Membrane Electrolysers for producing hydrogen gas [13].

Water electrolysis, despite being highly energy demanding, today offers significant benefits as it offers easy integration with renewable energy generation such as weather dependent solar and the wind. These benefits will increase as the proportion of renewable energies in the "mixed energy sources strategy" for the national grid is growing and would lead to a possible reduction in the cost of hydrogen produced by electrolysis by 20 % over the next decade, as shown in Figure 1-6 [14].

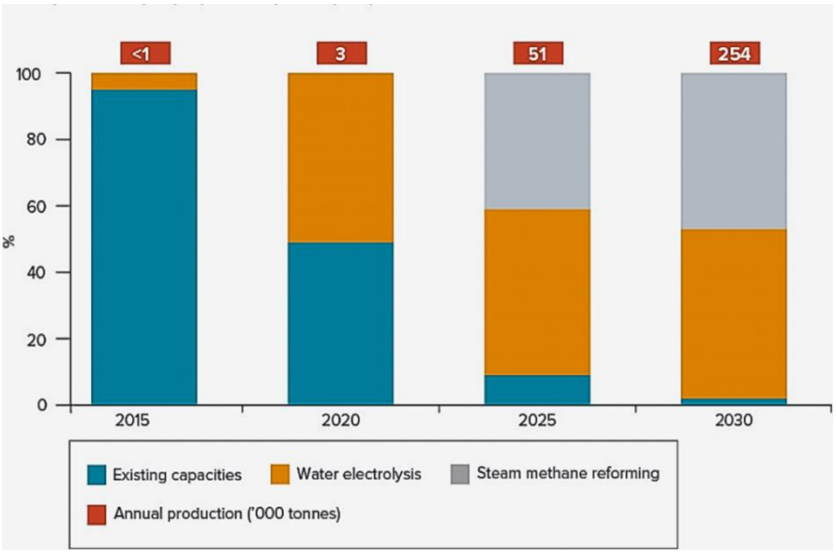

Figure 1-6: Development of hydrogen production capacities over time roadmap for the UK, comparing mainly steam reforming versus electrolysis [20].

Referring to hydrogen production from Biomass, even this process requires an external energy input (often fossil) for initiating the process and uses environmental unfriendly carbon dioxide for suitable process conditions. Other green biomass

routes are dark fermentation, photo-fermentation and biophotolysis. Dark fermentation is a fermentative conversion of organic substrates to produce *biohydrogen* and often employed by diverse groups of bacteria and a series of biochemical reactions (anaerobic conversion). Dark-fermentation differs from photo-fermentation, the latter being done in the presence of light and the former not. Bio-photolysis use the microbial production of hydrogen, often by algae. Although all these technologies mentioned above are environmentally friendly they do not deliver a good yield of hydrogen gas [15].

To make hydrogen generation commercially attractive the production process should be inexpensive; utilise renewable sources or renewable materials and be effective whilst at the same time to produce a pure hydrogen gas efficiently [17]. More recent publications such as [16-19], emphasise using water as the source of hydrogen due to its wide availability. Also, water provides a broad range of optional routes from which hydrogen could be liberated and the processes can be made more environmentally friendly compared to the classic hydrogen generation routes. It is important that the processes should aim only to use renewable materials or such resources that do not produce greenhouse gases [20]. The majority of techniques discussed above produce hydrogen off-site which has to be transported where needed. Two of the major obstacles seen in the overall hydrogen economy is shipment and storage. It is possible to store the hydrogen that is produced in three forms, i.e. gas, liquid and solid state. It can be stored as chemical hydrides such as MgH_2, $NaAlH_4$, $LiAlH_4$, LiH, $LaNi_5H_6$ and TiF-H_2 some of which are liquids at ambient temperature and pressure and others are solid, but none of these is ideal because of their environmentally hazardous properties. For example, in solid form, it is not very economical to store as 84 kg of metal hydride which can only carry 1 kg of hydrogen gas [21].

The major drawback regarding storage in the gas phase is the very high pressures required which further requires additional energy for compressors and the whole procedure come with a high-risk factor. Further to provide an idea compressing hydrogen is challenging, 1 kg of H_2 gas in terms of volume is equivalent to 11200 ~11000 litres of H_2 gas. This amount of gas would occupy a significant amount of space if stored at ambient pressure. Whereas for compressed hydrogen is stored in

tanks at 350-700 bar and at -285 ˚C, this process is energy intensive and challenging to maintain [10,22]. Once it is stored further disadvantage is associated with its shipment. Another concern is the fire hazard, hydrogen should be minimum 99 % pure when stored. If the purity decreases to 74 % or below, it can easily catch fire or explode in the presence of ignition source [23].

Due to the importance of the overall hydrogen economy and avoidance related to storage and transport obstacles, this research work focuses on on-demand hydrogen generation via a cost-effective and convenient method. A simple but effective route involving metal (Aluminium) and water reaction would be adopted and applied for hydrogen generation aimed at portable fuel cells. The process will be developed as environmentally and economically friendly as possible with widely available aluminium-based particles that are activated mechanically and using naturally occurring water as the feedstock. The water source investigation will begin with pure deionised water and later proceed in the direction of various tap water and typical industrial wastewaters. Process methods will be explored in order to seek ways to improve the particle synthesis and in particular how to treat the unavoidable oxidation layer on the aluminium surface. The thesis will begin the aluminium particle processing and optimisation. Currently, most commonly aluminium reacts easily and a strong alkaline at pH 10+ such as KOH or NaOH forming hydrogen despite the protective aluminium oxide (Al_2O_3) layer. For an on-demand hydrogen production aimed at portable fuel cells, the use of such strong alkaline will cause risk of corrosion of piping and damage the seals. As a gentler method of aluminium-water reaction, it has been found that using so-called “milling additives” that can cover the metal aluminium particles surface and rupture the Al_2O_3 surface layer, can promote the reaction to proceed at ambient conditions without strong acids or alkaline. Hydrogen can be produced from various processes as discussed above. There are a few technologies which have matured and have high efficiencies and they are some which are either in their development stages or early research and development work is ongoing. These can be seen in Table 1-2, therefore, a need for a more sustainable and environmentally friendly process is required.

Table 1-2: Listing of the cost and performance characteristics of various hydrogen production processes [24]**.**

Energy Required (kWh/Nm^3)					
Processes	**Ideal**	**Practical**	**Status of Technology**	**Efficiency [%]**	**Cost Relative to SMR**
Steam methane reforming (SMR)	0.78	2-2.5	Mature	70-80	1
Methane/NG pyrolysis	-	-	R&D	75-54	0.9
H_2S methane reforming	1.5	-	R&D	50	<1
Landfill gas dry reformation	-	-	R&D	47-58	~1
Partial oxidation of heavy oil	0.94	4.9	Mature	70	1.8
Naphtha reforming	-	-	Mature	-	-
Steam reforming of waste oil	-	-	R&D	75	<1
Coal gasification (GE Energy)	1.01	8.6	Mature	60	1.4-2.6
Partial oxidation of coal	-	-	Mature	55	-
Steam-iron process	-	-	R&D	46	1.9
Chlor-alkali electrolysis	-	-	Mature	-	by-product
Grid electrolysis of water	3.54	4.9	R&D	27	3-10
Solar and PV-electrolysis of water	-	-	R&D to mature	10	>3
High-temp. Electrolysis of water	-	-	R&D	48	2.2
Thermochemical water splitting	-	-	Early R&D	35-45	6
Biomass gasification	-	-	R&D	45-50	2.0-2.4
Photo-biological	-	-	Early R&D	<1	-
Photolysis of water	-	-	Early R&D	<10	-
Photoelectrochemical cell decomp. Of water	-	-	Early R&D	-	-
Photocatalytic decomp. of water	-	-	Early R&D	-	-

A method for this particle additive integration is through the use of high energetic milling technologies, such as planetary mills. The choice of active additives and the milling protocols planned will also be defended, including milling time and mill rotational speed, which have a direct impact on the cost used in the process in a hydrogen economic evaluation. In-depth particles material analysis will be employed such as particle size evaluation (morphology), scanning electron microscope (SEM), elemental analysis (EDS) and X-ray diffraction (XRD). Moreover, the hydrogen reaction mechanism will be considered. Initially, this will be done using deionised water and later commonly available surplus water such as domestic tap water and typical traces in wastewater such as urea, sucrose, anti-freeze and ethanol mixed with deionised water will be analysed. All throughout the project, hydrogen generation cost (energy use and cost of materials) will be evaluated.

1.2 Research aim and objectives

The aims of this research are to investigate the generation of on-demand hydrogen for portable fuel cells focusing on aluminium particle activation for the water reaction while developing the technology both in an environmentally friendly and economically feasible way. The research is using the working principle of an Energy- pod by iHOD USA [6] as a guide to the research development. The research is, therefore, aimed to produce hydrogen for such fuel cells to provide power up to 90 W in a cheapest, purest and simplest way.

iHOD USA's energypod (or powerpods) uses a low-temperature, low-pressure chemical reaction to produce hydrogen without any harmful greenhouse gas emissions and this will be the main criteria for this research.

Research objectives are broken down as follows:

1 To produce hydrogen gas using economical and readily available recycled aluminium.
2 To establish an activated particle process that is energy efficient, economical and environmentally friendly.

3 To establish a safe hydrogen gas generation by not employing hazardous chemicals such as alkaline solutions or elevated temperatures and pressure.
4 To evaluate the hydrogen reaction by using different types of water and further waters available for customers of portable fuel cells such as tap waters and typical wastewater and compare with less available but purer deionised water.

1.3 Structure of report

Chapter 1: Introduction

In this chapter, a brief outline was provided explaining the motivation of this study which includes why there is a need for an energy production change and relates to the growing demand. It will provide a description of existing hydrogen technologies and how hydrogen gas can be used for fuel cells. The term *Hydrogen Economics* is clarified, where it is seen that transport and storage are two important factors connected with both high cost and high risks. This is justifying the objective of finding a cheap and reliable on-demand hydrogen generation technique. Finally, this chapter provides an outline of study and stating the aims and objectives of the PhD Thesis.

Chapter 2: Literature review of hydrogen generation

This chapter provides a detailed insight into how aluminium-water reaction for hydrogen gas is generated and discussed the area that could be improved. It will explain the way of improving particle activation, reaction time and hydrogen yield by reviewing published data by researchers up to date.

Chapter 3: Methodology

This chapter provides a description of the proposed experimental setup and methodology used in this research. It will cover particle processing and analysis; reactor setup, gas analysis and different water analysis.

Chapter 4: Results and discussion

In this section, the outcomes and findings of the experiments will be discussed and concluded. Section A will cover the particle processing where the success is evaluated by hydrogen flow rate and yield. Section B will cover how the water

quality affects the reaction and finally, Section C provides a breakdown of the cost and the estimated process cost of hydrogen per kg in a hydrogen economy evaluation.

Chapter 5: Conclusions

A critical review and overall conclusion of this research are presented in this chapter, as well as future work.

1.4 Chapter 1 Conclusion

In this introduction chapter the current need for improving hydrogen generation aimed at small-scale on-demand power sources, to make it both economical attractive and simplified was presented. It introduces the reason for choosing metal-water reactions for the hydrogen reaction and reactive milling for particle processing. The content of the thesis chapters is described at the end.

Chapter 2 Literature review of hydrogen generation

The research presented in this thesis focuses on how metal particles can produce hydrogen in an aqueous environment, aimed mainly at on-demand hydrogen fuel cells. This chapter provides a review of the current status of hydrogen generation technology as found in the literature and how the technology might be improved. It will review the current state of the art in this field and discuss the novelty produced in this thesis.

The chapter also presents a review of different metals that can be used and explain why aluminium was chosen. Further, it will explain why additives are employed in the particle synthesis, review milling procedures for the particle synthesis and explore how these aluminium-based particles can be synthesised both environmentally friendly and economically viable. The chapter will go on to further review different on-demand hydrogen generator and types of aqueous solutions that can be used for the hydrogen generation reactor, i.e. effect of pH and temperature. Finally, methods for evaluating the reaction kinetics and activation energies for these types of hydrogen reactions are reviewed. Lastly, the chapter will establish the novelty of this research and which will provide a platform for the subsequent chapters.

2.1 Challenges associated with hydrogen production in large scale and storage

Hydrogen can be produced by different means, for example, from fossil fuels or from the water. As was mentioned in the previous chapter, steam reforming process is currently the most common method of produce hydrogen. While it may be the prime way of producing H_2 in today's market, in the context of on-demand production aimed at fuel cells which this research seeks to address, it is expensive and impractical.

Two major obstacles have so far limited the widespread implementation of hydrogen-based energy systems; The first being storage which is an issue due to the extremely low density of hydrogen gas which requires that it be stored in large high-

pressure tanks. Even when compressed to its liquid form, the density of liquid hydrogen is only 0.081 kg/m^3 [25]. In addition, for liquid hydrogen, there is a need for bulky insulated dewar storage tanks to prevent the rapid boil-off of the cryogenic liquid hydrogen (boiling point -252.9 °C). The second major concern is safety as H_2 when mixed with air, reacts with O_2 in a chain reaction with a high-risk of the explosion. Therefore, H_2 must be handled with great caution and care.

Due to high compression, the energy demand is consequently high, making the process expensive which has a direct effect on both the hydrogen economics and its carbon footprint. Therefore, the overall energy requirements for a hydrogen generation require most consideration. These include all possible means of transportation, which are mostly powered by fuels like petroleum and its derivatives. It is clear that the one of disinclination with hydrogen production is embedded in the cost from "cradle to grave".

In order to reduce CO_2 emissions from the cradle-to-grave, it may be possible to use hydrogen for transportation, e.g. in hybrid vehicles or fuel cell vehicles. Another alternative is to produce on-demand hydrogen for the fuel cell itself or simply focus on an on-demand hydrogen generation close to a fuel cell which it is aimed at. Hydrogen is mostly not a primary fuel but seen as an energy vector and produced from hydrogen-containing compounds. The chemical energy stored in H_2 molecule can be converted to other forms of energy such as by combustion in air or through the fuel cells. The cheapest and most abundant source of hydrogen is water, H_2O. Therefore, this study focuses on a hydrogen generation from water which reacts with carefully synthesised metal particles.

Metal-water reactions have had considerable attention over the recent years. In particular for its possibility to produce on-demand hydrogen gas for portable fuel cells up to kW range. Currently, researchers are trying to find the optimal metal particle composite or alloy for maximum hydrogen produced per gram particle. For commercial interest, the particle process, raw materials and amount of energy-rich hydrogen produced need to be balanced for a prospering hydrogen economics.

2.2 Strategies to improve the hydrogen generation

Recently, hydrogen generated from metal and metal alloys reaction with water has garnered keen interest because of its low cost and simplicity [26]. This thesis focuses on a route particularly suitable for portable fuel cell application.

For a given oxidation state, the theoretical amount of hydrogen produced from the metal-water reaction has no bearing on whether the reaction product is a metal oxide or metal hydroxide.

$$xM + yH_2O \rightarrow M_xO_y + yH_2 \text{ (metal oxide product)} \quad (2.1)$$

$$xM + 2yH_2O \rightarrow xMxOH_{2y/x} + yH_2 \text{ (metal hydroxide product)} \quad (2.2)$$

The above relations where M_xO_y is a metal oxide shows that the metal will oxidise and form either oxides or hydroxides and if using pure water only, pure energy-rich hydrogen gas is formed in an exothermic reaction. Due to the nature of the exothermic reaction, there will be an increase in temperature of the aqueous solution. This means on a larger scale that this principle can be developed as a combined heat and power energy source. The following section will review different methods that have been employed by researchers to improve further the water and metal particles reactions and how to avoid "*passive layers*" on the particles that prevent the reaction to proceed.

2.3 Hydrogen generating metals

Releasing hydrogen from water at the point of utilisation (on-demand) can be realised by reacting it with a metallic element. A number of environmentally-stable and widely-used metals such as aluminium, magnesium and silicon can be made to readily react with water releasing not only hydrogen but also a significant amount of heat, as mentioned above [29,30]. This means that many metals possess a volumetric energy density that is greater than that of gasoline if both the hydrogen and heat released from the exothermic reaction are utilised for energy conversion.

In these systems, the metal powders effectively serve as *secondary energy carriers*, storing primary electrical or heat energy in a chemical fuel that can be converted to hydrogen and heat when needed. Therefore, both the choice of metal and their

character in the reaction process are essential information for the hydrogen production. The metals most commonly investigated are aluminium, zinc, magnesium, iron and copper, all share one common characteristic: all these metals are usually found in ores and are protected by their oxide layers preventing water molecules to interact with the surface and produce hydrogen [27]. This natural occurring and stable oxide layer must be penetrated by water for a robust and optimal hydrogen generation and therefore, several particle process methods have been developed to expose the non-oxidised surface to the water. Besides hydrogen and thermal energy, the only rest products of the metal-water reactions are solid metal oxides and hydroxides. These end products are, in most cases, chemically inert and easy to collect and store. Metal oxides/hydroxides can be reprocessed back to pure metals using metal smelters [28]. Some of the reactive metals are useful but do not provide economic viability, which later will be discussed in the section of hydrogen economics. Although the majority of published work on metal-water reactions has made use of aluminium powder, other metals have been used, see example in Table 2-1.

Table 2-1: Example of metal–water reactions and enthalpy of reaction [29,30].

Hydrogen Production Reactions	
$Mg\ (s) + 2H_2O\ (l) \rightarrow Mg(OH)_2\ (s) + H_2\ (g)$	$\Delta H_r = -354.6\ kJ/mol$
$Al\ (s) + 3H_2O\ (g) \rightarrow Al(OH)_3\ (s) + 1.5H_2\ (g)$	$\Delta H_r = -280\ kJ/mol$
$Fe\ (s) + 1.5H_2O\ (l) \rightarrow 0.5Fe_2O_3\ (s) + 1.5H_2\ (g)$	$\Delta H_r = +34.1\ kJ/mol$
$Zn\ (s) + 2H_2O\ (l) \rightarrow Zn(OH)_2\ (s) + H_2\ (g)$	$\Delta H_r = -64.5\ kJ/mol$
$Cu\ (s) + H_2O\ (l) \rightarrow CuO\ (s) + H_2\ (g)$	$\Delta H_r = +130\ kJ/mol$

Most researchers have focused only on the hydrogen generation and very few on how to utilise the additional exothermic heat energy from the reactions. Owing to the aspiration to make the hydrogen generation process affordable and commercially attractive, the reaction conditions should not require stringent control measures, i.e. atmospheric pressure conditions and reasonable reaction temperatures. Several authors have investigated the optimal reaction conditions. For example, in 2013, Yavor *et al*. discovered that a combination of the elevated starting

temperature and the chosen particle size could help to increase the rate of reaction and hence the yield of hydrogen. The authors used a reaction temperature of 20–200 °C and got a yield of 97 % using 2 µm particles at 200 °C. It was suggested that with an increase of the particle size, the hydrogen yield was decreased, i.e. 93 % yield was reported for 4 µm particle [31]. The same author reported the maximum possible hydrogen yield obtained from various metal powders under same reaction conditions in 2015 [32], see Figure 2-1.

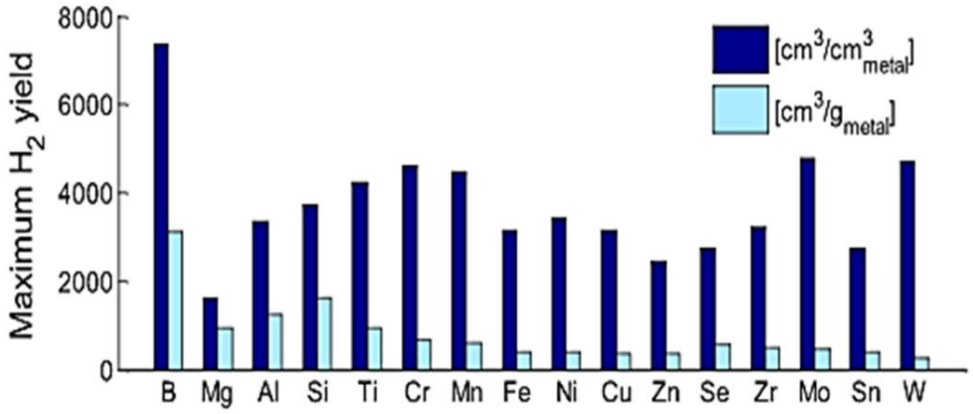

Figure 2-1: Volumetric hydrogen yield (cm^3/ cm^3 metal) and gravimetric hydrogen yield (cm^3/g metal) from a range of different metals [32].

Figure 2-1, displays a graph showing the generation of hydrogen gas per unit mass of the metal (cm^3/g) and per unit volume of the metal (cm^3/cm^3) for the investigated metals. The horizontal axis is arranged such that metal with smallest atomic mass (boron) appears on the left and the mass increases going to the right. At first glance, the chart appears to show that metals like boron (B), molybdenum (Mo), tungsten (W) and chromium (Cr) perform much better than other metals for hydrogen production, however, when taken into the account the viability, temperature of reaction (best achieved at 200 °C in the study) and the energetic heat energy released, show that both the aluminium (Al) and magnesium (Mg) powders would produce more hydrogen per unit mass than any other metal powder. Copper (Cu) also seems to be promising, but it is expensive and hence less commercially attractive than Al or Mg. Boron (B) possesses the highest possible hydrogen yield, both gravimetrically and volumetrically, but presents more difficulties for use and

is not considered a suitable candidate for commercial on-demand hydrogen production.

Table 2-2, shows a comparison of the yield of hydrogen obtained from various metals. Based on these figures, both aluminium and magnesium stood out as good candidates to be used in this research. Between the two, if one looks at the mass of metal required to produce 1 kg of H_2 gas, aluminium is the obvious choice especially, if the hydrogen generator is aimed at small portable sized fuel cells. Magnesium (Mg) has a disadvantage that it reacts relatively slow with cold water but faster with hot steam. The reaction products are magnesium hydroxide, $Mg(OH)_2$ and hydrogen gas, H_2, where 1 mol Mg will produce 1 mol H_2 gas.

Table 2-2: Chemical properties of metals which potentially can produce hydrogen [33].

Metal	Atomic mass (g/mol)	Density (g/cm^3)	Moles of hydrogen produced by 1 kg of metal (mol)	Hydrogen produced by 1 dm^3 of metal (mol)	Metal required (kg) to produce 1 kg of H_2 gas
Al	27.0	2.70	56	150	8.99
Mg	24.3	1.74	41	72	12.00
Fe	55.8	7.89	18	141	9.30
Cu	63.5	8.96	16	141	31.75
Zn	65.4	7.14	15	109	32.00

In 1996, a US Patent was filed by Vladimir *et al*. describes how a magnesium alloy was capable of generating hydrogen when it reacts with water in the presence of chlorines salt. It explained how the presence of salt and a co-metal such as zinc was used to prevent unwanted corrosion [34]. In 2007 Yu *et al*. used magnesium scraps from recycled products in solutions of salts like the common sodium chloride, NaCl, to improve the hydrogen generation. It was pointed out by the authors that only high-grade Mg is suitable for a successful hydrogen production and caution should be taken if low quality recycled magnesium were to be used [35].

Low-grade recycled Mg is cheaper but often contains a high level of impurities such as iron, nickel or copper which hamper its reactivity with water. Pure magnesium for hydrogen generation in ambient conditions was investigated and described by Grosjean *et al*. [36] using 1 M acidic solution rather than pure water. Later researchers avoided using any corrosive acids and a magnesium hydride MgH_2 was used instead for the hydrogen generation. Chemical-bonded metal hydrides are often used for hydrogen storage rather than hydrogen generation, but the principle of chemically bonded hydrogen can be utilised as a chemical catalyst to adjust hydrogen generation rate. Magnesium hydrates can be hydrolysed to produce hydrogen as:

$$MgH_2 + 2H_2O \rightarrow Mg(OH)_2 + 2H_2 \qquad \Delta H_r = -277 \text{ kJ/mol} \qquad (2.3)$$

The above reaction is a very slow due to the rapid formation of a magnesium hydroxide layer and therefore, a general consensus has been reached amongst researchers that Mg for hydrogen generation works best in acidic solutions. Another disadvantage of using magnesium described by Lui *et al*. is that when milled or as in powder form is very flammable with a low flame point [37].

Aluminium, on the other hand, is safer and also abundant. Aluminium powder from recycled aluminium scrap to even foil has shown high efficiencies [38,39], as much as 89 % according to one report [36]. Aluminium has become one of the most popular metal to use in reaction with water to generate hydrogen gas [31,32,39-42]. It has many advantages over the other metals such as stability, its abundance in the earth crust as well as in different forms such as powder and scrap metal. It has an ever growing to recycle market from cans, scraped aeroplanes and lightweight vehicle providing a plentiful supply of cheap material for particle synthesis [43].

When estimating the overall hydrogen economics for this type of technology, it must be beared in mind that producing aluminium from the earth crust is a very energy-demanding process in itself and therefore, recycled aluminium is preferable. Furthermore, aluminium is oxidised to the state 3^+ in the reaction, meaning that 1.5-mole hydrogen is formed for each mole of Al reacted. Magnesium on the other hand, which oxidises to Mg^{2+}, produces only 1-mole hydrogen when reacted with

water which means that more hydrogen will be generated per mole metal when aluminium is used [44].

In the last decade, researchers have shown how to improve the aluminium-water reaction by developing suitable metal particle processing techniques such as using high-energy ball milling with various additives or low melting metals for alloying [45]. The effective use of metal-additives and water to produce hydrogen was discussed in 2010 "Application of activated aluminium powder for generation of hydrogen from water" by Rosenband and Gany based on a similar study conducted by the same authors in 2008 [40]. Huang *et al*. in 2013 did a review titled "Feasibility of Hydrogen Generation from the Reaction between Aluminium and Water for Fuel Cell Applications" in which different *activation* of aluminium was described [46]. In the same publication, available hydrogen generators at that time were also reviewed. According to the book 'Alternative fuels-the future of hydrogen' , 2008 [47] using a starting batch of 8 kg Al can provide hydrogen with a mass flow rate of 1.6 g/s, meeting a target of 80 kW of power (or 140 kWh), which would be enough to run a car. These estimated values of energy and power are encouraging to develop this hydrogen technology further for everyday usage.

However, aluminium like many other metals have the issue of a formed oxide layer on the surface, which hinders the reaction from taking place between water and the metal [48,49]. The oxide layer is only a few nanometers thick 4 nm according to Sundaram *et al*. [50], but enough to protect the surface so that no reaction with water takes place. The outermost electron shell in pure aluminium is not stable with only 3 electrons and this causes it to react readily with oxygen as suggested by Hatch *et al.* [51] but on the other hand, when no oxygen is present this also promotes a fast reaction with water. The breakdown of the formed hydroxyl and oxide layers on the metal surface is, therefore, necessary to achieve a high hydrogen yield and a fast rate of reaction. This can be done by either activation in the particle processing or by modifying the water solution conditions.

2.4 Synthesis of the particles

Reactive ball milling is attractive for particle processing and has attracted huge interest for its utility in green engineering/ green technology [52]. Ball milling, mechanical ball milling, mechanical alloying or grinding describe the same technique in which usually a powder is crushed until ground using grinding balls. The milling balls can be of different material, such as ceramic or stainless steel and the number of balls size and type will affect the milling the quality of synthesised powder [19,41,53,54]. However, this process is energy intensive and therefore, can be ineffective. As a result, scientists and engineers alike have been trying to understand and, if possible, improve this technology of particle processing.

For milling metal aluminium together with chosen non-metal milling additives, stainless steel balls would be the primary choice in a planetary mill. In a planetary mill, the milling jar containing metal balls and powders is placed inside the milling device fixture, which spins at a fixed speed. The milling jar is swung to 180 º producing a large centrifugal force. Due to this centrifugal force, the balls collide with each other and any powder caught in between the balls and furthermore, the balls also collide with the walls of the jar as shown in Figure 2-2.

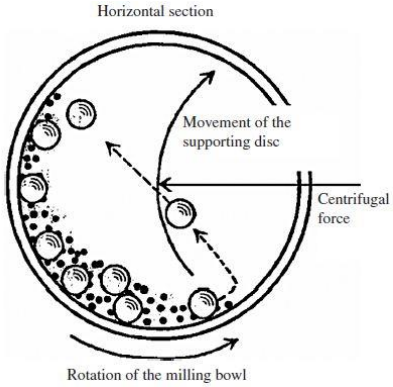

Figure 2-2: Influence of centrifugal force on the milling ball during milling [55].

It is suggested that powders ground in such mills experience up to 40 times higher acceleration than that due to gravity [34]. Such intensive energy causes changes of the metal particles as they undergo different phases as a result of plastic deformation, i.e. change in the particle shape, cold welding and fracturing seen in Figure 2-3 [55,56].

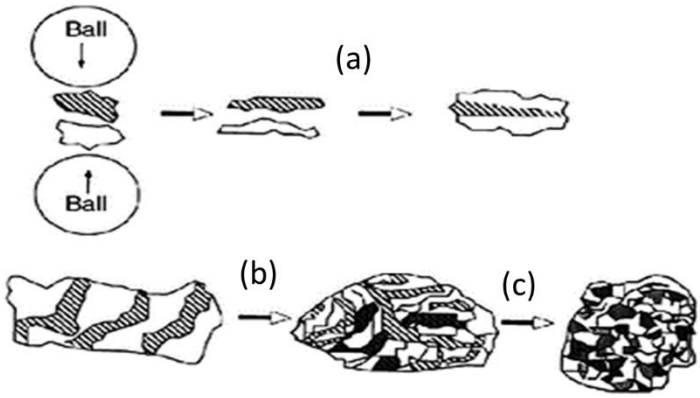

Figure 2-3: Schematic of morphological changes of materials during the milling process [57].

Referring to Figure 2-3, the morphology of the metal powder often changes and goes through different stages. These steps include: a) beginning stage b) transitional stage and c) finishing stage.

a) The beginning stage is when cold welding and process of agglomeration, i.e. increases in particle size takes place. Cold welding occurs when two particles join (also called immersing or enabling) at the interface due to significantly high centrifugal forces.

b) If milling is continued after the cold welding has taken place, it will result in the irregular distribution of additives which are being milled with the metal. The additive distribution depends upon the properties of the additives and metal particles.

c) At the last stage, the powder cannot be deformed any further. However, if milling is persisted with then it would then lead the particles to fracture (not shown in the diagram). Fractures in particles are produced as a result of particles splitting after the cold welding. These mechanisms are more profound when low melting additives are used with the aluminium. These include low melting metals such as bismuth and lithium or their hydrides, BiH or LiH forming alloys [58]. The fracturing of the particle occurs when a particle is stressed to a maximum limit of the plastic deformation [53,59,60]. The fracturing also reduces the particle size and increase the particle surface area. Furthermore, metal aluminium would be exposed again in the fracturing process and this is why the milling process is undertaken in the oxygen-free environment [60].

The reason for the particle changes described above is from the high kinetic energy and elevated temperatures from the high-intensity collisions [61]. The temperature change may also alter the crystal structure of the particle [62,63]. However, the extent of cold welding and fracturing depends mainly on the metal properties as well the milling additives. Other factors that also play a role in the final milled particle are milling jar size, machine type, filling ratio, ball-to-powder ratio, rotation speed, the number of balls, the weight of balls, the density of balls, the material of balls, the direction of milling and break in-between the rotations [64]. Moreover, different machines can have different sizes (diameter) of the disc on which the milling jar is placed resulting in a change of the centrifugal force. High-speed millings have provided researchers with aluminium particles that are able to produce hydrogen at a reasonable rate without the need for any corrosive acids or alkaline solutions or heating to more 'reactive' temperatures [65]. In this research, the milling process used a planetary ball mill (RETSCH PM 100) to prepare activated particles for hydrogen generation, more details Chapter 3.

Metal aluminium is usually not milled on its own because of the cold welding that makes the particles grow larger (and the effective surface area to be reduced). In order to prevent this, stearic acid is often used as it acts as a barrier between the particles reducing the particle fusion [66,67]. Zhang *et al.*, performed high-speed milling up to 5 hrs not using any fusion prevention agent and reported an increase in particle size by 50 μm of both Al and Mg particles [68]. For the best hydrogen generation at ambient conditions milling additives are recommended [69]. Milling duration also plays a role, as milling times can affect the morphology, the shape of particles, size and lattice imperfections and grains orientation [18,41,56,59,66,70-73]. It was suggested in 2013 by Tousi and co-workers they mixed 3 wt % stearic acid with aluminium and performed high-energy ball milling (with the ball to powder ratio of 30:1) of the powder with milling speed of 200 rpm that prolonged milling can cause the efficiency of hydrogen production to drop. The authors observed that the hydrogen yield increased at first as the milling time was increased up to 7 hrs, but after this, it started to decrease. After analysis of particles using XRD and SEM at different times in reaction, they attributed this tendency of first increase and then decrease the creation of pores. They suggested that the increase

in the number of pores at first increases the surface area of the particles leading to higher yields, but as the milling is performed for longer time, more impacts during milling can compress the particles so they are more uniform and have fewer pores, consequently lowering the yield [72].

Work continues with processing the hydrogen generating aluminium powder using advanced milling methods to understand better their applications [20,52,53,74,75]. When high kinetic milling is used, high temperatures are reached within the milling jar. This raises the possibility of annealing, which involves exposing the metal particles to extreme temperatures and then allowing them to cool. The annealing causes plastic and elastic deformations, affecting lattice structure and these changes could have an effect on the hydrogen generation. For example, Abdoli *et al.* milled Mg-Al alloy particles for an extended period of time up to 25 hrs, where they found that the crystallinity of the particles had changed and affected their stability and reactivity of the particles [65]. They also pointed out that annealing (a result of the high temperature builds up in the jar) affects the hardness of the metal, whereas Ghadimi *et al.*, proposed that annealing may help redistribution of the components in solid phase [73].

It is important that ball milling of the aluminium particles be performed under an inert atmosphere [26,41,75-78] as the process produces a considerable amount of heat due to constant collisions of the balls and friction between them. If oxygen is present in the closed milling jar, the elevated pressure and temperature could result in spontaneous combustion. Also, air would soon re-oxides the exposed metal Al surface to Al_2O_3 and in order to avoid any unwanted reactions, it has been suggested that the oxygen levels should be kept to a maximum of 5 ppm [61] by purging with inert gases such as nitrogen or argon of 99.99 % purity prior milling [66].

2.5 Breakdown of barrier layers

It is well-known that aluminium does not react with water at ambient conditions (room temperature, atmospheric pressure) due to the formation of solid and dense oxide film on its surface. Therefore, various activation methods aimed to dissolve or remove the oxide film are used in order to carry out the aluminium/water

reaction. Both in the actual particle processing and by immersing aluminium particles in water will soon create a passivation layer of Al_2O_3, AlO(OH) and $Al(OH)_x$. Removing or destroying these passive layers before the reaction will make the hydrogen reaction happen quicker and will be seen as a reduction of the "lag-time".

In the subsequent section, the importance of milling metals with additives will be discussed together with a review of the various additives that researchers have explored to enhance the water-aluminium hydrogen generation. The milling additives alter the aluminium particles surfaces due to the high energies in the milling jar [79]. When the milled powder is immersed into water, the additives which are embedded on the surface of metal particles, i.e. salts and metal oxides, also react or dissolve in water which then releases reactive ions into the solution such as OH^- and Cl^- ions. Both of these ions in solution affect the barrier layers, too. The oxide film on metallic aluminium, Al_2O_3, is hydrophilic and with the interaction of water, it soon forms a more porous Al-Oxyhydroxide layer, AlO(OH). Sites in the Al_2O_3 layer that are particularly susceptible to this hydration will exhibit a higher electronic defect density. These non-uniformity sites could originate from the milling and these defect points will be more susceptible to breakdowns, leading to the formation of local pits in the oxide barrier layer and making it more permeable to water [79].

Water penetrating through these defects will locally react with metallic Al generating hydrogen gas bubbles at the interface between the Al core and the protective surface layer. The growing H_2-gas pressure will eventually rupture the protective layer, thus activating metallic Al for reaction with water. A less stable crystal structure or more porous structure of the protective barrier layer would, therefore, be beneficial for the evolution of the hydrogen gas. The more porous the layer, the more water can penetrate through to the metal aluminium core by mass diffusion and this increase in hydrogen yield would be more evident if agitation is used in the reactor vessel and/or salt-gates has opened, see later in this section for clarity.

It has been found that salt and metal oxide milling additives work together to damage the different passive layers [80] and if these passive layers are not removed or disrupted, it will affect the hydrogen yield negatively. The reaction product, (which would effectively act as a second barrier layer) aluminium tri-hydroxide can have different morphologies depending on the nature of the experiment and reactants used. The formed $Al(OH)_3$ could be either crystalline gibbsite γ-$Al(OH)_3$, bayerite β-$Al(OH)_3$ or Nordstrandite $Al(OH)_3$ or even be amorphous. The three different crystalline polymorphs have different structural arrangements as well as different crystal density. All are composed of layers of octahedral aluminium hydroxide units with the aluminium atom in the centre and the hydroxyl groups on the sides and hydrogen bonds holding the layers together. The difference between them is how the layers stack together and what bonds are between the layers, see an example of configurations in Figure 2-4.

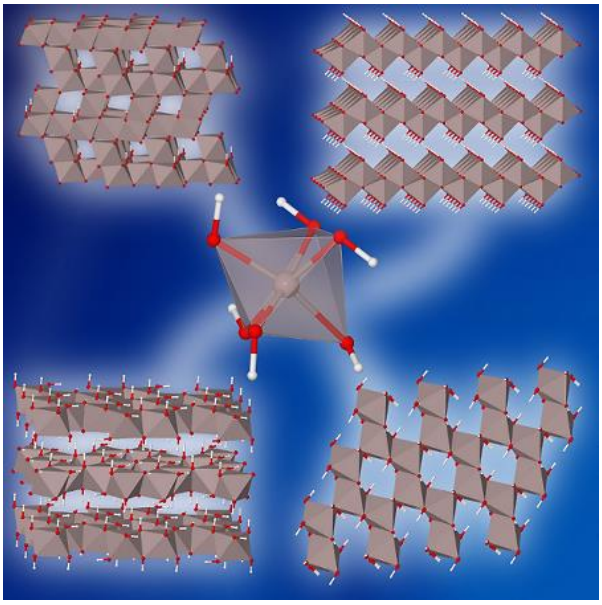

Figure 2-4: Different structure arrangement of $Al(OH)_3$ with the octahedral aluminium hydroxide unit shown in the centre and different stacking arrangements shown around [81].

In Figure 2-4, the octahedral aluminium hydroxide unit is shown and this octahedral is side sharing within the layers for all three common $Al(OH)_3$, however, the bonds between the layers differ which results in different packing order and different bond strength and bond length. Example of the different stacking of Bayerite α-$Al(OH)_3$, Gibbsite γ-$Al(OH)_3$ and Nordstrandite β-$Al(OH)_3$ can be seen in Figure 2-5.

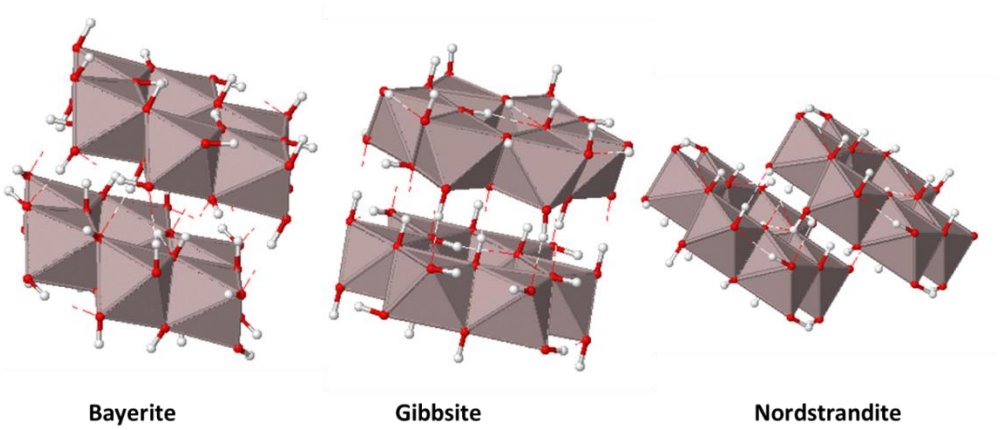

Figure 2-5: Different octahedral layer stacking of bayerite, gibbsite and nordstrandite $Al(OH)_3$ [82].

In this research, the aim is to understand which of these morphologies is formed. Different pH conditions and temperatures of the aqueous solutions used in the reaction as they affect the stability of the formed barrier layers will be tested. Aluminium oxide, Al_2O_3 found directly close to the Al-core is very stable and more or less impermeable to water. However, when it comes in contact with water it becomes hydrated and boehmite, γ-AlO(OH), is formed allowing water to diffuse into the metal core and react. At the end of the reaction, the aluminium Oxyhydroxide layer is transformed into a more stable hydroxide, which is also the end-product of the aluminium-water reaction. The most common morphology at the end of the reaction has been reported to be gibbsite γ-$Al(OH)_3$ [51,83,84] which can be proven by XRD analysis but eliminate the proof of the existence of any amorphous $Al(OH)_3$.

2.6 Metal additives

The reaction of water with metal alloys has been proposed for improvement of the hydrogen yield. Alloying can be either done by melting the metals together in a furnace or directly in a high-speed milling device due to the high energy and temperature reached. Milling aluminium together with low melting point metals has been studied for improving particle fracturing and particle size reduction in what is described as a mechanically alloying mechanism. Alloying is believed to prevent the formation of the barrier layer and is part of what is referred to as "*activated aluminium".* Fan *et al*. tested the metal additives Zn, Ca, Ga, Bi, Mg and Sn milled

together with Al on the influence on hydrogen generation [42,85]. The authors found that the alloy Al-Bi and Al-Sn significantly improved the production of hydrogen. They also reported that their particle size was 13 μm which was milled for 5 hrs with CaH_2 and Bi. However, when they reacted their sample in water it took a 30 min to achieve 80 % yield of gas [58].

Milling gallium together with aluminium was tested by Ilyukhina *et al.*, they found that the reaction temperature for Al-Ga particles could be reduced down to room temperature [19]. Despite successfully using ambient conditions for the reaction, the particle processing is still high-energy demanding and usage of rare earth metal gallium will also add to the high overall cost. However, in the hydrogen production process, the gallium is essentially an inert mat that could be reused if need be. Alloying of Al-Ga for hydrogen generation at ambient condition has also been described in two patents by Woodall in 2008 [86,87]. It is often considered that molten aluminium-gallium alloys will not possess the coherent and adherent oxide barrier layer. From mechanically alloyed particles, the constant deformation (cold welding and fracturing) will achieve similar exposure for the reaction to progress.

Metal-based additives in milling were further described by Fan and co-workers in 2011 [88]. In their study, the authors used a series of Al-Sn-Zn-X mixtures, where X corresponded to either a metal hydride or halide. They reported a hydrogen generation of 790 ml/g in less than 5 min for an Al-Sn-Zn-MgH_2 mixture. The powders were milled for as long as 20 hrs using a high-speed mill (speed not stated). Later on, Wang *et al.* in 2010 reviewed the available methods of making Al composites and alloys. The authors suggested that using low melting point metals in the milling helps in achieving higher activation of the aluminium, as more surface defects and grain boundaries are formed during the milling which promotes water reaching the Al core during the reaction [89].

2.7 Metal oxides additives

Metal oxides have also been used as milling additives to the Al particle process. Here it is not aimed at alloying or reducing melting temperature but to take part of the actual hydrogen generation reaction path. In 2002 and 2003 Chaklader *et al.*

produced two patents and proposing the use of α-Al_2O_3 and γ-Al_2O_3 as metal oxide milling additives [90,91]. In the patent "Hydrogen generation from water split reaction US 6440385 B1", 20 wt % additive ceramic powder and 80 wt % metal aluminium (80 μm average particle size) were milled and pressed as pellets and used in a reactor between 30 °C to 70 °C. It was described how the added Al_2O_3 have a tendency to hydrate in water (highly hydrophilic) which would activate a water split reaction assisting the aluminium- water reaction. The authors also pointed out that the total amount of gas release does not vary significantly with the different type of alumina oxide additive, produced from different aluminium hydroxides, (or aluminium oxyhydroxide), but significantly depended on pH of the water. If using the same Al-oxide composition, the maximum rate of H_2 depends majority on (i) nature of milling (ii) type of oxide additive (iii) temperature of reaction and (iv) pH of the water.

In 2011 Wang *et al.,* hand milled a series of nano-sized metal oxide additives including TiO_2, Co_3O_4, Cr_2O_3, Fe_2O_3, Mn_2O_3, NiO, CuO and ZnO together with Al for 3 min and reacted the particles with both deionised water and tap water at 25 °C and 35 °C [92]. The authors reported that all the metal oxides additives gave off H_2 upon reaction with water, but their reactions were slow, e.g. ZnO took up to 25 hrs to achieve 95 % hydrogen yield and additive Cr_2O_3 reported to the produce highest yield of 100 % needed 18 hrs. Their major finding conveys two key points, one that the water quality plays an important role in the reaction, as well as the choice of additives.

Wang and co-workers explored the effect of a more complex mixture of additives such as CaO, NaCl and low melting point metals such as Ga, In and Sn on the activity of Al-based particles in water. The authors prepared the Al-based mixtures using a high-speed planetary ball mill using a ball-to-powder ratio of 10:1 and milled for 8 hrs at 360 rpm. The composites were reacted with pure water at 25 °C and 60 °C. The authors reported that while all additives promote hydrogen production at both temperatures, the composite containing aluminium alloys, i.e. Al -CaO-NaCl performed much better than when using bare aluminium. They attributed this effect to a higher surface area for when alloyed Al was used (the role

of low melting point metal alloying) combined with NaCl in the milling, making the particle to fracturing and destroying the passive oxide layer more efficient [80].

Fan *et al.* commented in their 2008 paper that metal oxides additives, will result in high efficiencies of liberated hydrogen and at a fraction of the cost compared when low metal point metals are used [58]. Dupiano *et al.*, [75] tested the oxide additives of Bi_2O_3, MoO_3 and CuO and milled the Al-oxide mixture at 350 rpm in a high-speed mill. Here it was reported that mixture containing the CuO additive was able to produce hydrogen at a rate of 3.8 mL/min.gram Al, however, at higher temperatures of 80 °C. While MoO_3 and Bi2O3 produced 3.1 and 164.2 mL/min.gram Al, respectively.

Chen and co-workers [93] reaffirmed this notion in a study where they milled aluminium with CaO and NaCl (512 rpm between 30 min to 120 min) and reacted the mixture with water at temperatures between 10 °C to 80 °C. They reported their highest yield at 30 °C which produced 100 % of theoretical hydrogen yield in 2000 sec. They suggested the best composition of the mixture to be 65 wt % Al–25 wt %, CaO–10 wt % NaCl. They also suggested that the metal oxide plays a critical role in making the reaction possible as metal oxides in water release OH^- ions when reacted, which increases the pH in the solution, which in turn helps to break down the passive layer Al_2O_3.

2.8 Salt additives

Researchers have also tried salts as milling additives. Sodium chloride (NaCl) is arguably the most used salt additive for milling purposes. Nonetheless, potassium chloride (KCl), calcium chloride ($CaCl_2$), magnesium chloride ($MgCl_2$) and lithium chloride (LiCl) have also been employed. There has been significant work undertaken to understand the effect of milling time and speed using salt milling additives [26,48,58,94]. Tousi *et al*. work focus only on salt milled with aluminium [95], while Chen *et al*. work focused on salts dissolved into the reaction solution [93].

2.8.1 Salt solutions

In 2006 Grosjean *et al*. [96] prepared Mg and Ni and MgH_2 with KCl by milling for up to 10 hrs (speed not stated). They reported the highest yield of just 20 % in 60 min from powders that had been milled for just 0.5 hrs in 25 °C water. However, when the authors reacted the same sample with 1 M KCl solution at 25 °C instead of water, the yield reached 100 % in 60 min. While this may look like a good prospect, the use of nickel in the particle composite is not desired due to concerns for health and its negative environmental impact. Nevertheless, they rationalised the observed behaviour by suggesting that the chloride ions from dissolved KCl in solution cause pitting corrosion which damages the protective oxide layer making it more reactive towards the water. This claim about the salts (Cl^- ions damaging the oxide layer was later supported by Li *et al*. in [97], Chen *et al.* in 2013 [93] and Meng *et al.* in 2011 [98] and Zhao *et al*. in 2012 [99].

Using salt as milling agent was investigated by Liu *et al.*[94] where various salts such as the salts KCl, NaCl, $NiCl_2$, $LiCl_2$ and $MgCl_2$ were milled with Al-LiH composite. They performed the milling up to 3 hrs at 400 rpm and reacted their powder with water at different temperatures (25 °C to 75 °C). The authors discovered that KCl performed better than NaCl at high temperatures despite their similar chemistry. They attributed this to the solubility of the KCl salts which increases with temperature more than NaCl and is higher by 20 g per 100 ml of water (g/100 ml) at 90 °C temperature [149].

The salt milling additive magnesium chloride, $MgCl_2$ and NaCl were milled in a composite of; Al 80 wt %, Bi 10 wt %, $MgCl_2$ 10 wt %, for 5 hrs to 20 hrs, (milling speed not stated) by Chen *et al*. [93]. It was concluded that $MgCl_2$ performed better than NaCl for the H_2 production due to the high ionic concentration from the additional Cl^- ions. Chai *et al.* in 2014, also suggested the reason for improvement of hydrogen reaction being that salt enhances the conductivity of the solution when dissolved. In their work, cobalt (II) chloride, $CoCl_2$ and $NiCl_2$ were added into the water in which Al was reacted. It was found that increasing the concentration of $CoCl_2$ enhanced the reaction compared to $NiCl_2$. It could be due to the solubility $CoCl_2$ was higher, therefore, the authors proposed that by having more Cl^- ions help

in the by penetrating the oxide film on the surface of aluminium to promote the aluminium corrosion [100].

Zhao *et al.* [26] in 2011, milled aluminium with different ratios of Ca and NaCl varying the time from 10 min to 1 hr at 512 rpm. They reported that when the composition was Al 73 wt %, Ca 20 wt % and NaCl 7 % favourable hydrogen yields were produced. The authors also reacted their sample with various salt solutions containing $CaCl_2$, NaCl and $MgCl_2$ and reported that solution containing NaCl was more reactive and produced 100 % yield in 1400 sec. They explained that the presence of high concentration of Ca^{2+} ions will hinder the dissolution of $Ca(OH)_2$, thus preventing the production of OH^- ions and hence the complete hydrolysis of Al. The Mg^{2+} on the other hand, it was suggested to react with OH^- ions to form $Mg(OH)_2$ by the authors which again inhibits the reactions. They proposed that NaCl addition can be used to greatly improve hydrogen generation of Al–Ca alloys.

In 2016, Tousi *et al.* [95] prepared aluminium powder by milling potash (KCl) and NaCl separately with 50 wt % for up to 7 hrs at 200 rpm. The milled samples were reacted with hot water (80 °C) and KCl was reported to be better than NaCl for H_2 generation. To understand the reason for this behaviour, they analysed their samples using SEM-EXD and reported that KCl affected the aluminium particles structure more by being more embedded on the surface of the metal than NaCl.

Alinejad *et al*. [77] in 2009, presented a similar argument that salts milled with aluminium particles are easily broken down and adhere to the Al particles surface. When the prepared powders are reacted with water, the salt particles on them are dissolved. As a result, a fresh surface of aluminium metal is exposed to water for reaction. Wang *et al.* in 2014, milled NaCl and CaO together with aluminium for 8 hrs at 450 rpm. They found promising hydrogen production by using this combination of salt and metal oxide milling additive. They further reported that the salts and metal oxide ratio had a direct effect on reaction rate and reaction exothermic temperature. A ratio of 10 wt % of salt and 9 wt % oxide in the mixture provided the highest rate of hydrogen generation [80]. Furthermore, the additives CaO and NaCl are attractive to use as additive due to easy availability and abundance to keep the process economics low. Chen and his group [93] Chen and

his group in 2013 had reported similar findings for the case when aluminium was milled together with NaCl and CaO for 2 hrs at 512 rpm. More support came from other works [101-103]. Where it has been generally found that NaCl produces more reactive powders than $CaCl_2$ and $MgCl_2$. Therefore, it can be concluded that NaCl is the most favourable salt to mill with Al and that salt additives can play a major role in reaction kinetics and if used in an optimised composition will contribute towards getting a better hydrogen yield. Though salts are immediately dissolved in the water solution and soon form ions, the difference when using salts as milling additive is that it disrupts the mechanically the barrier layer during the milling and leave a so-called "salt-gate" when dissolved. An already dissolved salt will not provide this enhancing mechanism, though they will increase both the ion conductivity (electrolytic effect) and provide plenty of reactive Cl^- ion.

From above review, it is concluded that salt additives can play a major role in reaction kinetics and if used in an optimised composition can also contribute towards a better hydrogen yield.

2.9 Hydrogen reaction conditions

For a good hydrogen yield, pure water would theoretically be the best choice for the reaction. However, to make hydrogen generation technology more applicable different types of water needs to be tested as pure deionised water is not always available.

As established earlier, there are many factors that can influence the hydrogen reaction. These factors can be the type of solution used, temperature and pressure, the ratio of particles to the solution, the pH of the solution and agitation. Another measure of the reaction that can be used to determine what reaction conditions work best is the lag time. The lag-time can be defined as the time taken for hydrogen gas to be produced and evolve out of the solution where it is measured. There are possible causes for the lag; it can be associated with the time taken for water to hydrate the passive layer and diffuse out to reach the surface of the metal or the time the formed gas bubble takes to escape the particle and enter the solution to

finally reach where it is measured. The lag-time is used when comparing salt in solution versus salts as milling agent [17,104].

Some researchers have reported aluminium hydrogen reactions to seawater. Seawater is usually more corrosive than pure (deionised) water as salt water is a good electrolyte and promoting fast corrosion and dissolved salts (in particular the Cl^- ions) helps in damaging the protective oxide layer. This occurrence was recognised by Gutbier and Karl [105], they registered a patent on it using magnesium alloys in hydrogen generation that sea water helps in the corrosion process as it contains about 3.5 % salt.

Activated Mg-Ni-Co alloy particles and seawater were studied by Zou *et al.* [102] they reported a 97.1 % hydrogen yield in 10 min reaction time. However, the reaction demanded very high temperatures of ~ 800 °C which makes it unattractive from the commercial point of view. Huang *et al.* [106] milled Mg with activators MoO_2, MoO_3 and MoS_2 and reacted the sample with sea water at temperatures ranging from 25 °C and 75 °C. A hydrogen yield of 91.7 % was achieved at temperature 25 °C after 10 min. Activated Al particles have also been reacted with sea water and reported by Ma *et al*. in 2011. An aluminium mixture of Al–NaOH-$Na_2SnO_3.3H_2O$ was milled for 1 hr at 400 rpm in a high-speed mill reached a hydrogen yield of 90 % only in a couple of min and at room temperature of 25 °C [107]. Hydrolysis process can be made faster if the passive layer is removed or damaged prior to the reaction with water. As stated already, this can be achieved by the milling, but also, the metal oxide coating facilitates as it contributes to increasing OH^- ions which enhance the pH of the solution which in turn improves the reaction as was discussed previously [18].

2.9.1 Temperature and agitation

Both temperature and pressure can be used to adjust the reaction kinetics. Many researchers have used hot water from 50- 80 ºC for the reaction [75,95,108,109]. The use of temperatures around 80 ºC for optimal reaction rate has been supported by many groups working on hydrogen production, including Tousi *et al.* [95]

IIyukhina *et al.* [19], Rosenband *et al.* [40] and Nie *et al.*[110] to reference a few publications.

The reaction of aluminium with water is susceptible to temperature changes seen in the enthalpy of the reactions that occur. Al_2O_3, AlO(OH) and $Al(OH)_3$ formed on the aluminium particles blocking access of water molecules to reach the surface of the metal and must be removed for the reaction to proceed [74]. The removal or shedding of the formed hydroxide layer can be facilitated when agitation is performed during the reaction. Therefore, agitation (stirring) is another significant factor affecting the rate of reaction. Agitation can also be used to ensure that the all the reactants are properly mixed and can also improve both the mass transfer and heat transfer rate in the reactor vessel. Stansbury *et al*. [111] described how agitation improved the reaction of aluminium metal as it removed the hydroxide layer thus improving water diffusion to the metal surface. Improved hydrogen reaction when using agitation has also been supported by other authors [112,113].

Generally, it has been found that both high temperatures and agitation improve the reaction yields. However, in order to maintain the temperature in the reactor vessel, a hot plate or water bath would be needed, which is undesirable for on-demand hydrogen generation for commercial interest. It was also reported by Elitzur *et al.* [69] and Dupiano *et al.* [75] that it is possible to react synthesised Al powder with at 30 °C water to produce hydrogen gas.

2.9.2 Different aqueous solutions

This research is exploring different types of water to use in the on-demand hydrogen reactor. A review of typically available surplus water or wastewater was, therefore, done. The most commonly used water for an on-demand hydrogen generator for fuel cells is domestic tap water. Tap water is far from as pure as deionised water as it contains minerals, dissolved salts and carbonates.

Wang *et al.* [92] looked into the effect of the water quality on H_2 production and focused their attention on tap water and deionised water. The authors that the main difference between the two was in their conductivity, with deionised having higher conductivity than tap water. They reacted their aluminium powder, prepared by

hand milling, with the two different types of water. They reported that deionised water was more reactive and produced a higher hydrogen yield than tap water, which they attributed to higher solubility or greater dissolving capacity of Al_2O_3 layers at 25 °C than tap water. They also indicated that higher temperature of the water, i.e. 35 °C, was ideal for hydrogen production.

Rainwater can also be considered as an accessible water source and if used it is worth remembering that rainwater often contains formed carbonic acid due to a high level of CO_2 in the atmosphere. Other types of water to consider is wastewaters from industry. Effluent waters. The first to be discussed is the sucrose solution. The starch industry, for example, is one of the largest in the world and it uses water for various processes, however, surplus water is often discharged without any treatment. This type of wastewater may contain carbohydrates, cellulose, protein, and nutrients [114]. Therefore, it was decided to explore this type of wastewater. Fermentation would be the best choice of hydrogen generation technology to use for hydrogen gas generation has been a practice. In this research work, different carbohydrate specimens like sucrose in water. Sucrose ($C_{12}H_{22}O_{11}$) is made up of glucose and fructose linked together by glycosidic bonds [115]. A solution of sucrose will contain molecules forming hydrogen bonds with each other. The rationale for investigating this is the possibility of H_2 to be given off upon breakage of H-bonds.

Yet another possibility worth considering is alcohol. Alcohols sold in the chemical market such as methanol and ethanol, either come pure (100 %) or have some water added to them depending on the purity. The water content from them can be tested for H_2 generation. Other carbohydrate specimens found in wastewater examined in this thesis are ethanol and ethylene glycol (anti-freeze). Grosjean *et al.* prepared (Al) powder by milling Mg and MgH_2 for reaction with methanol and ethanol [96]. They reported that hydrogen could be detected by methanol reaction and that the rate was higher when pure methanol was employed instead of in diluted form. The reaction of the sample with ethanol, on the other hand, did not produce any hydrogen. The results of our investigation are reported in chapter 4.

Ethylene glycol is an organic carbohydrate which belongs to the alcohol family and is used as an antifreeze, e.g. it can be easily mixed with water to reduce its freezing point. It is believed that there will be high concentrations of antifreeze in wastewater in the vicinity of industries. If the water that contains antifreeze can be utilised for hydrogen generation purposes, it could prove to be beneficial in remote and very cold areas. As for sucrose solution, no literature has been found using ethylene glycol solutions for this type of hydrogen generation.

Another wastewater solution that represents an interesting type of wastewater is urine. Human urine waste consists of 94 % water (depending on the hydration of the subject) and urea (CH_4N_2O) 10.5 billion litres urine is produced worldwide by humans every day and therefore, there is a plentiful supply [116]. Using urine for hydrogen generation has been attempted by some investigation but using an electrolysis route [117]. Elitzur *et al.* prepared Al in 2016 with LiH and reacted it with human urine. Urine itself was considered not to be hydrogen-producing, only the water. A theoretical hydrogen yield of 90 % was reached within 10 min in a batch reactor at ambient room condition with a flow rate of 150-700 ml/min/g Al. The particles for the reaction were 9 μm Al-activated with 2.5 wt % LiH in the particle processing [116].

2.10 Hydrogen economy

For many years supporters of green energy have proclaimed the hydrogen economy will soon be a reality. Some energy experts claim that hydrogen from renewable energy is excessively expensive whereas other companies (like ITM in the UK) are proving that this technology is already competitive as producers of hydrogen for use in cars. For hydrogen to become a common alternative to the traditional fuels and power generation, its complete cost needs to be considered. Hydrogen is an attractive alternative to the traditional fuels and currently, the two sectors consuming most fuels are transportation and electricity generation [118]. Hydrogen has increased its usage in the transport sector, meaning that produced hydrogen could be transported to the end user, by a hydrogen-fuelled mean of transportation. In recent years, hydrogen has seen an increase in its usage in the transport sector and it may be that in the near future the majority means of transportation is

hydrogen fuelled in one way or another. This can be either by hydrogen fuel cells or by a combustion engine.

In 2005, Chevrolet introduced the Equinox, a car using hydrogen a fuel travelling up to 320 miles on a 4.2 kg hydrogen tank [119]. In the UK, H21 (Project LHNE), collected data from fuel cell powered delivery vans to observe the hydrogen performance in 2015 [120]. The EU project CUTE (Clean Urban Transport for Europe) studied fuel cells aimed at public transport across Europe, notably in London where fuel cell buses are extensively used. The aim of all these incentives is to show hydrogen as a friendly and economical fuel for the future. However, for this to be integrated fully into society, more refuelling stations are required.

Currently, the BOC Group plc is developing hydrogen refuelling stations in the cities across Europe, especially in London UK, to facilitate vehicles running on hydrogen. London had three refuelling stations in 2016 and more are being developed [7]. Cars that run on hydrogen fuel cells are designed in such a way that if the surplus amount of electricity is generated, it can be fed it into the national grid. This concept is known as Vehicle-to-Grid (V2G) [121]. As for the economy, hydrogen gas production still requires a significant capital cost making it an expensive source of energy. Additionally, coal reforming, natural gas reforming, biomass gasification and electrolysis still produce greenhouse gases indirectly which is detrimental to the environment [122]. Various techniques have been adopted by engineers and scientists around the world in order to develop straightforward and cost-effective processes while balancing safety concerns and running cost.

Making hydrogen mainstream is also challenging due to safety concerns around production, transportation and storage as has been stated previously. Taking the route of preparing Al particles to produce H_2 for fuel cells, every step in the process requires scrutiny regarding cost so that the overall hydrogen economics can be evaluated [123]. Electrical energy is utilised not only to produce hydrogen but also to compress, liquefy, transport, transfer or store and finally to be used (finally to make available for use, for instance, in a portable fuel cell device. There are no environmental or energetic advantages in producing hydrogen from natural gas or

other hydrocarbons sources for portable Fuel Cells. Therefore, this research work evaluates how the hydrogen can be produced at a relatively low cost and by using cheap (and often free) water sources.

After the production, hydrogen tends to be made into a transportable form either by compression or by liquefaction; both demand high energy input. To compress 1 kg H_2 adiabatically to 200 bar would need around 15 MJ/kg. Even more, energy input is required in the liquefaction of hydrogen because gas needs to be cooled down to 20 K (-253 °C) [124]. Hydrogen may also be bonded chemically to metal hydrides for a possible transport state and stored in metal hydride cartridges. If this form of storage is undertaken, then it needs to be recognised that only two grams of hydrogen can be stored in a small 230 g metal hydride cartridge. This makes this type of hydrogen packaging impractical for the purpose of this research. Also, the energy needed to load hydrogen in metal hydrides is more than can be recovered from the metal hydrides later. However, the energy cost of a delivery of hydrogen-metal hydrides is lower than when hydrogen is compressed at 200 bar and delivered.

Hydrogen economy evaluation also often involves the mean of transport, either by trucks or ships, to where it will be used, however, it would be most likely to be transported via road. As an example, a road transportation can illustrate the cost evaluation where a 40-tonnes truck is designed to carry a maximum load of hydrogen limited to only around 300 kg of hydrogen at 200 bar per truck [125]. This is because of the low hydrogen density consequences and the weight of the necessary pressure vessels and safety armatures for transporting such highly compressed gas. The financial cost of such transport vehicle must, therefore, be added together with the hydrogen production cost and the compression cost. In March 2017, the Government announced additional funding to support the development of hydrogen for transport until 2020. The “Hydrogen for Transport Programme” (HTP) will provide up to £ 23 m to increase the uptake of hydrogen fuel cell vehicles and grow the UK hydrogen refuelling infrastructure [126].

It can be said when reviewing the current hydrogen economy that the overall cost of hydrogen should be as low as possible, using as little energy as possible for the overall process, transport and storage. The hydrogen economics can, therefore, be

drastically reduced if hydrogen can be produced on-demand, avoiding the need for costly transport and compression. In the next chapters, these costs would be investigated based on the choices of starting material for particle production, the particle process and the necessary experimental condition.

2.11 Chapter 2 Conclusion

Different technologies for hydrogen production as well as reactive particle processes were reviewed. For the hydrogen production, it was found that majority of the technologies were not green processes and not economically feasible for small-scale hydrogen production. The current state-of-the-art for metal-water reactions was reviewed and it was found that optimal hydrogen yield was often achieved at elevated temperatures or using expensive components in the particles during the reactive milling process. Reviewing the research in reactive particle processing it was often suggested that intensive milling energy input was asked for making the particle process expensive, in addition of the costly milling additives such as rare-earth metals, barium oxide or expensive metal oxides or salts were employed. These findings explain the reasoning to balance the cost of particle processing with the outcome of hydrogen production to make this type of on-demand hydrogen generation effective and economical, while still achieving high hydrogen yield from the activated particles.

In the literature review, it was also found that majority published data were using deionised water in the reaction. Whereas deionised water should be used for comparison, other more accessible and readily available waters including wastewater should also be tested. From the literature review it was only found a small contribution using tap water and using sea water but no typical abundant waste waters or extended description how different types of water effect the reactive particle's components in their reactivity for obtaining the highest hydrogen yield.

It was concluded that reactive ball milling using cheap recycled aluminium will be used for this research. While using affordable and easy accessible milling additives such as CaO and CuO along with salts including KCl, NaCl and $CaCl_2$ would be used in this research work.

Chapter 3 Methodology

This chapter describes the different procedures undertaken in this research including synthesis of the particles, particle analysis and hydrogen reactor. Including how the generation of hydrogen was measured and the different aqueous solutions used for the reaction. The details of the methodology are crucial for repeatability in any process. Therefore, it is necessary that it be described in a manner which is easy to follow. A work flowchart demonstrating the strategy of the experiments can be seen in Figure 3-1. The flowchart shows the simultaneous routes for reactive powder preparation and the solutions that will provide the hydrogen.

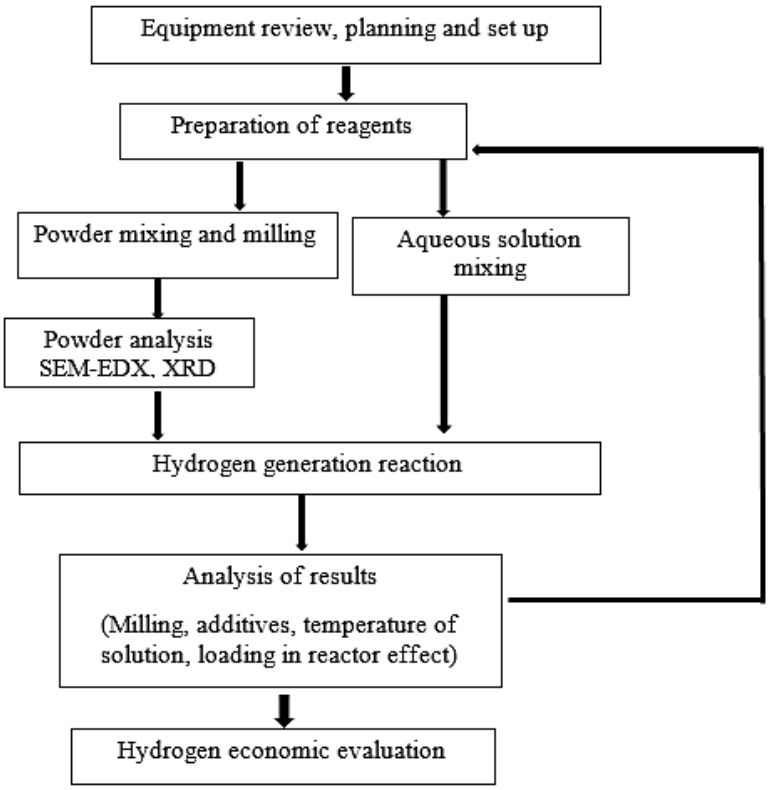

Figure 3-1: Work flowchart of the hydrogen generation research.

3.1 Experimental setup

In Figure 3-2a and Figure 3-2b, schematic and photographic description of the hydrogen reactor set-up can be seen. The setup was designed and constructed at LSBU and it was kept simple for ease of moving and adjusting when necessary.

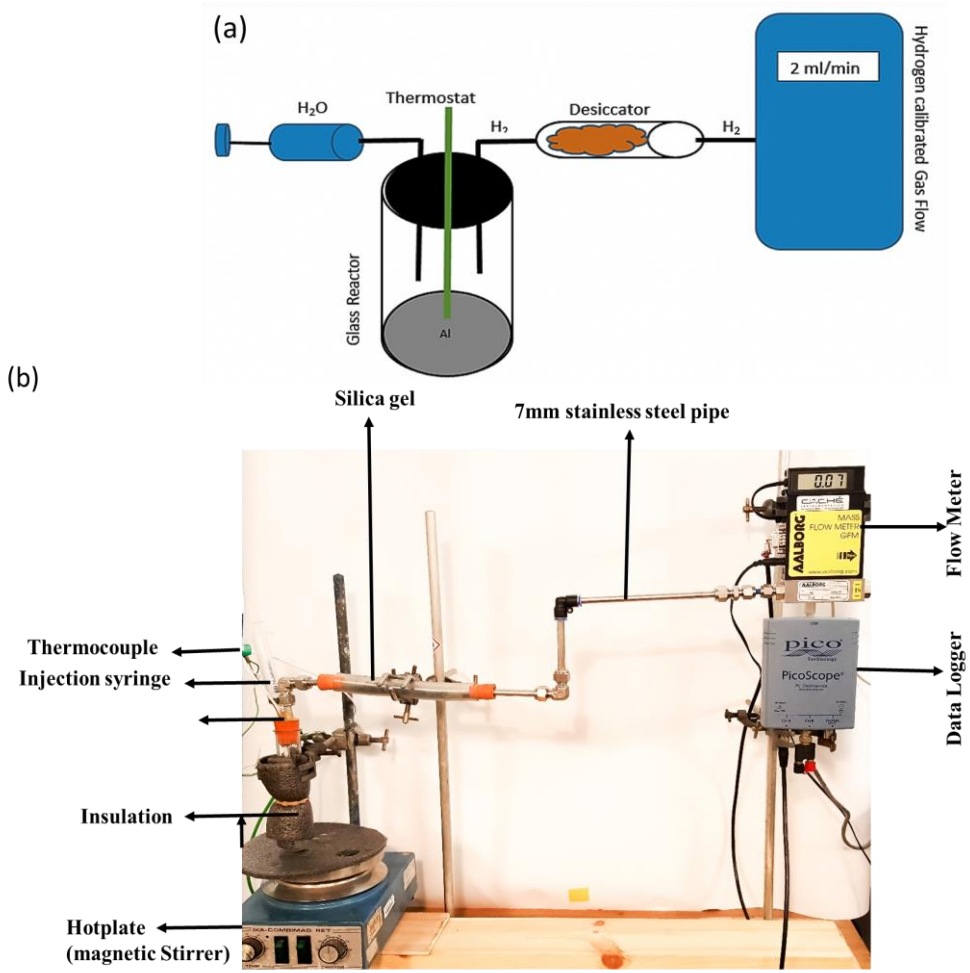

Figure 3-2: a) Schematic showing the working principle of the hydrogen reactor and b) Photograph showing the experimental set-up.

A Pyrex glass tube (60 ml, inner diameter: 21 mm) was used as the reaction vessel. A rubber stopper with 2 openings acted as a sealant for the connections. One of the openings in the stopper provided the exit channel for the hydrogen that was liberated in the reaction whereas the other opening was used to insert a thermocouple (k-type) connected to a digital data logger (Picotech, Model: 2204) in order to monitor the real-time temperature.

Before the start of the reaction, the vessel was thoroughly purged with pressurised argon gas (an inert gas) in order to keep the concentration of oxygen in the vessel as low as possible. A measured amount of prepared activated aluminium powder (0.3 g) was added to the reactor followed by water at 25 °C, 9 ml which were added using a syringe. The initial temperature of the water was varied only when analysing how it affected the hydrogen generation. In order to observe the developed temperature and prevent heat energy transfer, the vessel was wrapped with an insulating polystyrene sheet. The mixing of water and the powder was accomplished by agitation using a small capsule-shaped stirrer bar (5 mm, 1 g) added in the reactor. The vessel rested on the magnetic stirring plate (IKA-RH-Basic 2) used to control the agitation speed. In most of the experiments, the stirring speed was set to 700 rpm. When the effect of stirring speed was analysed it varied between 0-1100 rpm. The size and the weight of the stirrer allowed free movement of particles inside the reactor. Other sizes or shapes of the stirrer bar were not considered in the case as they proved detrimental to the success of the reaction.

The generated hydrogen gas was passed through a series of stainless steel pipes (internal diameter: 7 mm) with three elbow compression joints and one push-fit to avoid any gas leakage. To ensure that dry gas entered the gas flow meter as a reinforced plastic tube joint (5 cm x 3 cm) containing a desiccant (silica gel) was attached to a gas mass flow meter (Aalborg GFM-17). The hydrogen produced was recorded via a data logger connected to a PC using the relevant Pico Logger software with sample intervals of 1 sec. The connections to the data logger enabled that both the hydrogen flow rate and temperature were read and recorded simultaneously. For monitoring the pH changes during the reaction, a pH meter

(Mettler Toledo 3311) was employed and inserted into the glass reactor in separate experiments using different stopper arrangements and the recorded manually. In order to analyse the produced gas quality, a gas-tight syringe was used to collect the formed gas and transported to a gas analyser (gas chromatogram, GC). While it is acknowledged that ideally the system should have been connected directly to a GC for real-time/*in-situ* analysis, this was not possible during the course of this PhD due to limitations of access, i.e. the inaccessibility of GC at the premises.

3.2 Hydrogen flow metering

Two means to measure the rate of hydrogen generation and the total amount of hydrogen generated were employed; inverted column method and a gas mass flow meter. The gas mass flow meter had ± 0.01 ml accuracy in the flow range of 0-10 ml/min. The gas flow meter was pre-calibrated for hydrogen gas. The principle of operation of the mass flowmeter is described as the gas enters the mass flow transducer, the flow is split out of which a small portion goes through a narrow capillary stainless-steel sensor tube and the other portion goes through a primary flow pipe. Both pipe and tube are designed to allow laminar gas flow only. They are also aimed at having proportional flow rates which mean that the flow rate measured in the small sensor tube can be converted to the total flow reading. This means that the flow rate is measured only in the small capillary sensor tube. This is done by utilising the heat capacity C_p, of the gas and by a heat transfer mechanism. Heat flux is introduced at two sections by precision sensor coils (35 mm apart).

As heat is carried by the gas from the first heater coil position to the next coil, a temperature depended resistance differential can be detected from the gas. The device is a configuration that the molecular mass flow rate output signal is a function of the amount of heat carried by the hydrogen gas in the fluid flow. Sometimes inverted column was also employed to measure the amount of hydrogen being formed. This was done to ensure the reading with a mass flow metre was coherent. Error and uncertainty estimation for hydrogen generation is found in Appendix as well as calibration certificate for the gas flow meter (GFM-17).

3.3 Particle synthesis

For the synthesis of what is called “activated particles”, which will react with water readily, a high-speed ball mill was used to prepare them. In Chapter 2, different ball milling approaches were explained as was the expected role of adding various additives to the milling. Since one of the research aims is to estimate the energy consumption used in “particle activation” and then further to balance this energy consumption with the production of energy-rich hydrogen, the powder synthesis was worked out in detail to make it both highly reactive while using minimal energy. Prior to the reactive milling, all powders were dried in a vacuum furnace (Townson and Mercer Ltd) at 25 ºC for 24 hrs to remove any excess moisture. After drying, the powders were kept in a desiccator inside an oxygen-free glove box (Saffron Scientific Alpha) purged with 99.99 % pure argon gas to ensure moisture and oxygen-free environment. Inside the glove box, an oxygen sensor (SYBRON Taylor) was placed measuring to the oxygen level with ± 0.01 accuracy.

Aluminium powder as received from iHOD USA was made from recycled aluminium and therefore, was blended with different particle sizes. It was decided that it should be sieved and 3 different particle sizes would be separated to establish the effect of different particle sizes. For this purpose (Endecott Test Sieve Shaker E.F.L Mark II with Endecott’s Ltd) sieves BS410/1986 with size, 3-300 μm were employed. In literature, nano-sized particles have been mostly used [50,62,65,76,77,89] for production of hydrogen. All the sieves were placed in descending order placed on top of each other and on the topmost sieve was 300 μm were received aluminium powder was dispensed. The sieving process was set on for 48 hrs for a better homogeneous distribution. After sieving was completed and share distribution of particle sizes was taken into account. After all the separation has taken place sieves from 40 μm, 70 μm and 100 μm were selected and later compared to the SEM for verification. It was confirmed that from SEM analysis (Not displayed here) that in 40 ± 5 μm. On the other hand, for other sizes, their average was found to be at 75 ± 5 μm and 105 ± 5 μm, respectively. These sizes of particles would also provide a more cost-effective and realistic solution for keeping the process of hydrogen production commercially attractive. High purity aluminium

particles (which represent an expensive alternative) were also purchased to compare with recycled aluminium. Below is the list and details of the components used including aluminium and milling additives.

- Aluminium recycled (99.1 wt %, sieved from 3-300 µm to achieve 40 µm, 75 µm and 105 µm, obtained from iHOD USA).
- Aluminium pure (99.5 wt %, Alfa Aesar, 200 mesh, Fisher Chemical).
- Calcium oxide (99.0 wt % CaO, 65 µm, Fisher Chemical).
- Copper oxide (99.0 wt % CuO, nanoparticles, ACROS Organics).
- Barium oxide (90.0 wt % BaO, nanoparticles, ACROS Organics).
- Potassium chloride (99.5 wt % KCl, 65 µm, Fisher Chemical).
- Calcium chloride (80 wt % $CaCl_2$, 280 µm, VWR Chemical).
- Sodium chloride (98.0 wt % NaCl, 150 µm, Fisher Chemical).

All above-state additives, including metal oxides and salts, were blended with the metal particles as 25 wt % metal oxides and 10 wt% salt. Later it was discovered that two combined metal oxides (CaO and CuO) and a salt blend (NaCl, KCl and $CaCl_2$) was optimised to improve the hydrogen yield.

3.4 Milling setup

Preliminary milling conditions were investigated prior to this PhD research (not reported in this Thesis) where milling speeds between 200-550 rpm for 0.5-5 hrs were tested and evaluated by hydrogen reactions. The results provided a starting guideline for suitable milling conditions. As stated already, powder preparation for milling was performed under anaerobic condition inside a glove box. This was done for two reasons; one reason was to ensure that oxygen could not come into contact with the newly exposed surface of the aluminium metal during the milling process, which would otherwise cause the Al_2O_3 layer to form rendering the metal unreactive. The second reason was to prevent oxygen entering the glove box for safety. Metal balls colliding with each other during the milling process can cause a spark and in the presence of a combustible gas (of which oxygen is one) could ignite.

For the synthesis, the ball to powder ratio was kept at 10:1. Where 8 milling balls (spherical stainless-steel balls 7 mm diameter) and 3 g of aluminium powder along with chosen additives were placed into the 50-ml stainless steel milling jar while inside the glove box, see Figure 3-2.

Figure 3-3: High-speed plenary milling equipment used with a) stainless steel grinding pot and balls; b) fixture for stainless steel pot; c) the complete device with programmable settings and d) stainless steel pot locked.

The sealed assembly from the glove box was then transferred to the planetary ball mill device (Retsch PM-100) seen in Figure 3-3c. The total weight of the milling jar was adjusted with a counter balance on the milling machine station to avoid imbalance and rattling during high-speed milling placed in the fixture, Figure 3-3b and locked jar in Figure 3-3d.

Different milling programmes were setup in which the rotation direction of the mill and the milling speeds were altered. In milling programmes, a number of brakes and the duration of the breaks were varied. Milling programmes details are provided in Table 3-1.

Programme 1a and 1b differed in milling speed only and consisted of 1 min milling (set as 59 sec on the device), 30 sec breaks and change of milling rotation for another min, 30 sec breaks and so on until a total milling time 1 hr and 40 min.

Programme 2 was used to test the importance (if any) of the intermediate break time (so-called annealing time) where the break time was set to 5 sec instead of 30 sec as it was for Milling Programme 1a and 1b.

Table 3-1: Different milling programmes were used in this research.

Milling Programme	Total milling time	Time of milling set	Speed of milling	Break between milling set	Directions of milling
1a	1 hr and 40 min	59 sec	260 rpm	30 sec	Anticlockwise/ Clockwise
1b	1 hr and 40 min	59 sec	520 rpm	30 sec	Anticlockwise/ Clockwise
2	1 hr and 40 min	59 sec	260/520 rpm	5 sec	Anticlockwise/ Clockwise

After each milling, the jar was cleaned and washed with a dilute alkaline solution (NaOH) and dried thoroughly before milling again and placed back in the oxygen-free glove box. The milled particles were stored in air tight containers which were flushed with inert argon gas. A plug-in electricity cost monitor (Maplin) monitored the energy consumption during milling to be used for the hydrogen economic evaluation.

3.5 Particle analysis

The particles were analysed before and after milling by conventional material characterisation tools such as X-ray diffraction (XRD) and scanning electron microscope (SEM) with elemental analysis detection (EDX). Furthermore, same types of analysis were undertaken on reacted particles to examine the extent of the reaction between water and metal and the formation of the hydroxide layer $Al(OH)_3$ the by-product. The results of the reacted particle analysis were then compared with the hydrogen generation data to determine which additives were best suited for milling with aluminium for well-matched for an economical hydrogen production.

The reacted particles from the hydrogen generation, labelled as "after reaction", were collected once the reaction had stopped and no more hydrogen was produced and was prepared for analysis. The wet slurry in the bottom of the reactor vessel (glass tube) was poured into a petri dish with a filter at the bottom to prevent dried particles from sticking to the glass. The petri dish was then placed in a vacuum furnace for evaporation for 12 hrs at 24 °C. Please note all XRD and majority of SEM-EDX analysis were undertaken at University of Nova Gorica, Slovenia.

3.5.1 X-ray diffraction

X-ray diffraction was used to determine the crystallinity of the particles and for identification of the particle material. For the reacted powder, it was used to identify the different crystalline structure of $Al(OH)_3$ and see if the formed barrier layer was amorphous or crystalline. The X-ray diffractometer used (MiniFlex Rigaku, Cu K-alpha, 600W tube) could perform both qualitative and quantitative analysis.

The working principle of XRD consists of three basic elements: An X-ray tube (the radiation source), a sample holder where the samples are placed and an X-ray detector to record the response of the sample to the incoming the response of the sample to the incoming X-ray beam. The crystal structure information of the particle is then read on plots showing diffraction peaks over incoming X-ray beam. Different material gives different diffraction peak patterns depending on crystal structure and these can be identified with reference to the established XRD

databases. The principle of obtaining diffraction peaks can be described using the Braggs law [127];

$$n\lambda = 2d\,sin\theta \tag{3.1}$$

where λ is the wavelength of the incoming radiation, *d* is the interplanar spacing within the crystal, *n* is positive integer and theta *θ*, is the angle between the incoming and scattered X-ray beam, see Figure 3-4.

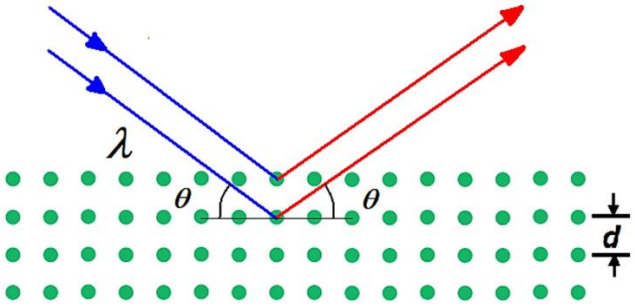

Figure 3-4: Working principle of XRD analysis of particle materials using Bragg's law [127].

The sample was placed evenly on a dedicated glass slide with a sampled groove for the sample (to assure constant distance, Z value). It was then irradiated with the X-ray source (40 kW, 15 mA, Cu source). The X-ray source was rotated to span a 2 θ theta angle between 20 and 100 degrees and the reflected beam from the aluminium powder mixture was detected for each angle incoming angle in the detector.

3.5.2 Scanning electron microscope

For evaluation of particle size, shape and associated elementary analysis scanning electron microscopy (SEM) (JSM7100f TTLS, JEOL, Japan) equipped with an energy dispersive X-ray spectroscopy (EDXS) detector (X-Max80, Oxford, UK) was employed for providing both chemical and morphological information on the aluminium particle mixture.

High-resolution images of surface topography were produced using a highly-focused, scanning (primary) electron beam. The primary electrons enter the surface with an energy of 0.5 – 30 kV and generate secondary electron flow of a lower energy. The intensity of these secondary electrons is largely governed by the surface topography of the sample. An image of the sample surface can thus be constructed

by measuring these secondary electron intensities as a function of the position of the scanning primary electron beam. High spatial resolution is possible because the primary electron beam can be focused to a very small spot (< 10 nm). The working principle of an SEM can be seen in Figure 3-5 where the specimen to analyse is placed inside a vacuum evacuated chamber and bombarded with the highly focused electron beam (primary electron beam) by an electron gun.

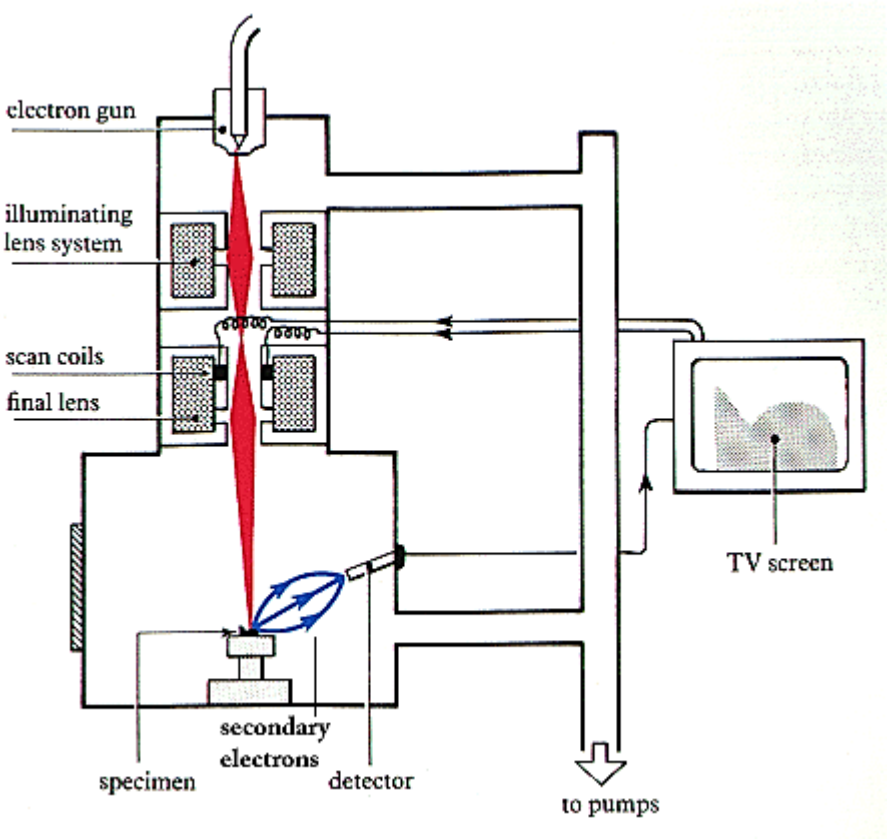

Figure 3-5: Working principle of scanning electron microscopy [128].

The focused beam (focused via different lens systems) is scanned over the specimen in a series of lines and frames called a *raster*. The raster movement is accomplished by means of small coils of wire carrying the controlling current (the scan coils). The sample inside an SEM chamber is bombarded with a highly focused electron beam (order of 10nm). The sample then absorbs some electrons and some are reflected back depending on the type of material and these reflections are detected by the suitably-positioned. The low energy secondary electrons are detected by creating an image analysis seen on a screen. The elemental analysis was conducted by energy dispersive x-ray spectroscopy (EDX) used in conjunction with SEM but by

using an EDX detector instead. In addition to the low energy secondary electrons, backscattered electrons and X-rays are also generated. The intensity of these backscattered electrons can be correlated to the atomic number of the element. The EDX analyses can identify elements within a specific area (mapping) or by spot sampling. Hence, in the SEM-EDX both qualitative/quantitative elemental information and image analysis can be obtained for the activated particles. For mapping EDX analysis, the powder was pressed do a flat prior analysis.

3.6 pH measurements

Both during the reaction and when preparing different water solutions, pH measurements were undertaken. The potential of hydrogen, (pH), is a numeric scale to specify the acidity or alkalinity of an aqueous solution. It is taken as the negative logarithm to the base 10 of protons and as such measures the concentration of hydrogen ions as [115]:

$$pH = -\log_{10} [H^+] \quad (3.2)$$

Water dissociation is an equilibrium reaction shown below as:

$$H_2O \rightleftharpoons H^+ + OH^- \qquad \Delta H_r = 55.8 \text{ kJ/mol} \quad (3.3)$$

As the equation 3.1 shows, water is split into positive hydrogen ions and negative hydroxyl ions and this is an endothermic reaction with an enthalpy change of 55.8 kJ/mol water. In aqueous solutions, the relative concentration of the two ions need not be equal, i.e. the solution may be acidic or alkaline. When the concentration of one ion is greater in the solution, the concentration of the other decreases and can be described by the following relationship:

$$[H^+] [OH^-] = 1 \times 10^{-14} (\text{mol/L})^2 \quad (3.4)$$

This is known as the ionic product of water, K_w and shows that it is always equal to 1×10^{-14} $(\text{mol/L})^2$ By using this relationship and by measuring the pH, the level of OH^- ions present at any time in the reaction mixture can be monitored. This is described in more detail in chapter 4.

3.7 Ion measurements

Inductively coupled plasma mass spectrometry (ICP-MS) is a type of mass spectrometry which is capable of detecting metals and several non-metals at concentrations at very low concentrations. First, the sample (here; various water) needs to be ionised with the inductively coupled plasma and then the mass spectrometer is used to separate and quantify those formed ions. Varian 820-MS was used for the different water analysis during this research work. It was employed to identify ions in different tap waters as, in particular, South East England and London, is regarded as "hard water" with a concentration of calcium carbonate, above 200 mg/l [129].

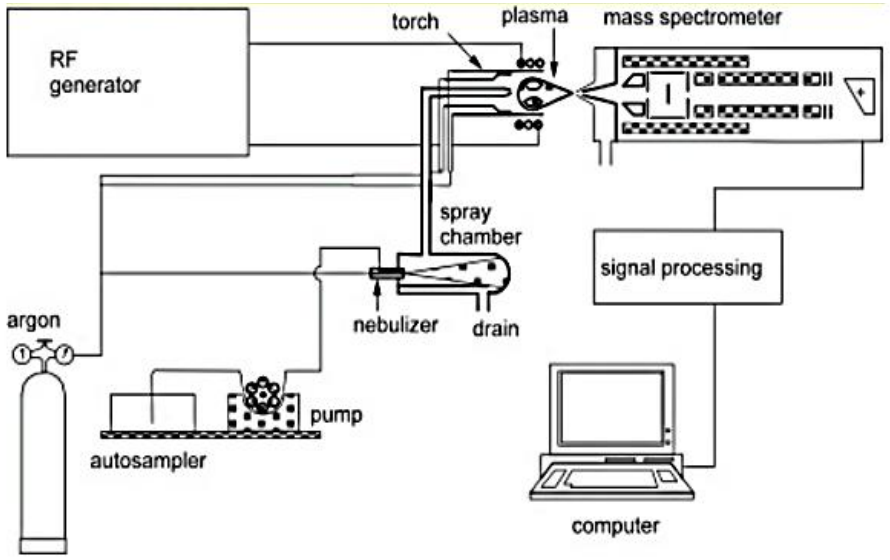

Figure 3-6: Working principle of inductively coupled plasma mass spectrometry [130]**.**

The ICP-MS instrument can be described by following components: torch, power supply and load coil, sample introduction system, a mass spectrometer and detection system. The *inductively coupled plasma* is plasma that is energized (ionised) by inductively heating the gas with an electromagnetic coil (RF coil). The plasma is sustained in an "ICP torch" that consists of three concentric tubes. The apparatus works using an inert argon gas, which carries the sample in vapour form, which flows inside the concentric channels, between the two outermost tubes of the ICP torch. When a spark is applied to the argon flowing through the ICP torch, electrons are stripped off of the argon atoms, forming argon ions. The sample to

analyse is typically introduced into this ICP plasma as an aerosol (for example by a nebuliser).

Once the sample aerosol is introduced into the ICP torch, the elements in the aerosol are converted first into gaseous atoms and then ionised towards the end of the plasma. When the elements in the sample are converted fully into ions, they are then brought into (nickel CRI cones) and separated based on their mass to charge ratio. After this, they are transported towards detector ETP AF250 Discrete Dynode Electron Multiplier (DDEM) detects the ions and sends signals to the recorder on that information [130]**.** This analysis was carried out at LSBU in the Applied Science Department.

3.8 Gas chromatography

The analysis of the hydrogen gas was an important feature of this research work in order to determine its quality. A high purity hydrogen gas (99.99 %) is desired for an optimal functioning fuel cell. Therefore, the hydrogen gas formed during the reaction was collected and examined by the gas chromatography (GC). Gas chromatography is one of the most efficient methods for gas analysis. It can separate and identify a variety of different gases providing both quantitative and qualitative information.

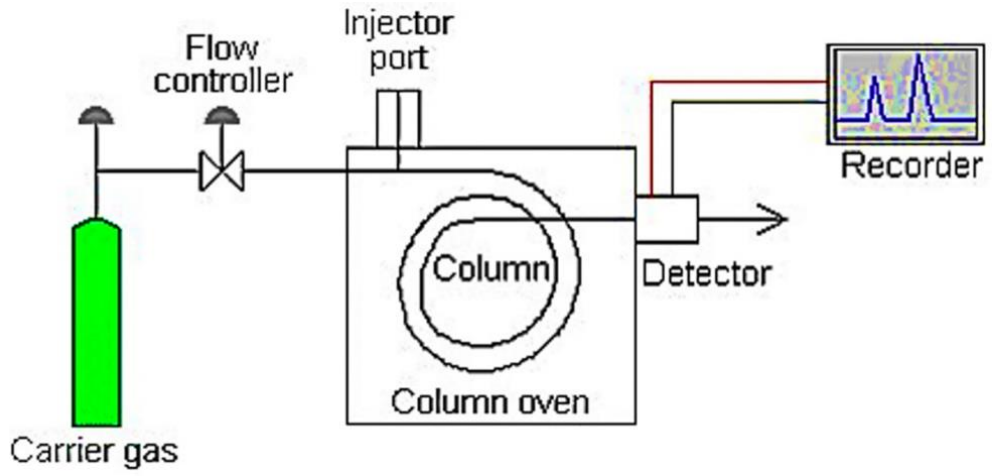

Figure 3-7: Working principle of Gas Chromatography [131].

The working principle of a GC can be seen in Figure 3-7. Gas samples are injected into the GC instrument via an injection port and are heated to temperatures of 250 °C inside the GC oven.

Owing to various thermal conductivities, different gases expand at different rates and are then transported towards the thermal conductivity detector, (TCD) detector. The thermal conductivity detector uses heating coils and two tubes running parallel to each other. Through one tube, a pure carrier gas (usually Helium) is passed and the other tube is used to pass the analyte of interest mixed with the carrier gas. The coils in each tube are heated by passing current through them and when a gas with high conductivity, e.g. He or H_2 is passed through it, it takes heat away from it, thus lowering the temperature of the coil. The resistance of the wire is temperature dependent and goes down as the temperature is lowered. As the carrier gas such as He is highly conducting, it will lower the resistance of the wire in the reference tube. When mixed with an analyte, the thermal conductivity of the mixed gas will usually be lowered and the coil temperature and resistance will rise. A TCD will sense the change in the resistance of coils in the column with effluent and will compare it to a reference flow of carrier gas [131]**.** The result of a GC experiment is a gas chromatogram which is a plot of peaks against time. The time is related to the how long a substance takes to pass through the column. This retention time, R_T for any substance can be compared with a standard reference data to help identify it. The height of the peaks represents the concentration of the species.

The gas analysis in this research work was carried out using a gas chromatograph (TRACE 1310 Gas Chromatograph, Thermo Scientific) equipped with a TCD (Instant Connect Thermal Conductivity Detector, Thermo Scientific™) for specimen analysis and a column (Trace plot TG-Bond M sieve 5A) of approximate dimensions: 30 m x 0.53 mm x 50 µm for separation. The 5A molecular sieve for the column was chosen to provide good separation of light gas peaks and well-defined peaks. For example, the Trace Plot column is designed to deactivate CO peak tails, making their detection clearer, if present. For manual injection of the gas, a dedicated GC syringe (10 µl, Hamilton™ 700 tight syringes) was used. 9 µl, Gas samples are injected into the GC where the injection port temperature was set

at 250 ºC and the thermal conducting detector at 200 ºC. The oven temperature where the column was located was kept constant at 32 ºC and 35 ºC on different occasions for 10 min for calibration purposes and later at 35 ºC for the same amount of time for most of the gas analysis. Argon gas was initially employed as a carrier gas for calibration. Nevertheless, it had some errors associated with retention times of the gases including for certain unknown reason, hydrogen was not detected and argon peaks were visible. Therefore, to eliminate any additional errors Helium gas was employed as a carrier gas and different high purity gas samples (used as standards) were used for calibration of the GC instrument. Each gas was injected at least 3 times to establish the protocol as listed in Table 3-2. The calibration sheets from Fisher Scientific were also consulted.

The retention times of gases eluting from the column at 25 °C and at 35 °C were recorded. Three different types of standards were prepared for the hydrogen gas. One using the BOC gas and other two were prepared from the reaction of aluminium with HCl and NaOH as shown in the equations below. However, the oven for these two standards was set to 35 °C.

$$Al + NaOH + H_2O \rightarrow NaAlO_2 + 1.5H_2 \quad (3.5)$$

$$2Al + 6HCl \rightarrow 2AlCl_3 + 3H_2 \quad (3.6)$$

Table 3-2: Gases used for creating standards.

Gases	Purity	Supplier
Hydrogen (H_2)	analytical grade	BOC
Nitrogen (N_2)	analytical grade	BOC
Oxygen (O_2)	analytical grade	BOC
Carbon Dioxide (CO_2)	analytical grade	BOC
Argon (Ar)	analytical grade	BOC

Gases obtained from BOC and from HCl and NaOH were injected into the GC using a gas-tight syringe. The data collected was sent to the PC equipped with the software (Chromeleon™ 7.2) for analysis and stored. Afterwards, the gas to be

analysed from different H_2 generation reactions was collected after an hour of reaction in a sealed gas syringe that had been purged with argon and injected into GC. The results of the measurement will be reported in chapter 4 of this thesis and discussed therein. The possible impurity gases to find in the hydrogen generation reactions were assumed to be the atmospheric gases found in the air, i.e. Oxygen, carbon dioxide, carbon monoxide, nitrogen, helium or argon might be present in the results.

3.9 Aqueous solution preparation

Part of this research was to investigate different types of water and their effect on the hydrogen generation. The first types of water investigated were readily available clean water such as deionised water and tap water. Tap water was selected because an on-demand hydrogen generation for power fuel cell is more likely to use this type of water rather than costlier deionised water. Furthermore, testing various types of water would help to observe the effect of dissolved ions and if they have any effect on hydrogen generation.

Subsequently, different pH variations of water were tested which was executed by using various concentrations of HCl for the acidic solution and NaOH for the alkaline solutions. Finally, more complex molecules found in the typical wastewater were tested, such as ethanol, ethylene glycol, sucrose and urea. Below is a list of the chemicals and waters used for the aqueous solution study. To obtain pH values below the natural value of 7, hydrochloric acid was dissolved in deionised water until reaching a pH of 3 and 5. For pH values above 7, sodium hydroxide was dissolved in deionised water until pH of 9 and 11 was reached. Please note all the concentrations stated below were prepared in 1000 ml of deionised water.

- Ethanol (C_2H_6O, M_w = 46.06 g/mol) concentrations were prepared by mixing 99.5 % pure ethanol with deionised water to 12.5 g (0.27 M), 18.9 g (0.41 M), 25.0 g (0.54 M) and 31.32 g (0.68 M).

- Different concentrations of sucrose ($C_{12}H_{22}O_{11}$, M_w = 342.3 g/mol) solutions were made by dissolving sucrose in deionised water to 3.1 g (0.009 M), 5 g (0.0145 M) and 7.5 g (0.021 M).

- Anti-freeze is a good example of surplus water that may be used for an on-demand hydrogen generation. The main component in antifreeze is ethylene glycol in the commercial product. Therefore, different concentrations of ethylene glycol were prepared and compared with a bought anti-freeze product. Ethylene glycol ($C_2H_6O_2$, M_w = 62.07 g/mol) powder was mixed with deionised water to make the different concentrations of 13.1 g (0.21 M), 31.7 g (0.51 M) and 47.8 g (0.77 M).

- For the urea solution, the ingredients usually found in the human urine were prepared using the recipe reported by Putnam [132]. Urea (CH_4N_2O, M_w = 60.05 g/mol) powder was mixed with deionised water to make solutions of concentrations 0.66 g (0.101 M), 0.9 g (0.15 M) and 3.5 g (0.05 M). As the concentration was increased, the salts weight percentage, i.e. NaCl and KCl wt % were also increased and were dissolved in the urea solution to represent the actual levels of human urine. Once the mixing had finished the beaker in which the solutions were kept were tightly sealed and stored in an inert atmosphere at 17 °C to avoid any oxidation and ammonia formation.

3.10 Hydrogen yield

The reaction setup was adequate for measuring the efficiency of hydrogen gas generation at a small and medium scale, however, due to a size of the glass reactor vessel and taking health and safety into consideration. It was decided that only 0.3 g activated aluminium powder would be used for each experiment in 9 ml of water.

For the hydrogen yield calculation, it was then assumed that only the metal aluminium was taking part of the hydrogen production and none of the milling additives. It was further assumed that in these temperature regimes used here following stoichiometric reaction is the most dominating.

$$Al + 3H_2O \rightarrow Al(OH)_3 + 1.5\ H_2 \qquad (3.7)$$

Equation 3.7, shows that for every mole of Al reacted 1.5 times more moles of H_2 is produced. Based on this information hydrogen yield from 0.3 g of activated aluminium can be calculated. It has to be reminded again that activated aluminium contains only 65 % of the Al. Therefore, 0.65 * 0.3 g = 0.195 g Al. In 0.3 g of activated aluminium, only 0.195 g is pure Al, which corresponds to 0.195 g / (26.981 g/mole) = 0.007 moles Al. If a 100 % hydrogen yield is achieved it would, therefore, correspond to 1.5 * 0.007227 = 0.010 moles of produced H_2.

To estimate the volume of 0.010 moles of hydrogen, the Ideal Gas Law [133] can be used as hydrogen is a small molecule and the gas is in ambient conditions.

$$\text{Ideal Gas Law:} \quad PV = nRT \tag{3.8}$$

Where P (bar) is the pressure of the gas, V (ml) is the volume of the gas, n is the amount in moles, R (83.14 $cm^3 K^{-1}$) is the universal, gas constant and T is the absolute temperature of the gas.

The volume can then be calculated as

Assuming temperature of water at 20 °C = 293.15 K, 1 atm pressure and R constant = 83.14 cm^3/K

$$V = \frac{0.010840 * 293.15 \text{ x } 83.14}{1} = \quad 264 \text{ cm}^3 \text{ (ml) of hydrogen gas.}$$

Majority of the reactions produced the most of hydrogen gas possible within 3 hrs (10000 sec). Since only 0.3 g of activated aluminium was used the total hydrogen possible was 264 ml~260 ml (depending on temperature) as shown above. A few reactions data were terminated just under 17 min (1000 sec) as a large part of the initial reaction kinetics majority takes place within this timescale and could be compared with similar to published data [67,104].

3.11 Volume of water

Based on to the stoichiometry, it was calculated that 9 ml of water which was used for each experiment are adequate for producing at least 5 litres of hydrogen gas. Nevertheless, only a maximum of 260 ml of gas was expected based on the yield calculations shown above. This extra volume of water would provide a cooling effect and avoid any temperature surge during the exothermic reaction.

3.12 Chapter 3 Summary

The experimental set-up is described including all the components used in the ball milling, GFM, XRD, SEM, ICP and GC and their basic principles are also defined. All the chemicals and solvents used are also labelled and their respective preparation techniques are given. It was concluded that milling protocols would be used for milling and milling will be performed at 260 rpm and 520 rpm for a maximum of 3 hrs using 3 g of the powder mixture in which 65 wt % was pure aluminium, 25 wt % was metal oxides and 10 wt % was salt. For reactions, only 9 ml of water was used with 0.3 g of activated aluminium.

Chapter 4 Results and discussion

This chapter is divided into three segments. At first, this chapter covers metal particle synthesis using different additives including metal oxides (MO) and salts and their respective hydrogen generation using deionised water at 25 ºC and stirring speed of 700 rpm (section A). The second segment reviews the impact of various aqueous solutions such as different water types, various dissolved molecules and ions with a focus to represent typical industrial wastewater (section B). The third and the final section (section C) briefly provide an economic evaluation of the hydrogen generation. It has been suggested that the necessary reactive milling (by high-speed ball mill) should be performed at either at high speeds (rpm) for a short period or for an extended period at reasonable speeds to produce good aluminium particles that it may be used to generate hydrogen with high yields and fast reaction rates.

It was noted in the literature [18,26,41,45,54,66,80,134-136] that authors of these publications have suggested milling procedures are often associated with an unfavourably high energy investment, see literature review section for more details. Therefore, as mentioned before, the focus of this research was to establish an optimised particle processing scheme which would aim to reduce the overall energy investment and at the same time achieve a high-quality synthesis of the Al metal particles that can be used to generate high hydrogen yield in a reasonable reaction time span. Reduced energy investment will further result in a greener process and be more cost-effective making this technology more attractive for commercial interest. In the next section, particle synthesis is discussed. Aluminium powder was synthesised using ball milling machine with salt and metal oxide additives. Different milling parameters were tested in order to measure the effect that it has on synthesised particles and these are discussed below in sections.

A) Particle synthesis
B) The effect upon hydrogen generation due to the varied solutions
C) Economical evaluation of the research

4.1 Section A Particle synthesis

As received recycled aluminium particles and after sieving, 40 µm, 75 µm and 105 µm were blended with metal oxides and the salt additive for conducting a variety of different studies, see chapter 3 for more details.

4.1.1 Effect of milling time and speed

An investigation was conducted to improve the understanding of the effect of varying the milling speed and length (time). Different reactions and particle process parameters were explored. Here for this study, only Al 40 µm sized particles were employed because they will provide a better reaction due to their larger surface area. Samples were milled at 260 rpm or 520 rpm, for durations of 1.1, 1.77 or 2.4 hrs and then reacted with deionised water.

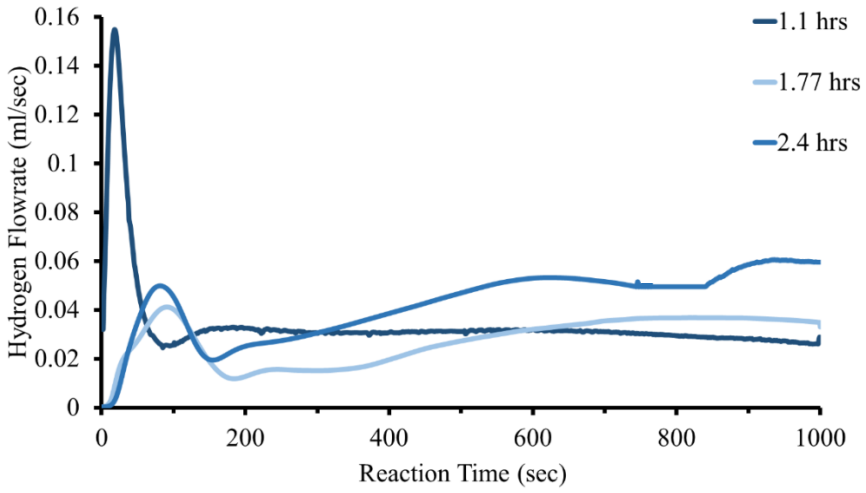

Figure 4-1: Hydrogen flow rate over reaction time using aluminium based powder milled at 260 rpm for 1.1, 1.77, 2.4 hrs.

Comparing the hydrogen flow rate in Figure 4-1 and Figure 4-2 (observe different y-axis scale), a significant difference can be seen between hydrogen production when using the two different milling speeds. Using a speed of 260 rpm appears to result in a favourable process that shows hydrogen generation is still ongoing and even increasing in some cases after 1000 sec. Whereas, In Figure 4-2 for the 520 rpm, the generation rate shows a rapid decline with only 0.005 ml/sec after 600 sec reaction time. It was established that the different milling times were also seen to affect hydrogen flow rate regardless of the speed, however, the change was

negligible when using 520 rpm. The in-depth analysis of this occurrence will be discussed later.

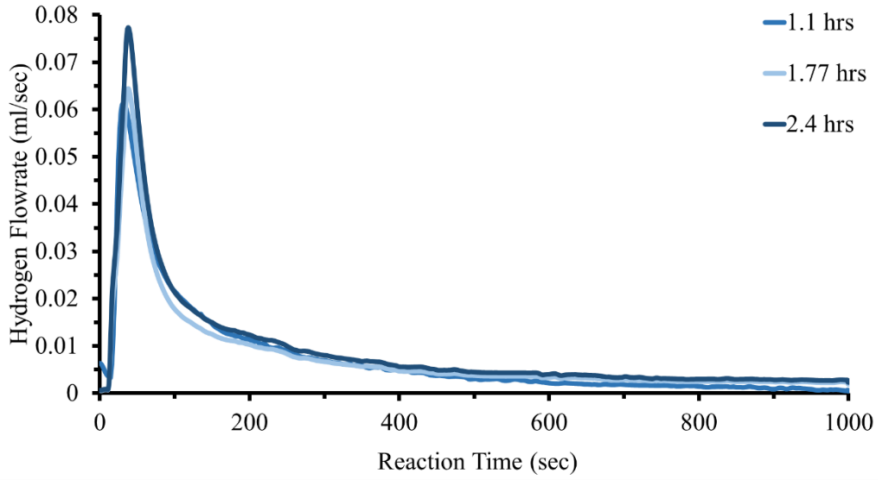

Figure 4-2: Hydrogen flow rate over reaction time using aluminium based powder milled at 520 rpm for 1.1, 1.77, 2.4 hrs.

Aluminium reacts with water in an exothermic reaction to produce hydrogen as shown in the equation below.

$$2Al + 6H_2O \rightarrow 2Al(OH)_3 + 3H_2 \qquad \Delta H_r = -280 \text{ kJ/mol} \qquad (4.1)$$

Therefore, to understand the reaction kinetics it is essential that its temperature should always be taken into account. Figure 4-3, shows reaction temperatures, while in Figure 4-4 hydrogen production results of both sets of milling speeds can be compared. All experiments started at 25 ºC and ambient condition in this study. One can see in Figure 4-4, from the powder prepared from 260 rpm, when it was reacted with deionised water hydrogen generation occurs progressively across the whole 1000 sec and was still ongoing at 10000 sec regardless of milling durations. The hydrolysis reaction is exothermic, therefore, production volumes can be linked with the reaction temperatures as observed in Figure 4-3. The volume of the H_2 (at 1 atm) for 260 rpm were; 220 ml, 170 ml and 230 ml for the 1.1, 1.77 and 2.4 hrs, respectively. Corresponding to 85 %, 65 % and 88 % hydrogen yield, respectively.

Results for 520 rpm showed no progressive hydrogen generation and after 1000 sec (only ~13 ml H_2 was generated), meaning that after 10000 sec no further H_2 would be produced. As with the results for 260 rpm, the 520 rpm reaction can be analysed with respect to reaction mass temperature change. Unlike for the 260 rpm, there is no significant increase in the temperature after 1000 sec (all three milled samples at 520 rpm only rose from 25 ºC to ~ 31 ºC). The reason for this will be explained further, and discussed together with scanning electron microscope images, later in this chapter.

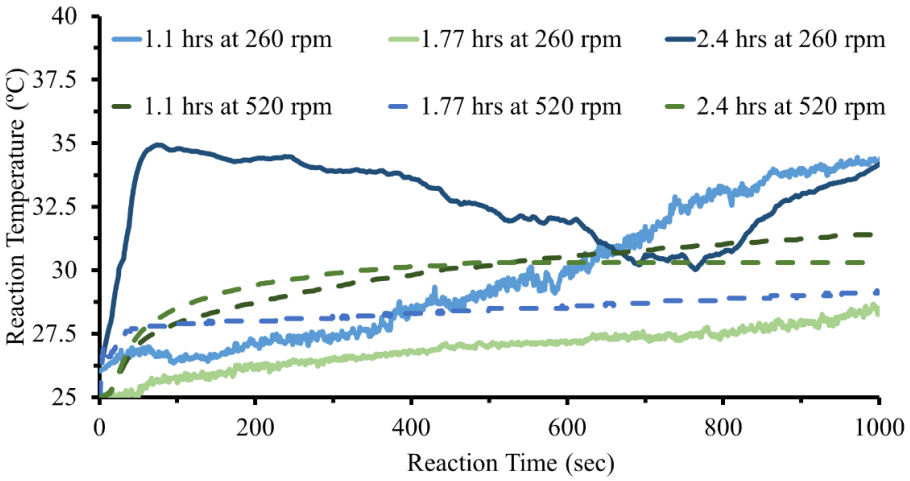

Figure 4-3: Exothermic reaction temperature plot over reaction time using aluminium based powder milled at 520 rpm and 260 rpm for 1.1, 1.77, 2.4 hrs.

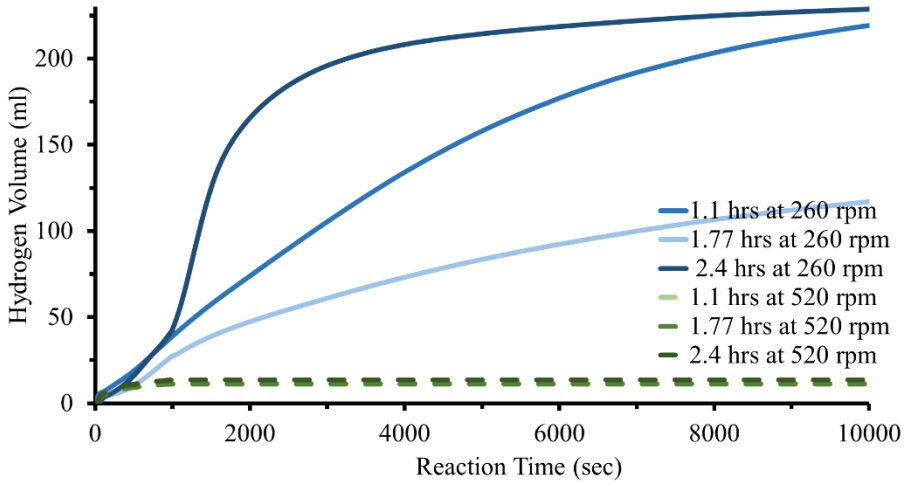

Figure 4-4: Volume of generated hydrogen over reaction time for the two milling speeds over different milling times. Hydrogen volume is normalised to the mass of aluminium in the particle used as (ml/g Al).

It was noted that for 1.1 and 2.4 hrs milling using the lower speed showed better hydrogen generation than when 1.77 hrs milling was used. The test was repeated several times, but no further explanation of this deviation was established. However, in the 1.77 hrs test, it is possible different particle deformations are created. Effect of milling on the particles will be discussed further later in the thesis.

4.1.2 Comparison of different milling programmes

In this study, three milling programmes were compared for their effects on aluminium particles and hydrogen production. Similar to previous study all the compositions of the additives (Al 65 wt %, MO 25 wt %, Salt 10 wt %) including particle aluminium particles size, i.e. 40 µm were kept constant. Milling programmes include:

- Milling Programme 1a (30 sec intermediate break time) with a milling speed of 260 rpm.
- Milling Programme 1b (30 sec intermediate break time) with a milling speed of 520 rpm
- Milling Programme 2 (5 sec intermediate break time) with a milling speed of 260.

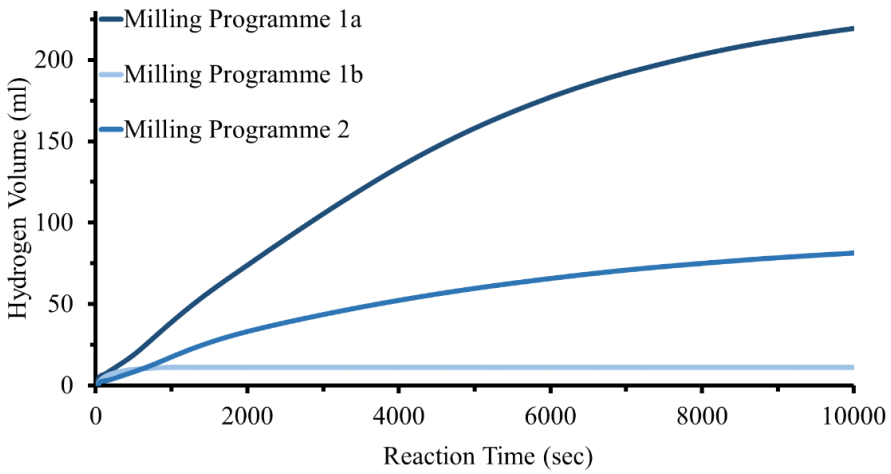

Figure 4-5: Comparison of the hydrogen generation effect when using different break-time and speed used in different milling programmes.

As seen in Figure 4-5, there is a striking difference in hydrogen production between the three different Milling Programmes. Milling Programme 2 produces far less hydrogen (total of 80 ml H_2, yield of 30 %) after 10000 sec compared with Milling Programme 1a (220 ml H_2, yield 85 %). However, Milling Programme1b produced the lowest volume with only 13 ml H_2 (H_2 yield of 5 %).

Two reasons can be highlighted to explain the difference in the yield produced by these three milling programmes. One reason is that due to intensive energy investment the particles have been milled to a degree making the aluminium particle defective. The last reason can be said to be related to an insufficient break in the milling, due to the metallic characteristics. During high-speed milling method, a significant amount of kinetic energy is introduced into the milling jar. Therefore, a significant heat is built up inside the milling jar. The extent of the break time allows the particles to cool down from the heat generated during the milling. The heat generated in the milling jar is a direct result of the collision of the balls both between themselves, colliding with the wall of the milling jar, and friction between additives and the aluminium particles may also contribute towards generating additional heat. The heat built up in the milling jar will be dissipated during the milling breaks and then heat will be built up again during next milling segment. The continuous expanding and shrinking mechanism results in elastic and plastic deformations, causing stress to the aluminium metal.

This deformation can explain the differences in the hydrogen generation. Most researchers expose their aluminium synthesised powders to very high temperatures of excess 300 °C after milling [73,104,137] to change the characteristics of their prepared powder [41,138]. However, it was not practised during this research to keep the synthesis process cost-effective and environmentally friendly. It is important here to highlight the fact that the ball milling machine used in this research has a cooling fan installed in the milling chamber outside the jar and helped to cool the milling jar. The total milling time for Milling Programme 1a and 1b was in 1 hr 40 min (100 min). Due to the difference in break-time, the cumulative milling time for Milling Programme 1a and 1b was 1.1 hrs and 1.7 hrs for Milling

Programme 2. Thus, the milling machine was stationary for 34 min for Milling Programme 1a and 1b and only 8 min for Programme 2.

This means that the total energy consumption using Milling Programme 1b is greater than using Milling Programme 1a and Milling Programme 2, indicating that it had the highest processing cost. In addition, aluminium powder produced from it failed to produce optimal hydrogen gas yield.

4.1.3 Effect of additives on milling

The effect of adding additives to the metal powder during milling was investigated to observe its influence on the particle synthesis and overall hydrogen production. Milling aluminium metal powder without any additives results in large agglomerates (collect or form a mass or group) as shown in Figure 4-6. When aluminium was placed in water with an additive such as metal oxide and salt, no reaction was observed to give off hydrogen whether aluminium was milled or non-milled. Likewise, when the non-milled Al sample (as-received) with no additives was introduced to water, it did not produce any hydrogen either at room temperature. From the literature review presented in chapter 2, it was concluded that additives including metal oxides and salts would be beneficial for breaking down barrier layers on Al particles. These additives will also help in changing the morphology of the particles during the milling.

Figure 4-6: Particle size change with milling with and without additives. From right to left: aluminium powder non-milled, milled no-additives aluminium and aluminium powder milled with additives (metal oxide and salt).

4.1.3.1 Metal oxides additives

Aluminium alone can theoretically react with water to produce H_2, but, this reaction is hard to drive in pure water at ambient conditions for reasons that have been mentioned previously. Adding additives can help to overcome this obstacle and an in-depth investigation of them is, therefore, required. This is due to the protective layer formed on the metal surface; Al_2O_3 and then the $Al(OH)_3$ after that when in contact with water.

Activated aluminium used in this work contained 25 wt % metal oxide (MO) and 10 wt % salt. Chen *et al.* 2010, used the same composition. They investigate different additive ratios and found using a composition of (Al 65 wt %, MO 25 wt %, Salt 10 wt %) the highest H_2 yield. However, they applied external heat [93,104] to increase the starting reaction temperature to drive the reaction but failed to justify the reasons as to of why this ratio worked best [80,140].

As with investigations on milling time, speed and break intervals in the previous segments, this study provided background to decide the most suitable metal oxides and salts to use in later millings. Inspiration was taken from Chen *et al.* 2012, and it was decided that the weight percentage of the component would be 10 wt % for salt and 25 wt % for metal oxides component. The selected metal oxides for this the study were Barium oxide (BaO), Calcium oxide (CaO) and Copper oxide (CuO), milled with Salt (NaCl) as shown in Table 4-1. The powders were milled using Milling Programme 1b (520 rpm mill speed for 1.1 hrs and 2.4 hrs, as was described in Chapter 3). A 0.3 g milled powder was used together with 9 ml deionised water with starting temperature of 25 °C.

Table 4-1: Powder composition with different metal oxide additives.

Powder composition (wt %)
Al 65 %, BaO 25 %, Salt 10 %
Al 65 %, CaO 25 %, Salt 10 %
Al 65 %, CuO 25 %, Salt 10 %

In Figure 4-7a and b, it can be seen when using BaO, the hydrogen gas was produced instantly and generated a total of 12 ml H_2 in 1000 sec (corresponding to only 4 % H_2 yield). Whereas, for CaO and CuO, diminishes after 600 and 400 sec for, respectively. Overall, BaO additive appeared more reactive and extended the reaction time when compared to than the other metal oxides. After the reaction, the sample mixture was re-milled for 2.4 hrs using the programme 1b protocol and the test was performed again, the result of which is shown in Figure 4-8. Once again BaO showed a more favourable reaction compared with CaO and CuO. Also after 1000 sec 17 ml, H_2 was produced after the 2.4 hrs milling compared with 12 ml for the 1.1 hrs, showing that milling time does affect the hydrogen generation positively when BaO was used. However, for the CaO and CuO, no improvement was recorded despite several repeats of the experiments.

However, one should be cautious as the 1.3 hrs extra milling would require far more energy input compared with the small gain (of a few millilitres) in the liberated hydrogen and is thus not very useful. The improved hydrogen generation when using BaO as the metal oxide additive can be explained by understanding the reaction mechanism between BaO and water. When BaO is mixed with water, it reacts and forms barium hydroxide $Ba(OH)_2$ as:

$$BaO + H_2O \rightarrow Ba(OH)_2 \quad (4.2)$$

The formed $Ba(OH)_2$ is dissociated in water into Ba^{2+} ions and OH^- ions and therefore, an increase in pH occurs.

$$Ba(OH)_2 \rightarrow Ba^{2+} + 2OH^- \quad (4.3)$$

As already stated, when the reactive Al metal is exposed to air and water, a layer of Al_2O_3 is formed which is highly hydrophilic and form a hydroxyl surface layer, Al_2O_3–OH as;

$$Al_2O_3 + H_2O \rightarrow Al_2O_3\text{–}OH \quad (4.4)$$

The increased pH formed by the dissociated $Ba(OH)_2$ may promote the dissociation of the $Al(OH)_3$ layer and therefore, increase the possibility of water diffusion to reach the metal Al surface and as a result, more hydrogen can be produced [19]. In the above studies, the salt fraction in the particle composition was kept constant for the three batches. Different metal oxides used displayed a huge variation in the

reaction rate. Despite not having a very high yield after 1000 sec, the rate of reaction reflects the reactivity of the particle composition. Regardless of Milling Programme and time used, BaO always showed the highest reactivity, which was explained by its ability to increase pH in the water solution. While BaO showed high reactivity, this metal oxide was not pursued because of its relatively high price which is deviating from the aim of the research.

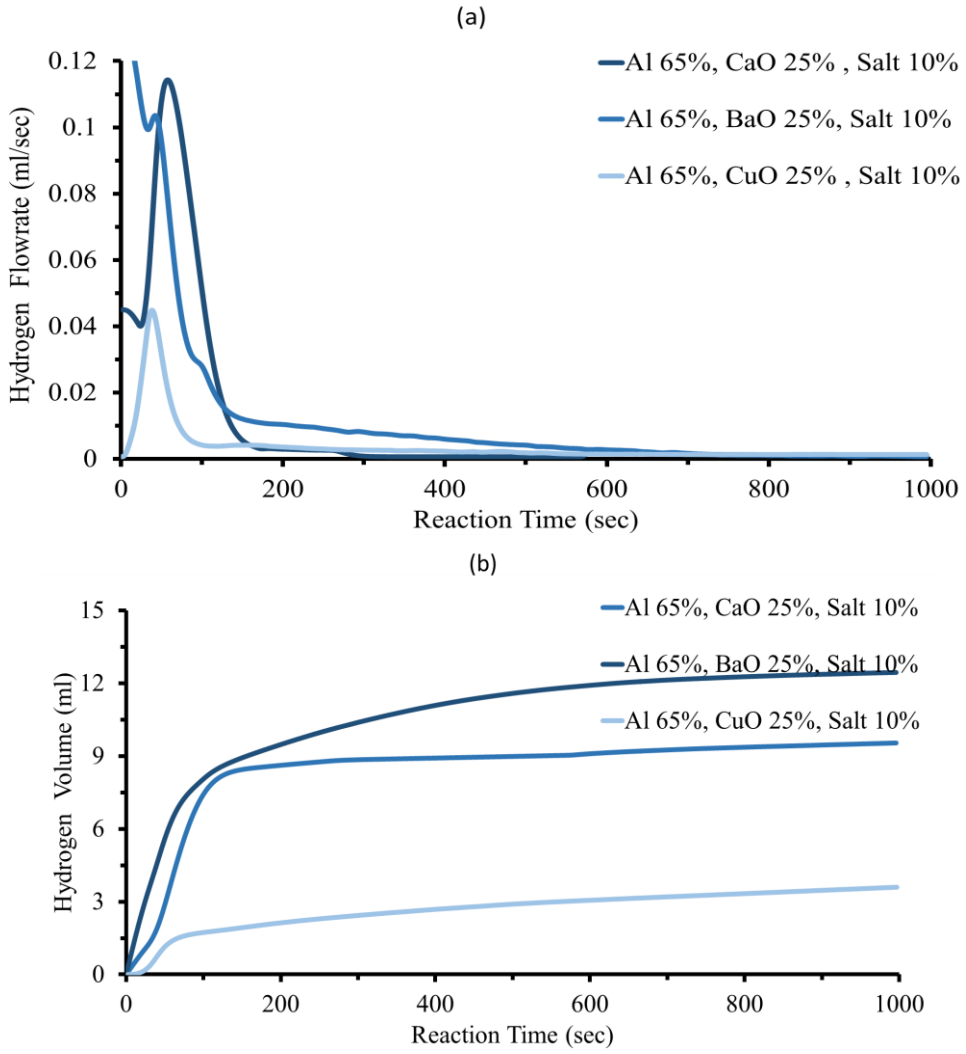

Figure 4-7: Effect of metal oxide additives seen; a) hydrogen flow rate b) accumulated a volume of hydrogen for powers milled 520 rpm/ 1.1 hrs.

A comparison of the metal oxide cost/kg can be made from a price estimation acquired from Fisher Chemicals [141] and is as follows: BaO = £ 345/kg, CaO = £ 77/kg and CuO = £ 179/kg. As stated many times before, it is important that the hydrogen economics is kept commercially attractive. Therefore, selection

of the raw materials was given extra attention. As mentioned already, the cost of BaO per kilogram is much more than the cost of Cao and CuO per kg combined, which was a major factor to consider the other metal oxides. Furthermore, from the safety point of view, both CaO and CuO are much less toxic than BaO. Moreover, CaO can be produced from recycling eggshells and other cheap methods and therefore, is economically beneficial.

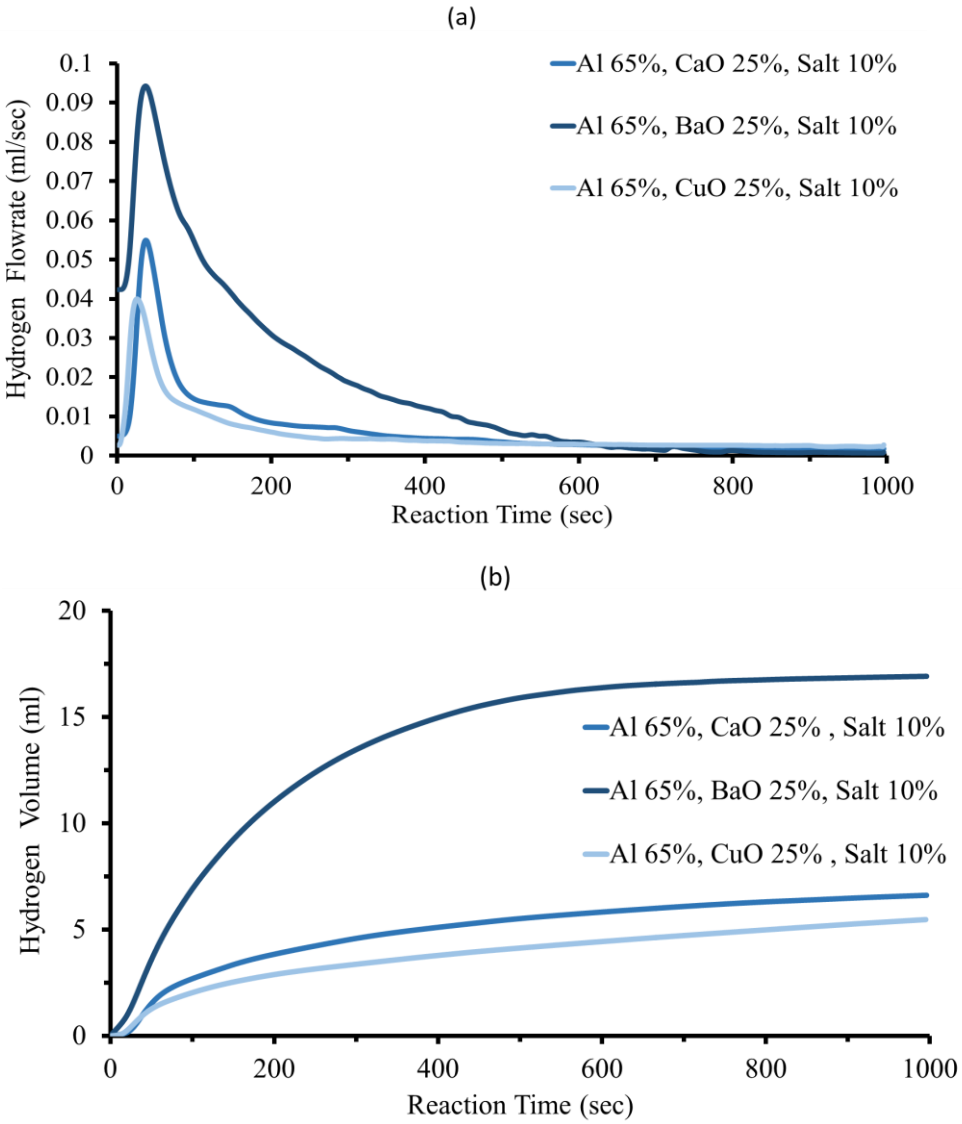

Figure 4-8: Effect of metal oxide additives seen; a) hydrogen flow rate b) accumulated a volume of hydrogen for powers milled 520 rpm/ 2.4 hrs.

To further analyse the role of the metal oxide additives in the overall reaction, an experiment was performed combining the above metal oxide additives. To focus on the line of the subsequent research, only the CaO and CuO are described below. It

was decided that CaO-CuO would be milled together with 50-50 ratio, but the total weight % was kept to 25 % of the total particle composition. Once prepared it was compared with the powders which only contained a single metal oxide, i.e. CaO and CuO. For this study, all the powders were milled using Milling Programme 1b (using 520 rpm). As stated above that, this segment is providing background to explain the reasoning for the selection of additives, additionally, any effect caused by the additives would be the same under different milling programmes. From Figure 4-9, it can be seen that when the two metal oxides, i.e. CaO and CuO are combined in a 50-50 ratio, there was more of an immediate, albeit slower rise in the generation of H_2 whereas there is a delay in production of H_2 when CaO and CuO are used separately in the mixture. CuO was also observed to produce less volume of hydrogen.

For the combined metal oxides, a total of 11 ml hydrogen was produced after 1000 sec which is comparable to the previous use of BaO additive, seen in Figure 4-7a, demonstrating that a combined metal oxide additive of two cheaper alternatives can be investigated further for an improved hydrogen economics. The same experiment of the metal oxide effect of combining the metal oxide was conducted using longer milling time of 2.4 hrs. In Figure 4-10, the combined metal oxides produced 13 ml hydrogen after 1000 sec while the CaO and CuO produced only 6 ml and 5 ml, respectively. In addition, it was noted that the high reaction rate seen previously for the CaO sample when it was milled for 1.1 hrs had also been affected, with it, resulting in an inferior hydrogen reaction. Although numerous research has been conducted using CaO as a milling additive with aluminium particles [13,80,142], it has its drawbacks for generating H_2 as these powders are aimed at portable fuel cell devices, the rapid exothermic reaction would increase the reactor vessel temperature towards water evaporation point. Water reacts with CaO strongly exothermically, see equations 4.6 below, which will add heat to the water-aluminium exothermic reaction.

For practical reasons, this water evaporation risk should be avoided as it could lead to damaging the on-demand fuel cell. The presence of water vapour inside the fuel cell causes the voltage to drop decreasing active surface exchange between the

gases resulting in current density which in result causes the temperature to increase leading to damage of membrane [143].

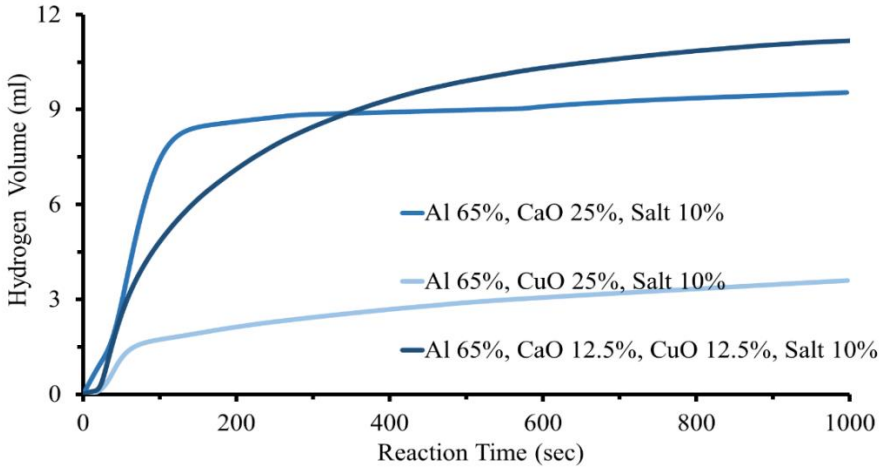

Figure 4-9: Hydrogen generation when combining metal oxide additives in the particle process compared with each metal oxide separately when milled using Milling Programme 1a for 1.1 hrs.

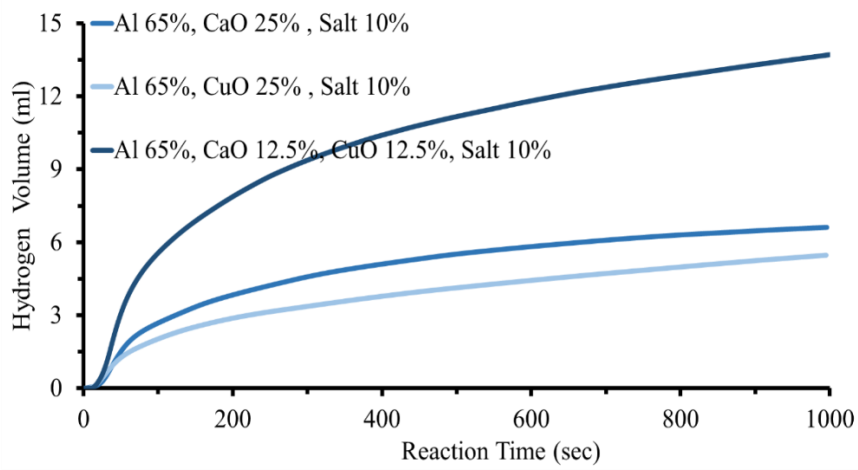

Figure 4-10: The hydrogen generation effect when combining metal oxide additives in the particle process compared with each metal oxide separately when milled using Milling Programme 1a for 2.4 hrs.

Additionally, the increased temperature inside the reactor would promote the production of an $Al(OH)_3$ with different morphology, which slows down the hydrogen reaction [109]. Also, CaO addition may lead to raised pH levels that could be corrosive to the metal piping and reactor vessel. To provide more control of the rapid reaction kinetics and its consequences, CuO was used together with CaO in the milling process. By using these two metal oxides, a new reaction occurs which

helps with the objective of keeping a controlled fuel-cell. One plausible explanation as to why this helps could be that when milling CaO and CuO together with the salt and Al in a high-speed oxygen free reactive milling procedure, there will be sufficient kinetic energy input to reduce the metal oxides to metal such as:

$$Cu^{+2} + 2Al \rightarrow Cu + Al_2O_3 \quad (4.5)$$

For verification of possible reduction of Cu(II) in an oxygen-free milling jar, only aluminium and CuO were milled, however, for an extended milling time of 20 hrs to improve the sensitivity of the analytical results. The milled sample was then analysed by XRD as shown in Figure 4-11, XRD was used to study the effect of the prolonged milling in aluminium lattice and orientation of crystallites.

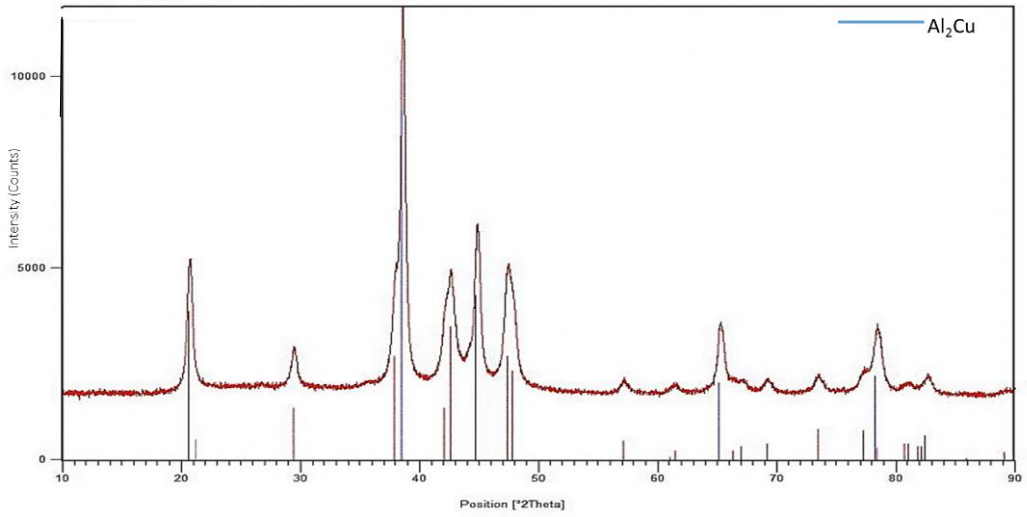

Figure 4-11: XRD results of prolonged milling of CuO and Al powder in the oxygen-free environment.

From the below XRD plot, it can be seen that sample produced peaks at different intensities and from all the peaks, the one at 37 ° indicates the formation of Al_2Cu. Furthermore, on the XRD analysis, there is no detectable metal Cu peak was observed. This alloy formation reaction was triggered by the mechanical energy during high-intensity milling. CuO reacted with Al and formed the alloy Al_2Cu. During the milling process, the powders are subjected to intense forces inside the milling jar in an inert atmosphere. The collision and fractures due to the collision of the metallic balls produce a substantial amount of heat. If the metal oxides, i.e. CuO is subjected to prolonged milling, it can result in reacting with aluminium

while being milled. XRD result provides support to that claim and Al_2Cu was formed. Cu will be in in the metallic state, not an ionic state like in CuO.

It cannot be verified that if any possible metal formations from milling could be taking part of a galvanic reaction while the milling salts are dissolved in water. Such galvanic reaction would most likely add to some kind of pitting corrosion of the Al_2O_3 layer.

4.1.3.1.1 Metal oxide ratio

To further explore the increased hydrogen yield when using combined metal oxide additives, different ratios of the metal oxides were tested. The hydrogen flow rate produced for samples with CuO: CaO ratio corresponding to 65 wt %: 35 wt % (sample 65-35) was compared to 50 wt % Cu and 50 wt % Ca (sample 50-50), as seen in Figure 4-12. Sample 50-50 displayed a higher flow rate than sample 65-35. This was sometimes almost twice as high, e.g. at 1000 sec, there is a rate of 0.04 ml/s for sample 50-50 versus 0.02 ml/s for sample 65-35.

The difference in volumes and flow rates between them can also be seen in Figure -4-12, where generated hydrogen volume on the right-hand y-axis, where the sample 50-50 produced 220 ml (85 % H_2 yield) after 10000 sec compared with 140 ml (53 % H_2 yield) for sample 65-35. In both cases, the reaction was allowed to continue running beyond 10000 sec shown in the figure (Not displayed in the plot). As stated above, the increased pH was one of the key reasons enabling the reaction to take place, the influence of pH by combined metal oxides must, therefore, be considered. Figure 4-13 shows the pH during the first 1000 sec of a reaction.

In Figure 4-13, it can be seen that as deionised water (pH 7) comes into contact with the powder its pH is raised to a pH of 12 within 100 sec for sample 50-50 and to a pH of 10.5 for the sample 65-35. This indicates that the aqueous solution becomes alkaline, i.e. more OH^- ions are present in the solution than before. It is known that dissolved OH^- ions will react with the passive oxide layer, Al_2O_3, on the aluminium particles and this is the main reason KOH is often added to promote the $Al + H_2O$ hydrogen generation reaction.

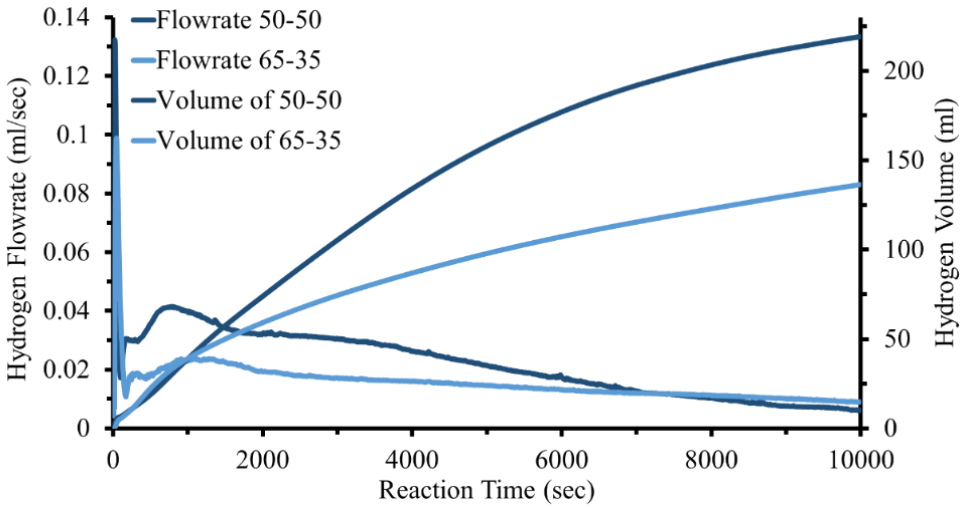

Figure 4-12: Hydrogen generation comparison when changing the CaO: CuO ratio additives. Hydrogen flow rate (y-axis to the left) and generated hydrogen volume (y-axis to the right).

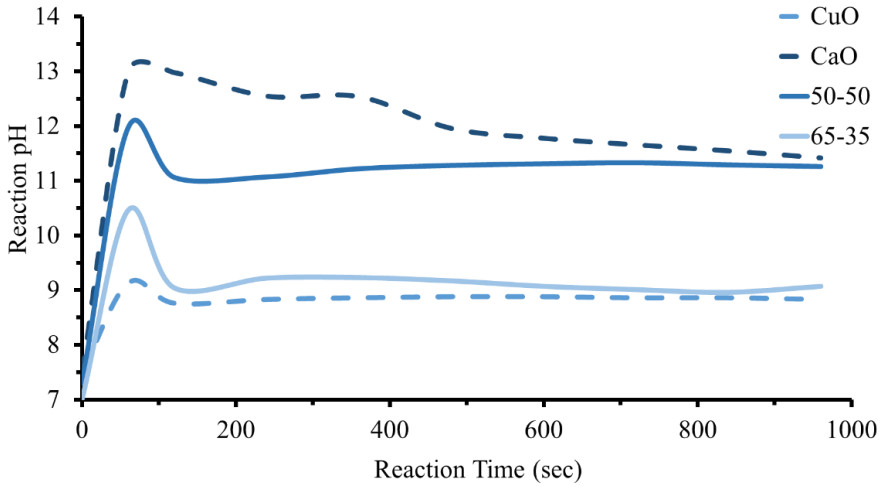

Figure 4-13: The pH variation within the first 1000 sec reaction time when comparing metal oxide ratio samples 65-35 and 50-50.

It should be noted here that KOH is another expensive component, especially when higher purity KOH is used which would be detrimental to the hydrogen economics as it costs £1100 per kg [141]. Referring to the pH change, here it is important to emphasise that simultaneous reactions are taking place with CuO and CaO in water. The proposed mechanism is presented below, is also suggested by Wang *et al.* [72]; however, the case of CaO will be discussed first. As a CaO, it is noticed that it reacts with water to form a solid calcium hydroxide as :

$$CaO + H_2O \rightarrow Ca(OH)_2\ (s) \quad \Delta H_r = -64.8\ kJ/mol \qquad (4.6)$$

The $Ca(OH)_2$ will dissociates in the presence of water as:

$$Ca(OH)_2\ (aq) \rightleftharpoons Ca^{2+} + 2OH^- \quad \Delta H_r = -16.64\ kJ/mol \tag{4.7}$$

$Ca(OH)_2$ dissociation in water results in an increased concentration of OH^- ions leading to increased pH as was shown in Figure 4-14. The solution with high pH reacts with the thin oxide film Al_2O_3. Despite only being a few nanometres thick the oxide film is adequate to prevent aluminium from reacting with water to form H_2 [50]. Although, milling the powder with the additives most likely does damage the film, a part of the film remains. When the alkaline solution reacts with the thin film, it hydrates it and potentially forms a hydrophilic layer of aluminium hydroxide oxide, also known as aluminium Oxyhydroxide (boehmite γ-AlO(OH)) on the surface of Al_2O_3 as shown in Figure 4-13, a similar mechanism was suggested by Huang *et al*. [106].

$$Al_2O_3 + H_2O \rightleftharpoons 2AlO(OH) \tag{4.8}$$

Oxyhydroxides layer on the surface of Al, due to its high porosity, can further permit water diffusion into the Al particle and hydrogen diffusion out of Al particle through *salt gates/tunnels* as shown in Figure 4-14.

$$2Al + 6AlO(OH) \rightarrow 4Al_2O_3 + 3H_2 \tag{4.9}$$

Moreover, this reaction will possibly simultaneously produce H_2 gas along with the metal and water reaction:

$$2Al + 6H_2O \rightarrow 2Al(OH)_{3\,+}\ 3H_2 \tag{4.1}$$

Referring to the CuO reaction, it can be hypothesised that the salt in the milling has enabled Al to be exposed and hydrogen can be produced as: However, the CuO most likely be reduced to metal Cu if a formed H_2 gas bubble is grown nearby as:

$$Cu(II)O + H_2 \rightarrow Cu(O) + H_2O \tag{4.10}$$

This possibly can explain the inferior reaction when CuO is used as the single metal oxide. On the contrary, CaO will not react similarly with the formed H_2 and the fastest reaction when using CaO is to form the dissolved Ca^+ and OH^- instead. If CuO is reduced to metal Cu in the reactor, a new scenario needs to be investigated for better determination. Copper metal is, unlike Al, unreactive towards the water. The presence of oxygen in the water (dissolved oxygen in 20 °C water is about 8-

10 ppm), can result in oxidation of the metal Cu back to CuO, therefore more elementary analysis such as TEM would help to determine the mechanism better.

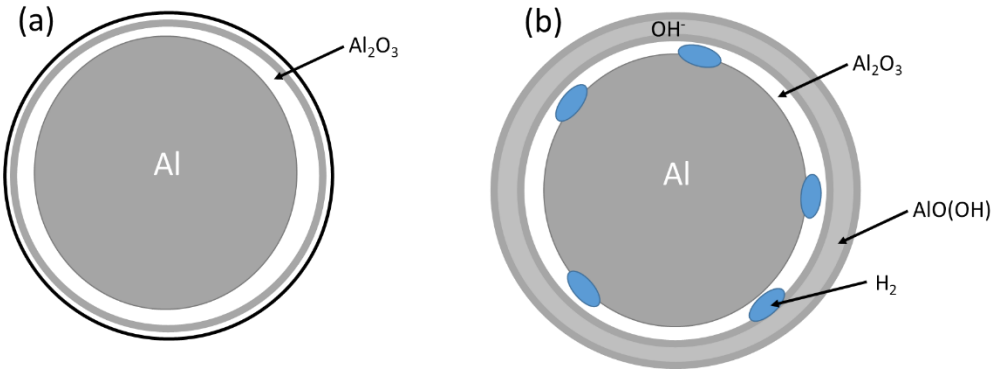

Figure 4-14: a) Hydrated Al_2O_3 layer b) Hydrogen bubbles formation on Al_2O_3 layer.

4.1.3.2 Salt additives

It has been established that both salt and metal oxides are necessary as milling additives for prolonged hydrogen reaction (promoting higher H_2 yield) and for an enhanced reaction rate. In the following section, the role of the salt additions is further investigated. Different salts; NaCl, KCl and $CaCl_2$ were milled together with aluminium powder and MO (combined CaO-CuO as 50-50) as listed in Table 4-2 and were synthesised using Milling Programme 1a.

Table 4-2: Composition of additives in the sample.

Powder composition (wt %)
Al 65 %, MO 25 %, NaCl 10 %
Al 65 %, MO 25 %, KCl 10 %
Al 65 %, MO 25 %, $CaCl_2$ 10 %

As Figure 4-15 shows, it is clear that by using 10 wt % $CaCl_2$, hydrogen gas is generated both faster right from the start and more plentifully when compared to NaCl and KCl within the first 1000 sec of reaction. At 1000 sec the $CaCl_2$ sample had generated 22 ml 8 % yield of hydrogen compared with 15 ml 5% yield for NaCl and 14 ml for the KCl sample. The small difference can be neglected as it falls within the error bar 1-2 ml for the analysis. One cause of the higher reactivity of $CaCl_2$ is that it produces more ions when it dissociates than NaCl and KCl. It will

still produce the same type of "salt gates", or tunnels, but will increase the conductivity of the water even more [93]. This conductivity helps to corrode the Al metal.

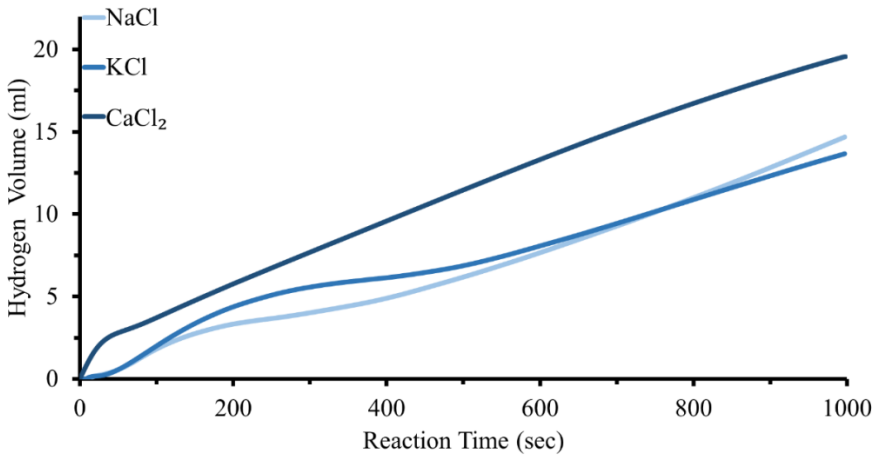

Figure 4-15: Generated volume of hydrogen gas when using NaCl, KCl and $CaCl_2$ in the particle milling using Milling Programme 1a.

Inspired by the effect, when two different metal oxides were combined producing promising results, similarly, Similarly, different salts were mixed together to create a synergy effect. Synergy effect is an effect arising from two or more agents, entities, factors, or substances that produce an effect greater than the sum of their individual effects [133]. The salt mixture contained three salts; $CaCl_2$, NaCl and KCl which from here on it would be known as PO (as in *potash*). The predominant salt in the mixture is NaCl, a commonly used salt additive in milling [40,74,77,95]. According to the authors of [42,135,136,140], Al metal particle size can be reduced if NaCl is employed during the milling. It is assumed that the three different salts would be able to etch, penetrate and damage the surface of Al particles simultaneously during the milling due to their different hardness and structure. The effect of salt on the Al particle will be discussed in the following section. In order to investigate if there is a synergy effect, salt additive PO was compared against $CaCl_2$. For this purpose, Milling Programme 1a at 260 rpm was employed to mill both particle composites under identical conditions for 1.1 hrs.

One can see in Figure 4-16, that the hydrogen formation is improved when using the PO sample compared with $CaCl_2$. Already from the start, PO had generated 22 ml, 8 % yield of hydrogen gas after only 600 sec compared to 13 ml, 5% yield by

$CaCl_2$. This can be compared to 9 ml from NaCl or KCl from demonstrating its superiority over them.

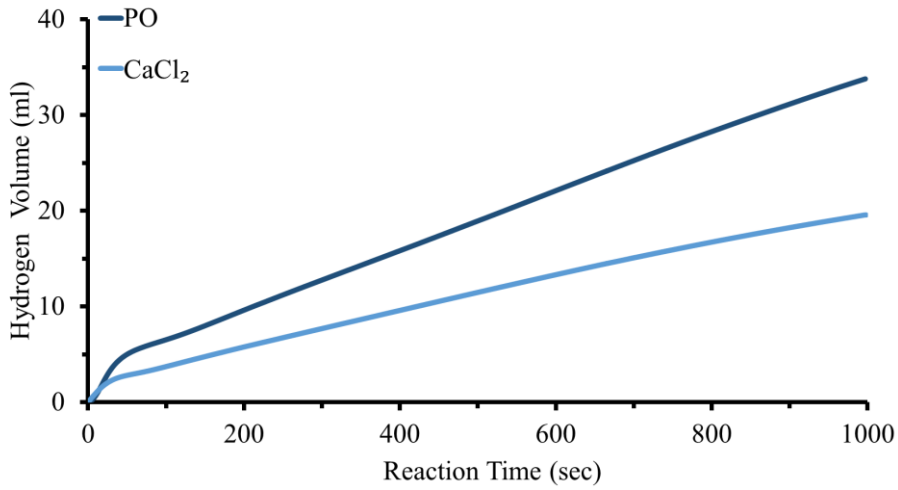

Figure 4-16: Effect of salt additives on the generated hydrogen volume when comparing sample PO with sample $CaCl_2$.

It is important to point out that this huge improvement of hydrogen generation by using a combined salt can be compared favourably with the results obtained when expensive BaO was used as an additive. This tells us that it is possible to source and select cheaper additives and with the appropriate mixture provide an advantage for the hydrogen economics. Different scenarios, described below, can describe this improvement. Salts were embedded in the metal aluminium as a result of the high-energy ball milling and dissolved when exposed to water, leaving behind salt gates or tunnels as shown in Figure 4-17. Due to these changes on the surface of the particles, water can then diffuse to the Al metal where the H_2 generation can take place as shown in Figure 4-24 and Figure 4-25.

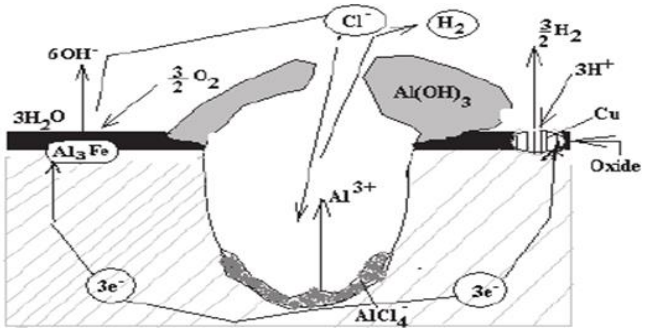

Figure 4-17: Illustration of salt gates and pitting corrosion mechanism [144].

This is the major reason for hydrogen generation enhancement resulting from the addition of the sale additives for milling. This was verified by comparing a blended powder mixture that was not mechanically milled with a one that was milled powder to verify whether the hypothesis was correct or not, Figure 4-19a. Another contribution to the observed hydrogen generation enhancement is carried out by the dissolved Cl^- ions from the salts used, which are highly aggressive anions and could possibly attack the passive Al_2O_3 film making it unstable and dissolving it. The salts NaCl, KCl and $CaCl_2$, in the mixture are dissolved when particles are introduced to water. This would result in a passive film breakdown and is referred as to *pitting corrosion*, as shown in Figure 4-17.

NaCl dissociates into Na^+ and Cl^- ions while 1 mole $CaCl_2$ is dissolved into the water as 1-mole Ca^+ ions and 2 moles of Cl^-, which results in increased pitting corrosion, seen in Figure 4-15. The effect of the PO mixture on H_2 generation can be explained by the different salts hardness and by their various dissolution reactions [26]. Dissolving salts in water can be either exothermic or endothermic. Potassium chloride, KCl absorbs heat from its surroundings when it dissolves in water (endothermic process) as does the commonly used NaCl, whereas calcium chloride, $CaCl_2$ reaction is exothermic [149]. Therefore, using different salts in a combination could create synergetic reaction kinetics. To further explore the effect of salt additives it was decided that two powders would be prepared.

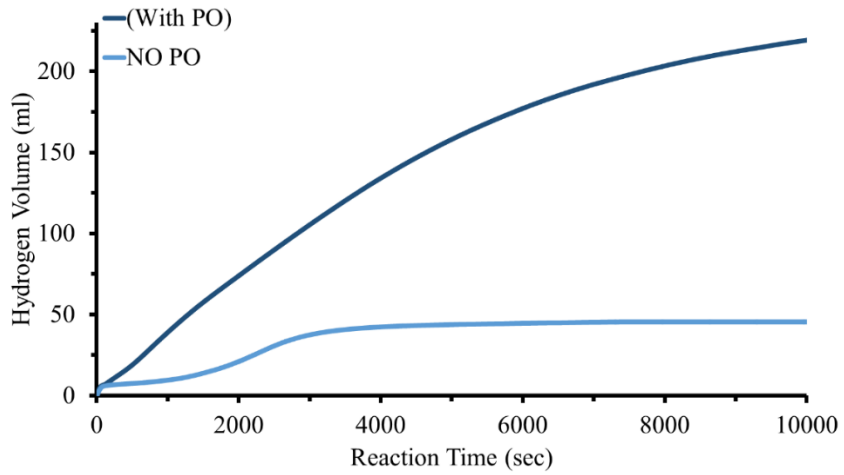

Figure 4-18: Salt versus no salt additive effect on the generation of hydrogen.

One contained all the additives, i.e. (Al+MO+PO) and other was prepared that did not have any salt additive, i.e. powder (Al+MO). These are called “No PO” and “With PO” in the results, respectively. Here it was necessary to adjust the weight % accordingly. The absence of salt in the sample No PO was adjusted by increasing the portion of metal oxides, i.e. (Al 65 wt %, CaO 17.5 wt %, and CuO 17.5 wt %) to keep the ratio 65-35. Powders were milled using Milling Programme 1a at 260 rpm and reacted with deionised water at 25 ºC for 10000 sec. From the Figure 4-18, it can be seen that milled NO PO powders only produced 48 ml of H_2 in 4000 sec and after that stopped producing any further. On the other hand, With PO powders displayed an increased hydrogen generation straight from the start. The sample With PO generated 130 ml (50 % yield H_2 yield) while only 48 ml (19 % yield H_2 yield) for the NO PO sample in 4000 sec.

Another important observation is that for NO PO the reaction rate is slow for the first 1700 sec and then increases rapidly until 3000 sec reaction time where it comes to a halt. A plausible explanation for this is that the pH (and the dissociated OH^-) from the CaO reaction has become sufficiently high to propel the reaction forward at 1700 sec, but at 3000 sec the barrier layer of $Al(OH)_3$ is preventing any further H_2 generation.

4.1.3.3 Combined additive effect (MO + Salt)

From above-described studies, it can be seen that several possible reactions can occur in the reaction vessel depending on the milling process and choice of additives used. As a continued study to highlight the importance of milling and the additives to the hydrogen production, it was decided to prepare three samples via milling. These included (Al+MO), (Al+PO) and (Al+MO+PO) and were compared with a non-milled sample of (Al+MO+PO). By doing this, a clearer picture of milling effect and additive effect emerges. As before, All powders were milled identically using Milling Programme 1a. From Figure 4-19a, it can be clearly seen that using both additives together with the milled sample (Al+PO+MO) is most beneficial for hydrogen generation producing a hydrogen volume of 1050 ml (corresponding to 220 ml out of 260 ml total) after 10000 sec corresponding to an approximate hydrogen yield of 85 % per mol of Al in the particles.

Without milling, the same composition produced only 700 ml (corresponding to 135 ml out of 260 ml total) hydrogen after 10000 sec, corresponding to an approximate hydrogen yield of 54 % per mol of Al. The high amount of hydrogen by Non-Milled (Al+PO+MO) sample was unexpected.

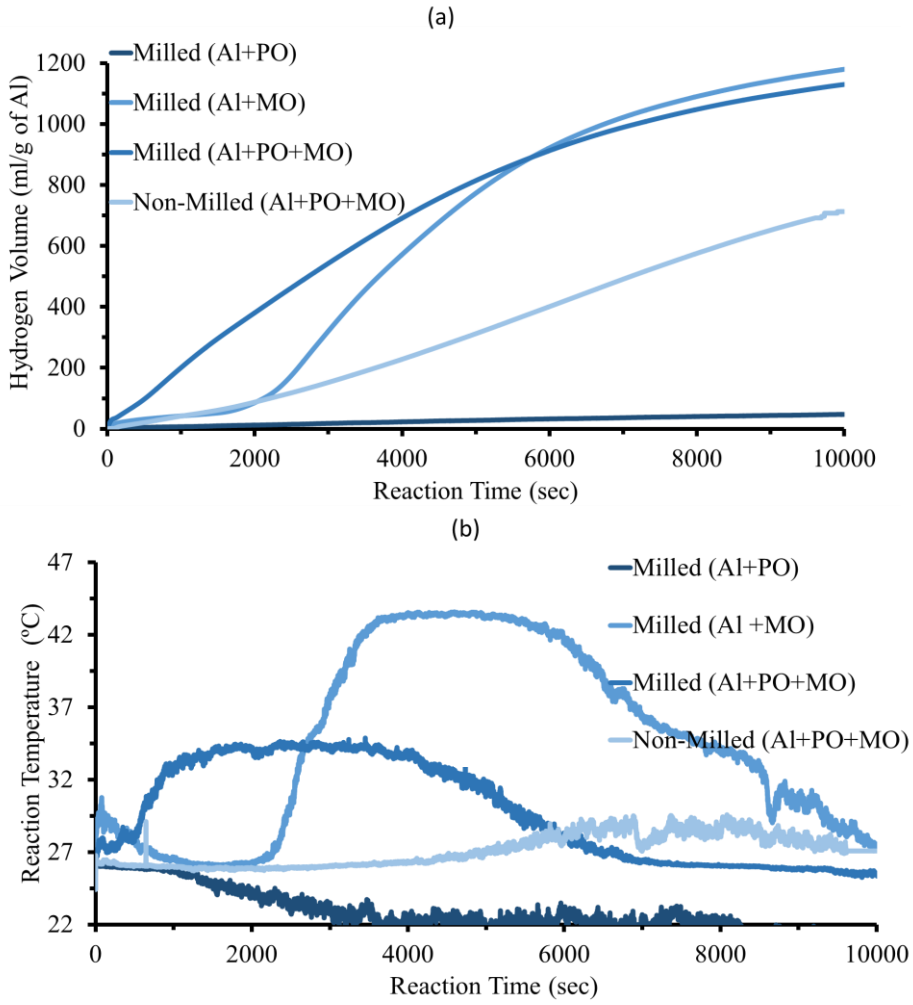

Figure 4-19: a) Generated hydrogen volume per gram Al for milled samples with various additives compared with a non-milled sample b) corresponding exothermic reaction temperature for the same samples.

A possible explanation for this occurrence may be that the hydrogen reaction depends mainly on the CaO reaction with water and the subsequent pH increase associated with it, as was discussed previously. Once again it can be seen that milling with salt additives removes the observed incubation time known hereon as the lag time of the hydrogen generation the generation is efficient right from the start. It should be mentioned that powders which were not milled and had no

additives did not produce any hydrogen at all at room temperature (not shown in Figure 4-19). When samples milled with salt (Al+PO), metal oxide (Al+MO) were compared it was found that only when the salt additive was present was there any amount of hydrogen being produced with the liberated amount < 20 ml after 1000 sec. Milled (Al+MO) samples yielded 100 ml/ g Al (corresponding to 17 ml out of 260 ml total).

The sudden rise in the rate of reaction for the milled (Al+MO) sample can also be seen in the temperature plot, see Figure 4-19b, where the exothermic reaction results in a temperature increase from 26 °C to 44 °C. Again, to emphasise the importance of salt additive in the mixture, when the (Al+PO+MO) sample is reacted with water, it could be seen that the lag time lag-time observed for (Al+MO) disappears. From the Figure 4-19b, it can be seen that the temperature at first rises from 26 °C to 33 °C and a then plateaus out after 750 sec for approx. 5000 sec (83 min) indicating a more stable kinetics than for (Al+MO). When only metal oxides (Al+MO) were used, the generated hydrogen volume in 10000 sec was 250 ml, which is similar to when both metal oxide and salt additives, i.e. sample milled (Al+Salt+MO). Also for this sample, there was a 2000 sec lag time before the reaction accelerated dramatically.

For the same reaction time, sample (Al+ MO+ PO) had already produced 400 ml/g Al (corresponding to 73 ml out of a maximum 260 ml). Furthermore, when 0.3 g of (Al+PO+MO) was allowed to react with 9 ml water for 12000 sec, it produced a total of 235 ml which correspond to a hydrogen yield of 90 % per amount of metal reacted. The mechanism and dynamics of the hydrogen generation appear more controlled when (PO+MO) is used which is evident in a stable reaction and furthermore a high hydrogen yield. The effect of milling with various additives will be further explained with the aid of scanning electron microscope (SEM) and elemental analysis (EDX) in the later section.

4.1.4 Effect of milling on Al particles size

As this research is aimed at using recycled aluminium particles, which can have a significant variation in particle sizes depending on the supplier, a study of typical recycle alumina particle sizes was conducted. This was later compared with highly pure micron-sized aluminium. Recycled aluminium (provided by iHOD USA) with particle size 3-200 µm was sieved to obtain representative batches of 40 µm, 75 µm and 105 µm sizes prior milling. The different sized batches were then mixed with the additives (combined metal oxide 50-50 and salt PO) and milled by Programme 1a. It should be mentioned that these were the average sizes before milling.

In Figure 4-20, the results are plotted that reflect the effect that the particle size has on the production of hydrogen. It can be seen that the recycled particle size does have a profound effect on the hydrogen reaction. The smallest starting Al particle size, 40 µm, showed the highest hydrogen generation followed by 75 µm, whereas 105 µm was considerably slower and produced the least amount of hydrogen of them all. After 500 sec, the larger starting batch of 105 µm slows down while both the batches 40 µm and 75 µm progress steadily.

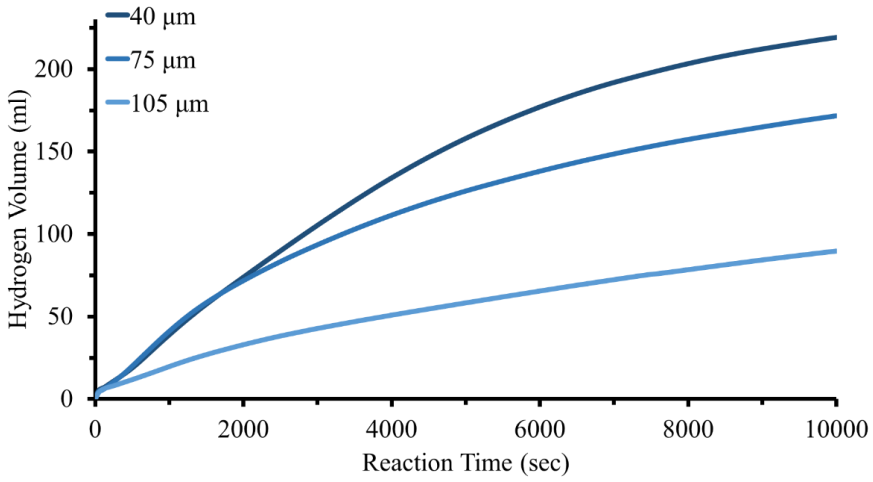

Figure 4-20: Effect of Al particle sizes (40 µm, 75 µm and 105 µm) used in milling and their corresponding hydrogen generation.

At 10000 sec reaction time, the 40 µm batch had produced 220 ml and the 75 µm batches produced slightly less of 172 ml whereas using the largest sized recycle aluminium particle batch of 105 µm only produced 90 ml hydrogen corresponding to a hydrogen yield of 85 %, 66 % and 35 %, respectively. In what follows, the

SEM images will further explain the final particle size of these three batches after milling with additives. It is well known that a smaller particle size will provide a larger surface area notion also supported by the authors of [19,50,103,109] and it is, therefore, not unexpected to see that the three different starting sizes showed a similar trend. Smaller Al particles sizes used in the milling would provide a larger surface area to be *tempered* by the salt additives. This results in the higher ratio of salt-gates per mass of Al used in the process. An opened salt-gate through the barrier Al_2O_3 layer would facilitate water diffusion to Al particle core allowing faster corrosion.

4.1.4.1 Comparison of fisher and recycled micro size Al particles

To continue the study of raw material, particle size and purity, a 40 μm recycled Al batch was compared to finer 10 μm aluminium particles (Fisher Chemicals, 99.9 % purity) named "Fisher Al". For comparison, powder compositions were kept same as from previous experiments, i.e. (Al 65 wt %, CaO 12.5 wt %, CuO 12.5 wt % and PO 10 wt %) and was prepared using milling Programme 1a (260 rpm). Shown in Figure 4-21a, b and c, one can see a strikingly similar trend in all figures.

A distinctive reaction lag time of up to 2000 sec was observed in the case of Fisher Al particles, but a much shorter lag was witnessed for the Recycled Al 40 μm sample. For the Fisher Al particles, following the lag, the reaction temperature escalated rapidly from 26 ºC to 52 ºC and resulted in a massive increase of hydrogen flow rate as seen in Figure 4-21a. The flow rate of hydrogen generated from the Fisher Al particles continued to rise until the 2800 sec mark, after which a levelling off was observed which was outside the sensitivity range of hydrogen mass flow meter (GFM-17 for flow rates <10 ml/s), therefore, impossible to record the peak flowrate properly. The result of the higher flow rate is also be reflected in Figure 4-21a, b and c.

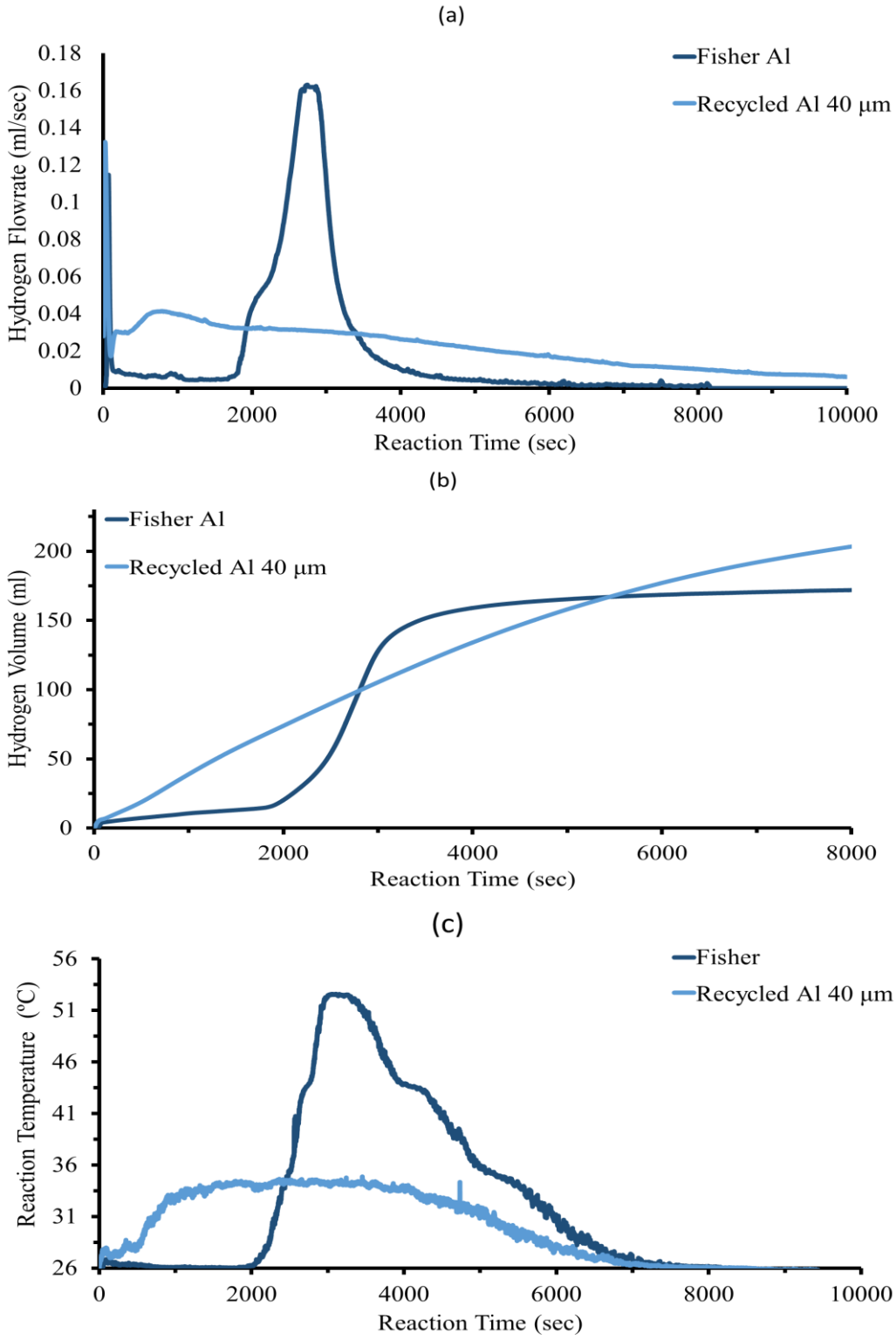

Figure 4-21: Comparison between Recycle 40 µm and Fisher Al particles in; a) hydrogen volume flow rate, b) generated hydrogen volume and c) exothermic temperature development.

The same experiment was also performed using an inverted column due to the limit of GFM, which provided a more accurate hydrogen volume of 240 ml just after 4500 sec of reaction. The amount of hydrogen generated by the Fisher Al corresponded to 92 % hydrogen yield compared to 220 ml by "Recycled Al 40 μm" corresponding to 85 % hydrogen yield, both after 10000 sec reaction time. From this study, it can be said that reactive milling had a variable effect on the two samples. At first, it was believed that different behaviour in reaction might have been caused by purity differences between the two samples however, that was not the case which was verified by the materialistic analysis. To verify this, analysis of these two different aluminium samples was conducted using SEM-EDX for an elementary evaluation.

Table 4-3: Shows the of elemental analysis by EDX for Fisher aluminium

Element	Weight %	Atomic %
Aluminium	100.00	100.00
Total	100.00	100.00

Table 4-4: Shows the elemental analysis by EDX for iHOD USA.

Element	Weight %	Atomic %
Aluminium	98.22	98.79
Calcium	1.78	1.21
Sodium	0.00	0.00
Total	100.00	100.00

The result of EDX for batches of "Recycled Al 40 μm" and "Fisher Al" are presented in Table 4-3 and Table 4-4 and in Figure 4-22. As the two batches contained the same milling additives and identical reaction conditions were employed, it was concluded that the difference must be due to some other mechanism in the milling process. Therefore, the SEM-EDX was thoroughly studied. In Figure 4-23, Recycled Al 40 μm and Fisher Al are compared in a high-resolution SEM image. It can be seen that the surfaces of the two particles appear different after the milling.

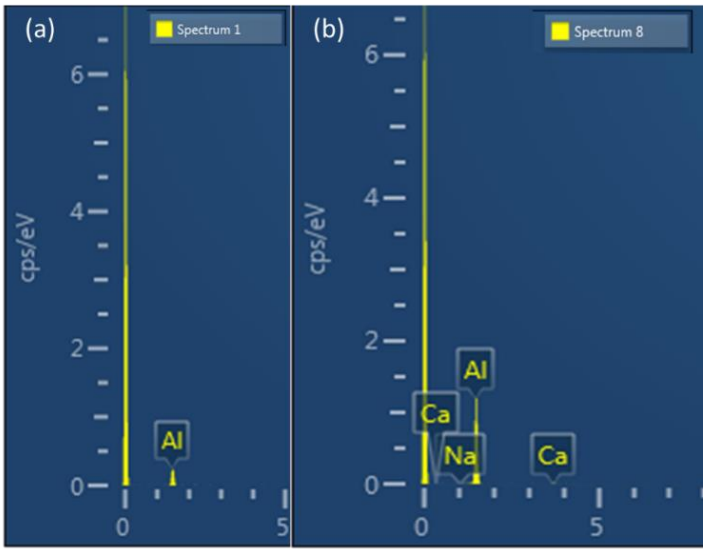

Figure 4-22: EDX spectra of the two types of aluminium particles: a) Fisher and b) Recycled Al 40 µm.

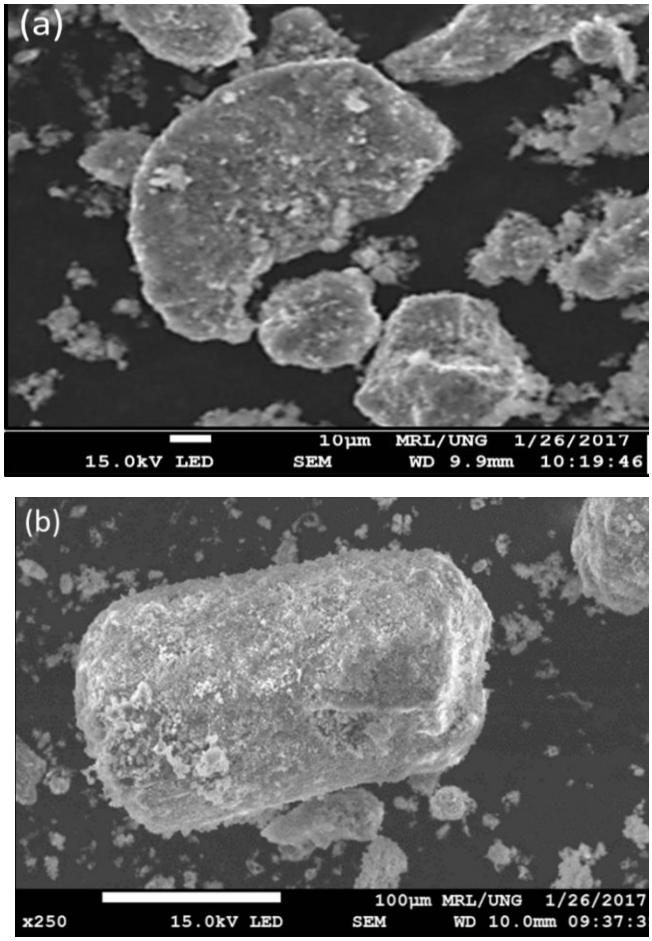

Figure 4-23: SEM zoomed in images of milled a) micro-sized Al Fisher b) 40 µm recycled Al.

The Recycled Al 40 µm shows clear evidence of additives covering the surface. For the purer micro-sized Fisher, the additives appeared scattered around as free particles. For the hydrogen generation, this would make a large impact as these unattached scattered additives will not take part in the hydrogen generation reaction. It should be said that similar lag time was observed when salt additives were not present during milling. Therefore, it was established that the salt additives used when milling Fisher Al particles do not generate the necessary "salt gates". These salt gates are essential for the mass diffusion of OH^- ions and for H_2 evolution at the metal Al core as emphasised already. The conclusion of this investigation is that finer aluminium powders would not be suitable for small on-demand hydrogen generation. One important reason for this is that small particles sizes generate higher reaction temperatures, subsequently generating hydrogen at a higher flow rate in a short time span. Such a surge of reaction kinetics would not be appropriate for the portable fuel cell. Another important reason is pure and well-refined aluminium particles would be costly, especially if upscaling is considered.

4.1.4.2 Particle characterisation

To monitor how aluminium particles were affected after each step of the whole process, samples were collected at three different stages: before the milling (sieved without additives), after milling (with additives) and after the reaction with water had finished. Figure 4-24 shows, a collage of SEM images of recycled aluminium particles sieved to a range of 40 µm, 75 µm and 105 µm and compared with the pure averaged 10 µm (Fisher). They are arranged from left to right displaying different stages of the particle synthesis whereas; the rows represent different starting particle sizes. From the SEM images below, it can be seen that the metal particles before milling and after milling, underwent changes in the morphology as well as the milling additives.

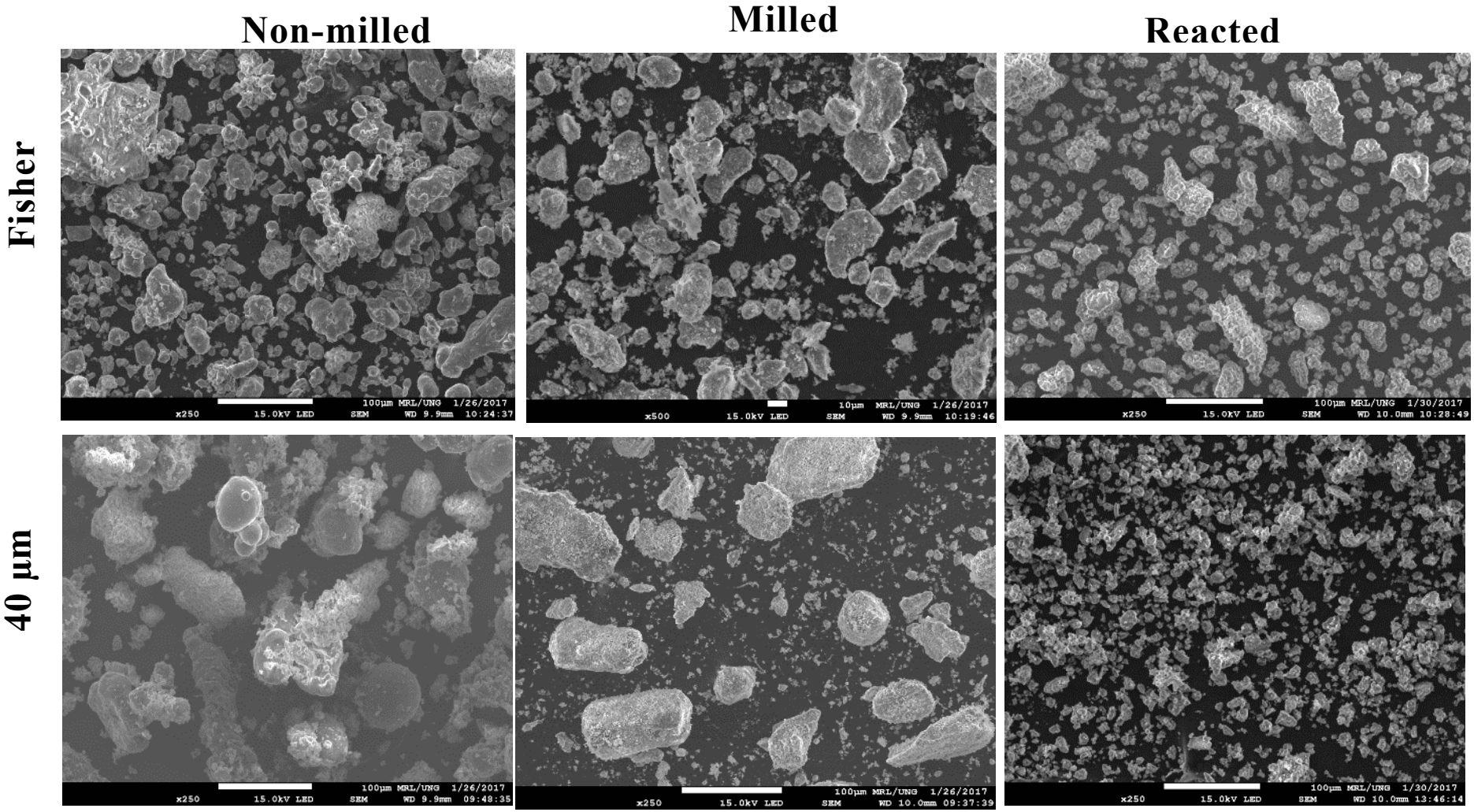

Figure 4-24: Particle evaluation by SEM of sample 40 µm and sample Fisher at three different stages; aluminium not-milled, milled with additives and after the end of the reaction.

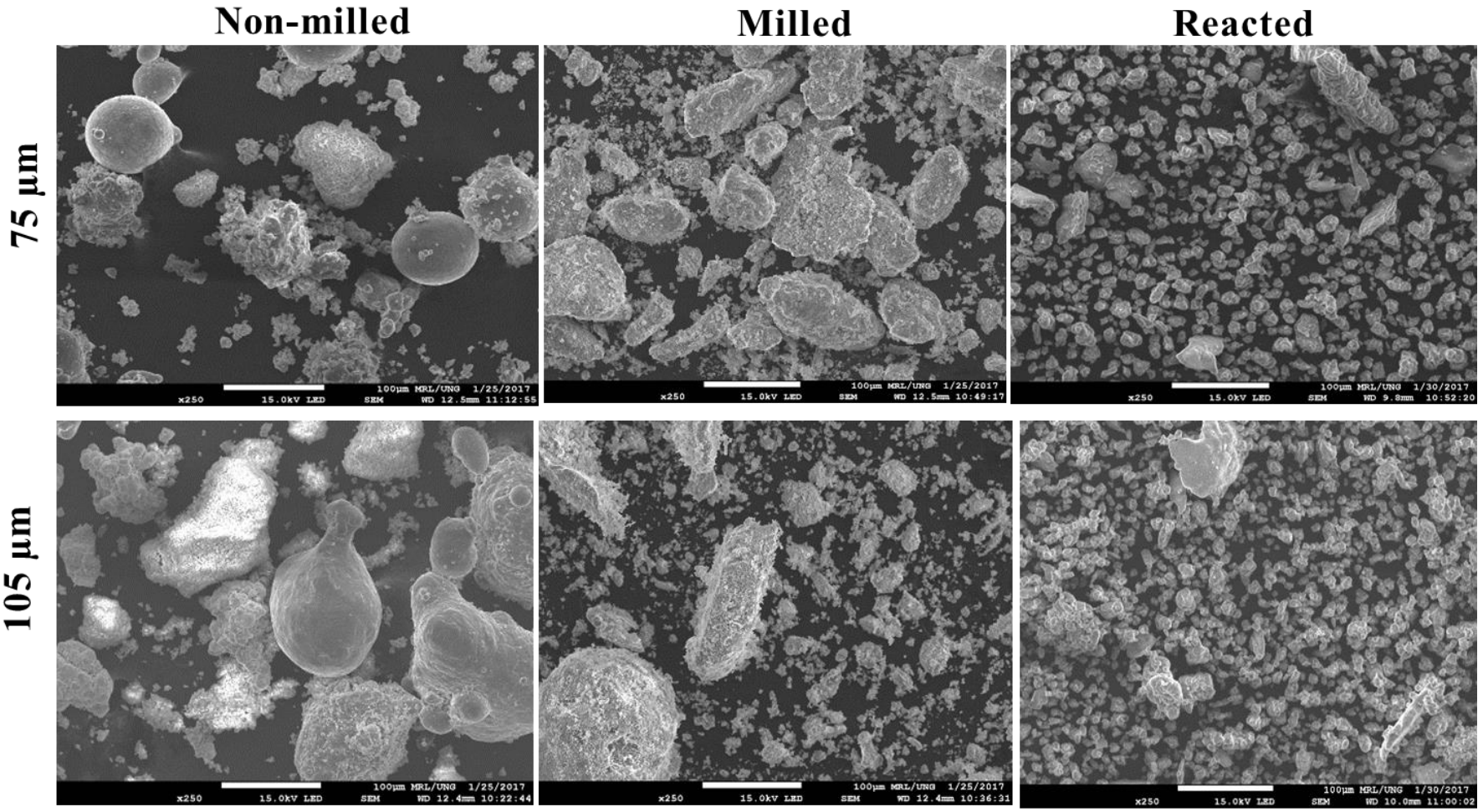

Figure 4-25: Particle evaluation by SEM of sample 75 µm and sample 105 µm at three different stages; aluminium non-milled, milled with additives and after the end of the reaction.

Due to the high kinetic energy and softening of the metal particles during the milling process, it can be seen how the additives have adhered to the metal particle surface. Due to this occurrence, it is expected that at least the hard salt additive has damaged the Al_2O_3 layer and formed "salt gates". This surface coating of crushed additives can be seen in all samples of 40 µm, 75 µm and 105 µm sieved recycled aluminium particles, but not in the smaller and purer Fisher aluminium powder. The particle size appears slightly larger after milling for the 40 µm, 75 µm and 105 µm particles, which is not the case for the Fisher sample. For instance, before milling sample, 40 µm samples were found to have an average particle size of 40 ± 5 µm and after milling the average was found to be at 60 ± 5 µm. In normal practice, the metal particles size should reduce, however, it was not seen here.

The powder size, in the beginning, was 40 µm and once it was milled it was again analysed using three samples under SEM, not shown here. This analysis was conducted for further verification purposes to observe powder size and ratio i.e. particle distribution.

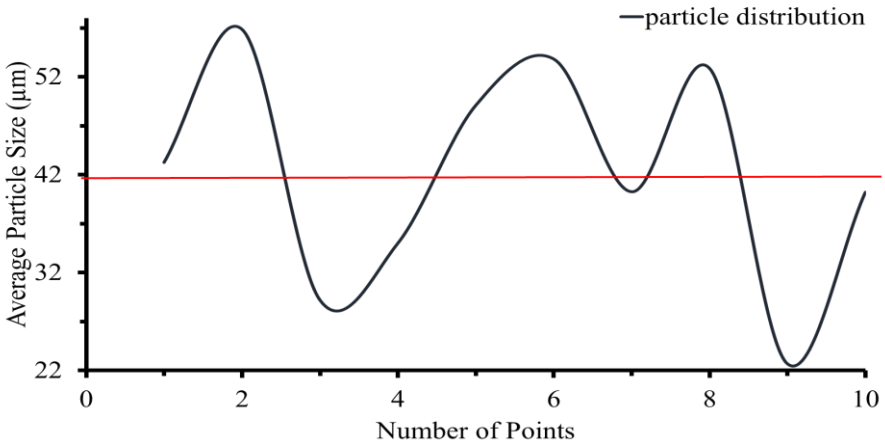

Figure 4-26: Particle distribution of 40 µm after milling for 1.1 hrs.

From Figure 4-26, one can see that the particle size does vary after milling and it is between 40 ± 18 µm, however, the average particle size was 42 µm. It is important to recognise that different particle sizes would significantly affect reaction kinetics as it was verified and explained in the earlier tests. Therefore, to develop a more accurate kinetic model it is recommended that metal particles must be sieved in an inter atmosphere (argon) after the milling to reduce the average distribution.

An explanation that particle size distribution is large could be that during the milling processes the additive gets coats the metal particles making their overall size larger. A similar increase of the Al particle size was observed by the authors of [54] when authors do not employ a processing control agent which provides a lubricant that minimises the cold-welding effect (stearic acid) for milling. Throughout this research work, stearic acid was not used because it would have avoided any additives to be embedded on the surface of Al particles. From Figure 4-24 and 4-25, the coating of the additive on the Al metal particles also appears to have altered the surface structure of the aluminium particles from uniformly smooth and spherical to more irregular and flaky in shape. This is intriguing as it was thought that to bring such morphological changes of aluminium particles would require higher speed or longer period milling. All samples were milled using Milling Programme 1a at 260 rpm, which is far less energy demanding than related research publications in which author also reported structural changes of the metal particles by additives [45,93,94,134,140]. Here it is concluded that a less energy demanding milling process was still able to integrate the additives successfully upon and in extreme cases within the aluminium particle and still provide excellent hydrogen generation yields.

After the hydrogen generation reaction, the residue was carefully collected onto a filter paper and placed in a vacuum furnace for 24 hrs at 25 °C to dry. In the SEM images in Figure 4-24, it can be seen that following the reaction all particles of sample 40 µm, sample 75 µm and sample 105 µm have shrunk considerably. It can also be seen that the sample 40 µm decreased in size considerably more, compared to other samples. This shrinkage is due to the aluminium consumption during the reaction. Particles, during the hydrogen reaction, undergo a considerable amount of change especially when there are changes in temperature and pH. Changes in Al particle sizes can be explained by the *shedding effect* of the outer hydroxyl layer until all the aluminium particles are have been converted into aluminium hydroxide each. This shedding effect is further improved by reactor agitation. Sample 40 µm had the smallest amount of $Al(OH)_3$ and also produced the highest hydrogen yield. As each sample had an equal amount of additives (as confirmed by SEM and EDX),

the fact that sample 40 µm produced the most hydrogen means that higher number of salt gates are present. It can be said this is because more additive-assisted reactions take place on the particle surface for small particle sizes than for larger ones because of the additional surface area available on smaller size particles. The Fisher sample, which showed the characteristic lag-time in the reaction, was found to lack such a uniform outer layer of additives despite the same protocols being followed for milling as for sample 40 µm. One can see in Figure 4-24, that a lighter appearing coating has formed on the reacted samples. This coating is most likely to be by-product aluminium hydroxide which was later confirmed by XRD. Inspecting the SEM images shown in Figure 4-24 and Figure 4-25, it is concluded that the reactive milling is essential for greater hydrogen yield. This is particularly important if the hydrogen generation is aimed at ambient temperature and pressure. Therefore, it is important to understand the mechanism in detail. It was seen earlier in Figure 4-27, that the aluminium particles increase in size during high-speed milling by up to 0.8-0.9 mm in the absence of additives. Figure 4-27 shows the initially smooth aluminium particle surrounded by additives in a normal blended mixture, i.e. not milled.

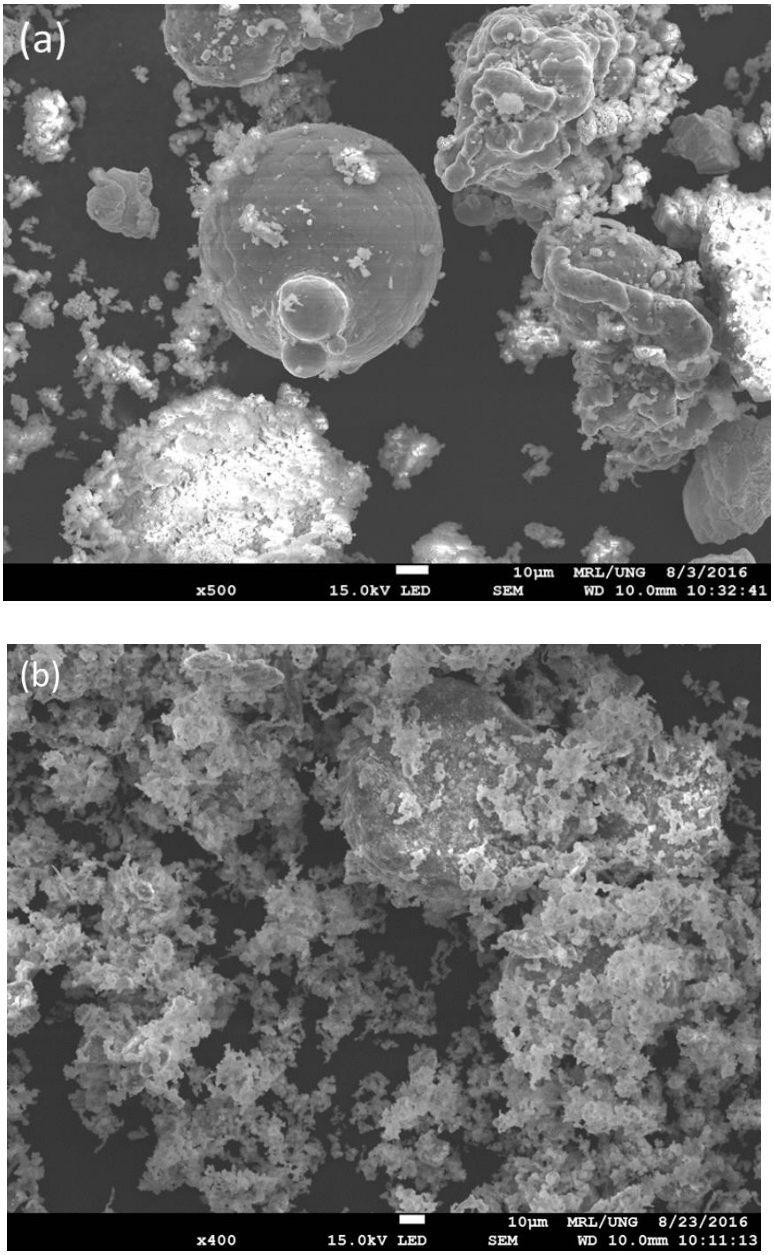

Figure 4-27: a) SEM image of an additive + aluminium mixture showing the smooth Al particle surrounded by the crystalline structure of the additives b) SEM image of an additive + aluminium milled sample showing plastic deformed aluminium particle covered.

Aluminium particles were divided into three batches as stated earlier 40 µm, 70 µm and 100 µm. However, their average was 40 µm, 75 µm and 105 µm. For these studies, the 75 µm sample was employed. From the SEM image, it could be interpreted that if such powder were reacted water, the additives (MO+PO) would be dispersed rapidly in water, the salt would dissociate and CaO will form $Ca(OH)_2$. This additive will further contribute to the pH increase and dissolution of a passive

layer of Al particles that subsequently will aid the hydrogen reaction, e.g. as in Figure 4-19 where it was observed that some hydrogen generation at ambient conditions does occur when using an additive combination (PO+MO). For further analysis purposes, Al particles of 75 µm were compared before and after milling using Milling Programme 1a at 260 rpm. In Figure 4-26b, one can see that the additives (MO+PO) have been crushed and subsequently surrounding the Al particles. Additionally, the shape of the spherical particle has also changed into an irregular sponge-like shape despite a relatively short milling time. This is a consequence of elastic deformation and softening of the metal, which results in more additives sticking to the surface, thus disrupting the Al_2O_3 layer. Since the reactive milling is very energy intensive, it was important to ensure that no chemical reaction took place while milling, for example, Al_2Cu was produced during persistent and high-speed milling as stated previously.

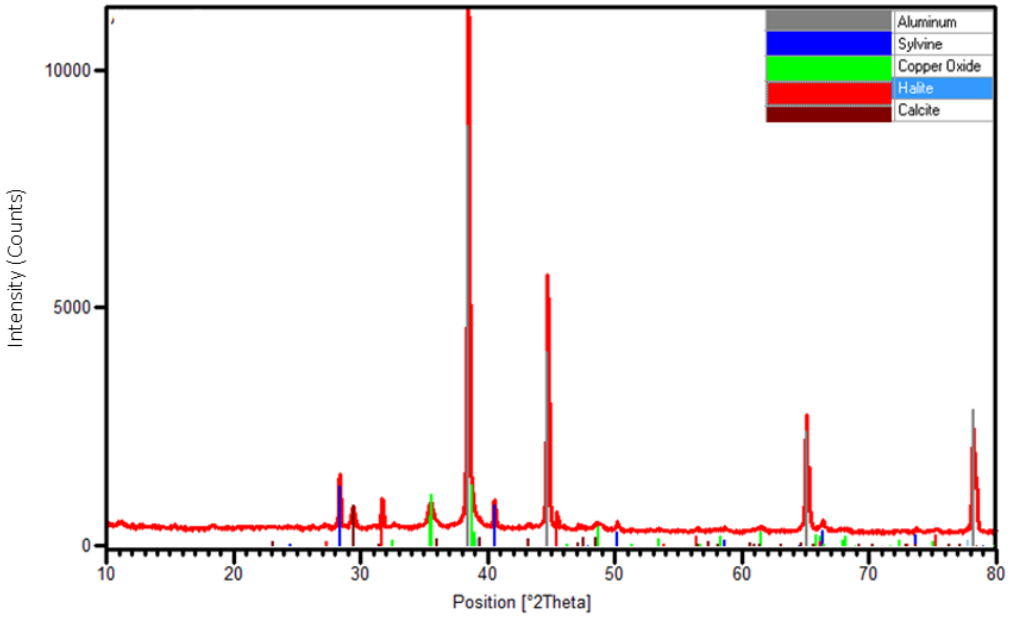

Figure 4-28: XRD of a milled sample showing only peaks from the additives and aluminium and none from products of possible reactions while milling.

Furthermore, milling was carried out in an inert atmosphere to prevent this. In order to check whether a reaction occurred during milling or not, the milled sample Al with 75 µm size was also examined by XRD, see Figure 4-28. The separate component peaks were identified (using Peak Fit Software) and no reaction product such as Al composites was found to be present.

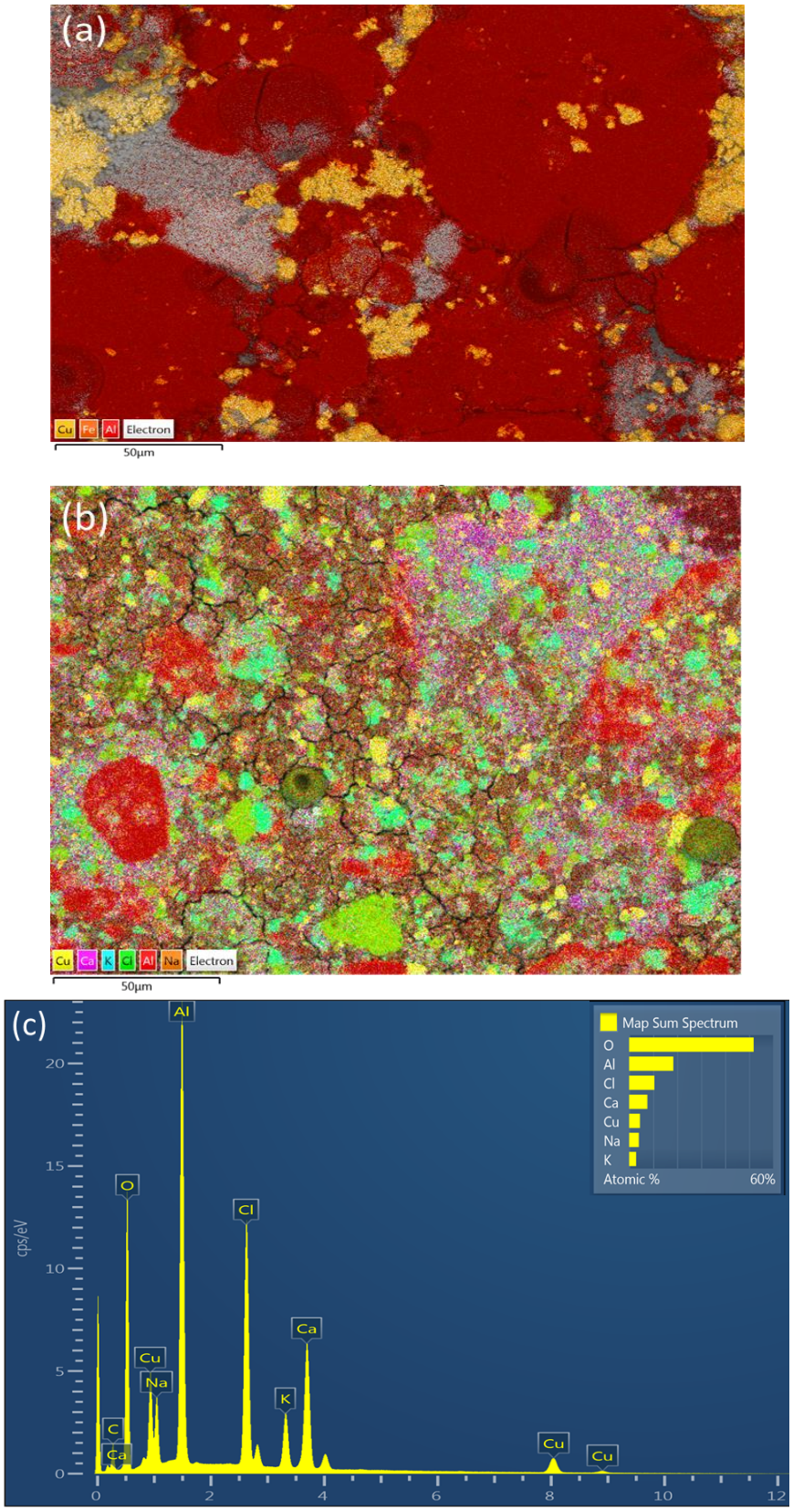

Figure 4-29: a) EDX analysis of sample 75 µm before milling b) Elementary EDX mapping after milling, c) EDX of the milled sample.

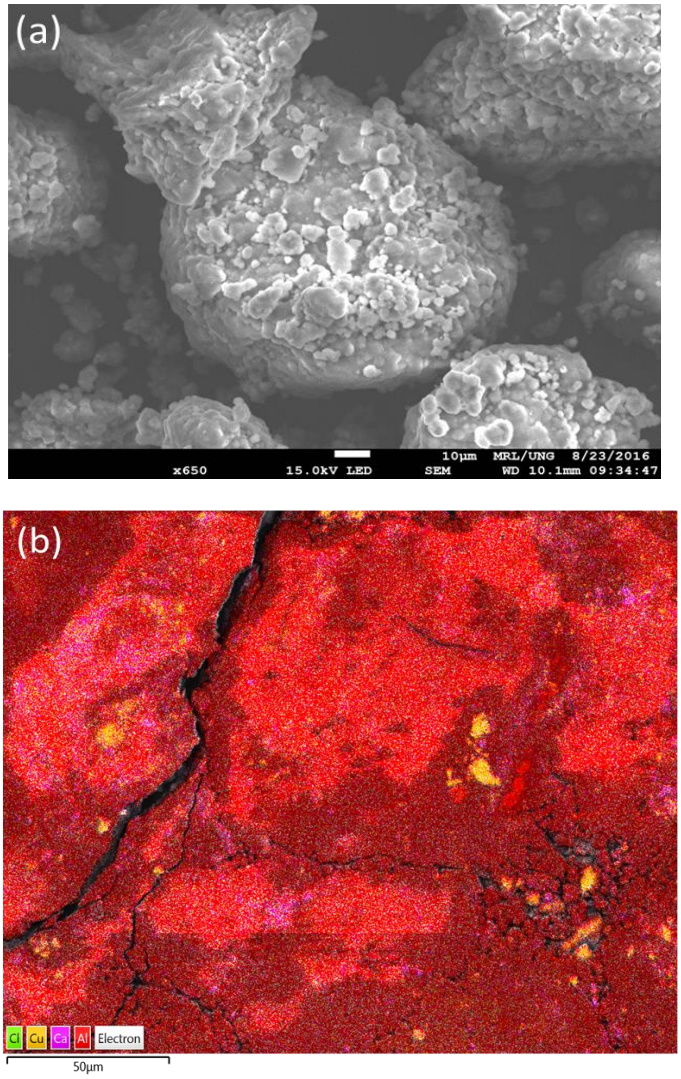

Figure 4-30: a) SEM image of 75 µm particles after 3600 sec reaction showing the barrier layer and the unreacted Al after milling and b) the elemental EDX mapping of the sample.

It has to be acknowledged here that the data collection and analysis was performed externally in Slovenia at the university of Nova Gorica. The same sample, before and after milling, was also subjected to elementary mapping analysis with SEM-EDX pressing the powder flat prior analysis. As an additional measure to check if any products could be identified. Figure 4-29a, b and c, shows the elemental maps together with the EDX spectrum for milled and unmilled samples. In Figure 4-29a, relatively bare Al particles (shown here in red) can be seen with additives (shown here in various colours) only pressed around the borders indicating there is no physical attachment. After milling Figure 4-29b, there is clearly a homogenous

distribution of additives coating the aluminium particles. Figure 4-29c shows the presence of all the additives, however, there is a large quantity of oxygen also detected perhaps because of metal oxides.

It can be hypothesised that the kinetic forces may have been strong enough to break the salt additives enabling the creation of salt-gates when immersed in water. After a 1 hr (3600 sec) reaction, when approximately 40 % hydrogen yield had been achieved with sample 75 μm, the powders were sieved and dried for further analysis. In this instance, loose $Al(OH)_3$ and AlO(OH) were assumed to be removed by filtering the slurry from the solution using a filter paper. Figure 4-30a, shows aluminium 75 μm particles have shrunk. An explanation could be the formation of $Al(OH)_3$ impermeable barrier layer, which prohibited any further reaction. It is important to note that what is not shown in Figure 4-32 and 4-33 was the whitish loose products of by-product $Al(OH)_3$. This analysis only represents a study as to why certain particle sizes and milling conditions appear to show a lower yield. The success of driving the reaction forward for complete formation of hydrogen depends on how the additives are interacting with aluminium core.

From Figure 4-30 a homogenous spread of Al can be seen and a few spots of Ca and Cu originating from surface bound CaO and CuO additives. The small degree of shrinkage of Al particles indicates that the sieved and dried samples 75 μm consist of Al particles that do not optimally produce hydrogen. There is also no indication of the presence of salt additives which points to the possibility that they may have been dissolved in the aqueous solution. Therefore, it can be concluded what is seen here is the barrier layer of Al_2O_3 and $Al(OH)_3$ distributed on approximately 50 μm particles. When XRD was carried out on the stated sample, it showed a considerable amount of Gibbsite γ-$Al(OH)_3$, see Figure 4-31. It was established in the investigation, “Effect of milling time and speed”, that higher milling speed is not favourable as it does not produce desired hydrogen yield. In order to understand the reason of this occurrence, synthesised powders after milling at 520 and 260 rpm were subjected to SEM before and after the reaction with water and their results can be seen in Figure 4-32 and Figure 4-33.

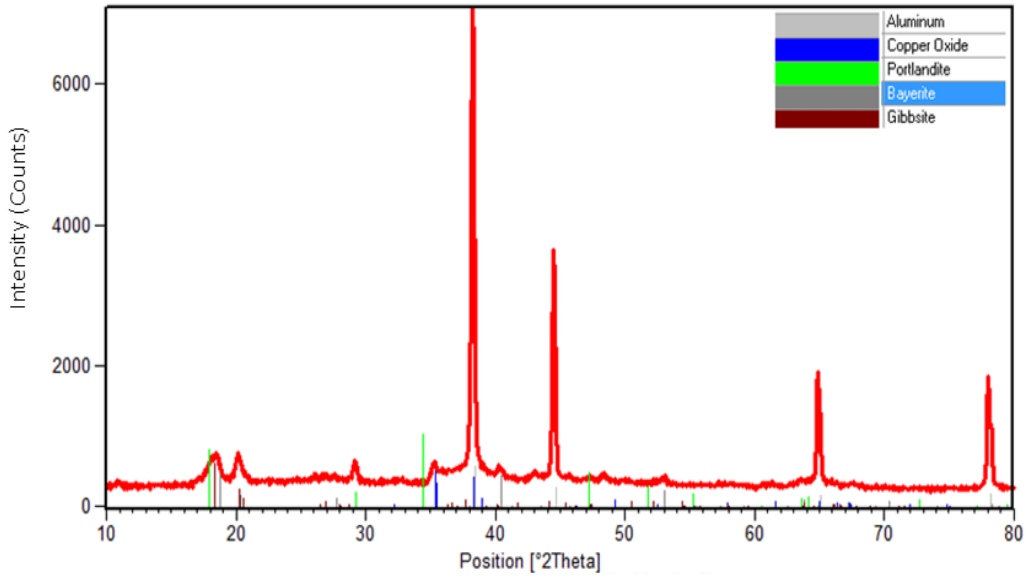

Figure 4-31: XRD analysis of the slurry by-product showing the formation of the surface-bound barrier layer of $Al(OH)_3$.

Based on the SEM images in Figure 4-32 and 4-33 one can understand why high-speed milling during this research was not a suitable choice and why were Al particles prepared from higher speed failed to deliver a good reaction and hydrogen yield. It can be deduced from the SEM images that additives coated the aluminium particle surface. It was also discovered that some of the Al particles sizes have increased and were deformed after the milling. The increase in sizes could be associated with some additives which may have were encapsulated into Al particles.

That meant when synthesised Al particles were reacted with water some of the additives were not exposed and thus were unable to dissolve. It is important that these additives be dissolved or dissociated in water as they help in the formation of salt-gates and increasing the conductivity of water. Whereas, CaO for the critical exothermic reaction and pH increase. Without these additives, the reaction would not be able to progress for long as the formation of $Al(OH)_3$ would not permit water contact with the surface of Al.

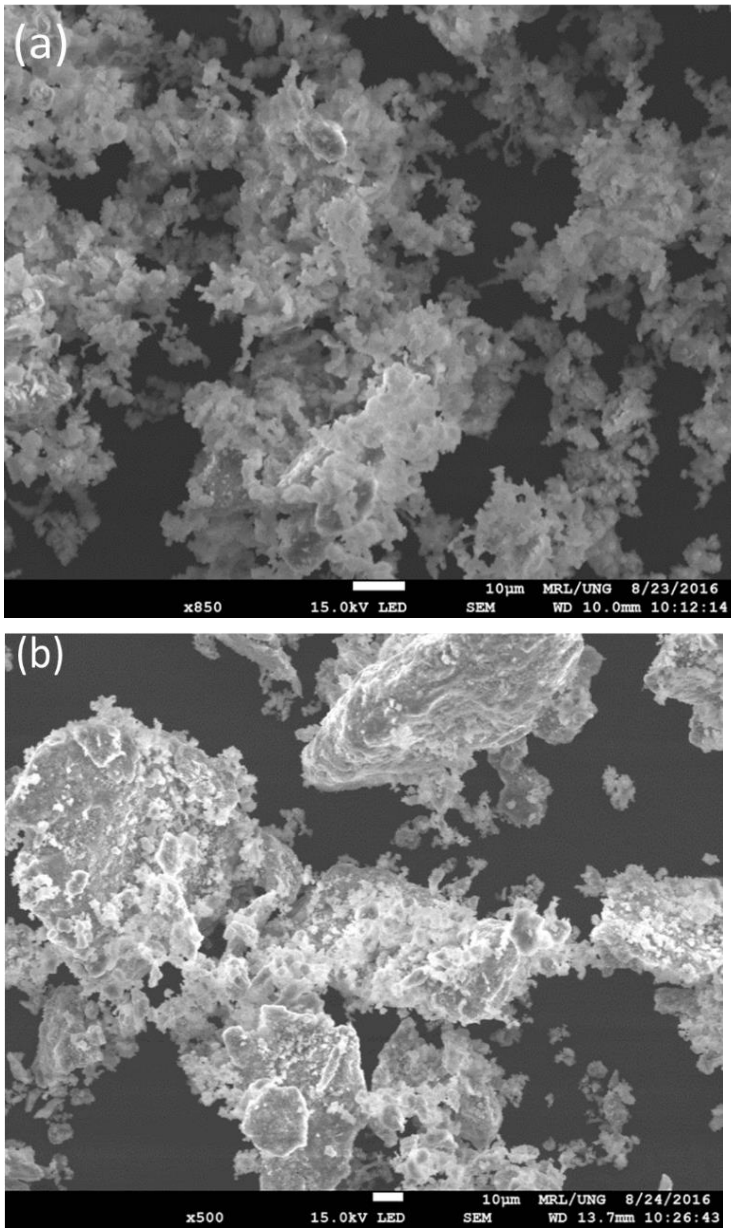

Figure 4-32: SEM of Al + additives milled at 260 rpm a) 1.1 hrs and b) 2.4 hrs.

XRD and EDX from the samples milled at 520 rpm and reacted for 3600 sec indicated the presence of NaCl, CaO and CuO. This further supports the additives encapsulation inside the enlarged particle. Studies conducted in this particle synthesis section provided confirmation that milling of the powder at 260 rpm for 1.1 hrs proved to be a better for hydrogen formation and improving the overall yield, for Al 40 µm sample with (Al 65 wt %, MO 25 wt % and PO 10 wt %). The success of the synthesis can be associated with appropriate mixing and adequate milling conditions, i.e. sufficient temperature fluctuations and the less intensive collisions

during the milling allowing particles to expand and contract and thus helping the additive to form a coat on them.

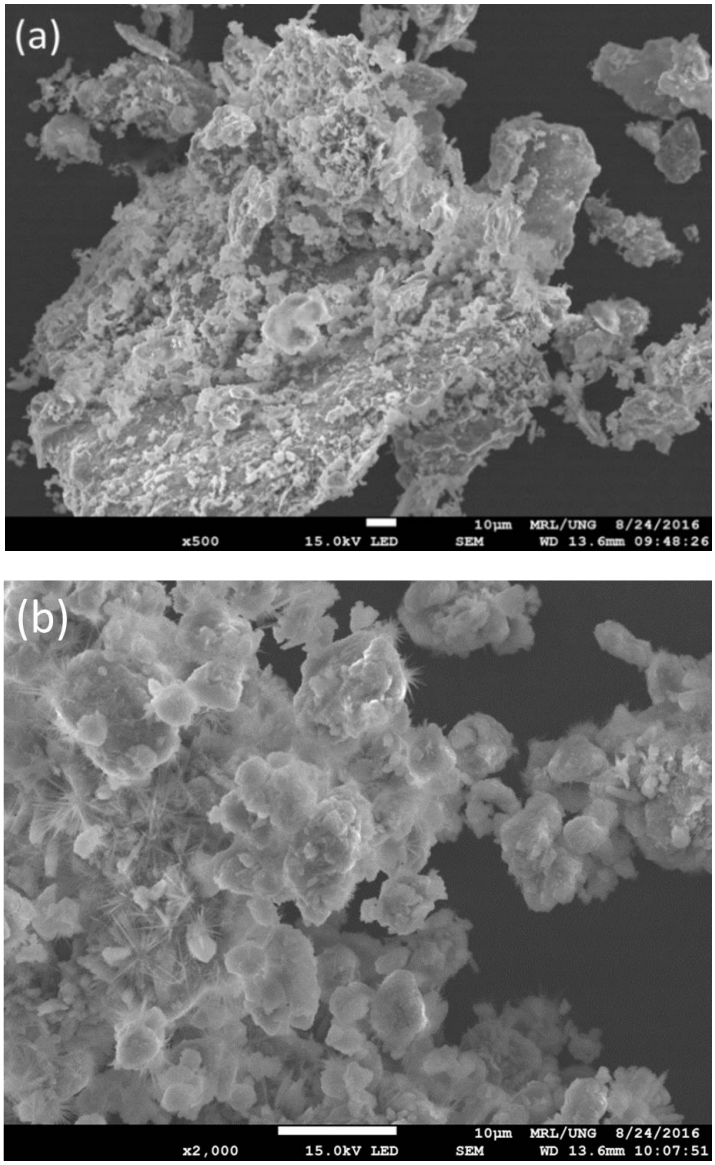

Figure 4-33: SEM of Al + additives milled at 520 rpm a) 1.1hr b) 2.4 hrs.

In support of the proposition that milling of the powder at 260 rpm for 1.1 hrs can provide a better hydrogen formation and improve the overall yield, Al 40 µm with (Al 65 wt %, MO 25 wt % and PO 10 wt %) was prepared. After milling, the synthesised recycled Al powder was reacted with 25 °C deionised water. After 3 hrs reaction time, the by-product was carefully collected and dried at room temperature in a vacuum furnace to avoid the continuation of the hydrolysis reaction. After all the water had evaporated (5 days), the residue was sent for XRD

analysis to Slovenia. The results obtained are presented in Figure 4-32, which provided a comparison of two different XRD's; Red is for the reacted powder and blue for unreacted but milled powder. One can clearly see that majority of the aluminium is gone (note difference in scale). The by-product contained, to the largest extent, Bayerite followed by Nordstrandite and small traces of Gibbsite, all of which are different types of $Al(OH)_3$ of different morphologies. Note, no salt was detected but the $Ca(OH)_2$ has formed some residual $CaCO_3$ that was detected. There are two plausible explanations for the detection of $CaCO_3$ crystals; one being $Ca(OH)_{2,}$ long exposure to air (CO_2) in following step reactions:

$$Ca(OH)_2 \rightarrow Ca^{2+} + 2OH^- \quad (4.7)$$

$$CO_2 + H_2O \rightarrow CO_2 \bullet H_2O \quad (4.11)$$

$$CO_2 \bullet H_2O + 2OH^- \rightarrow CO_3^{2-} + 2H_2O \quad (4.12)$$

$$Ca^{2+} + CO_3^{2-} \rightarrow CaCO_3 \quad (4.13)$$

This hypothesis was also presented by Shih *et al.* [145] and Wang *et al.* both identified $CaCO_3$ from XRD analysis of their by-product, however, they did not comment further on its presence. Another possibility can be related to the purity of the CaO which was used for this research. It can be concluded that 40 µm Al particles when milled with the right combination of additives, (MO+Salt) and adequate milling parameters can achieve favourable results.

As stated earlier in the literature review that, different crystals forms of $Al(OH)_3$ can be produced during the reaction. These different crystal structures and one of these crystal sutures and density reflects on their physical stabilities where it, which allows the water movement inside and out these layers. As it can be seen in the Figure 4-33, XRD, when it was performed after the reaction a large amount of Gibbsite and Bayerite, was found. Bayerite is slighted better as it holds the aluminium particles together, while a slower reaction continued to consume aluminium core while also dissolving and recrystallizing existing bayerite, forming a more porous layer [148].

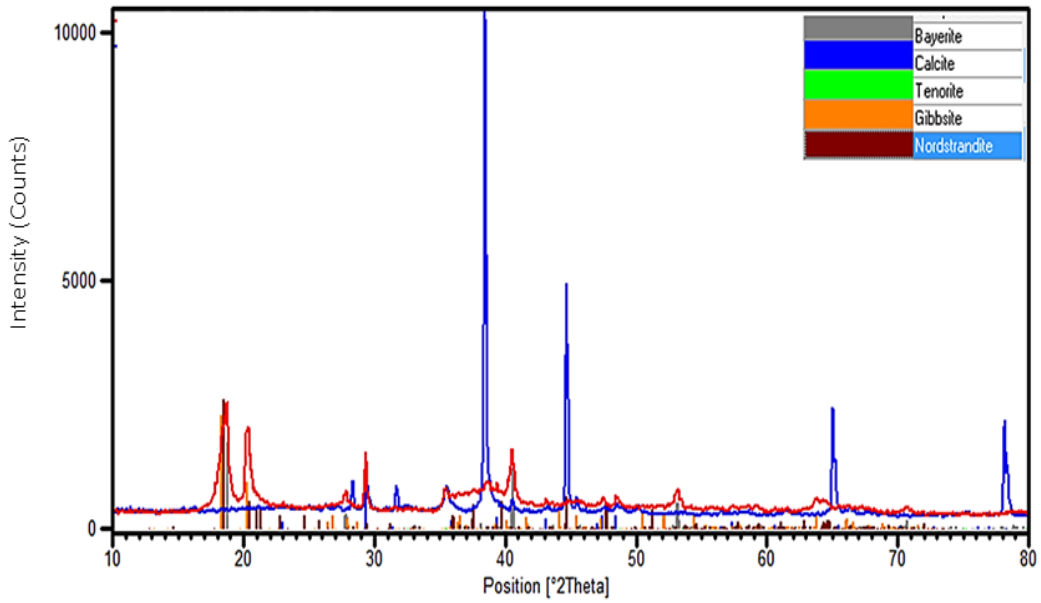

Figure 4-34: XRD of 10000 sec reacted particles showing the formation of the surface bound $Al(OH)_3$ with various morphologies, Blue is representing unreacted and red reacted.

During the complex course of the ageing of aluminium hydroxide, which is first formed in an amorphous form (and will therefore not be detected in XRD), still another aluminium tri-hydroxide, gibbsite or hydrargillite, can also be formed, especially if ions of the alkali metals, i.e. CaO are present, therefore, i.e. Na^+ or K^+ from the dissolved salts. From the XRD is was concluded that both $Al(OH)_3$ structures of Gibbsite and Bayerite were formed which can be described by the above discussion.

4.1.5 Conclusion for Section A Particle Synthesis

Based on the findings from section A, it can be concluded that aluminium particles on their own milled not milled do not produce any hydrogen at ambient conditions. During high-speed milling changes the particles morphologies and possibly physical properties because of the high temperature generated during the process. This was found to be beneficial for hydrogen generation. It was established that the metal oxide and salt milling additives synergistically were able to produce high hydrogen yield from 85 % to 92 %. It was found that a specially developed milling programme was able to produce highly reactive particles with a comparatively small energy input, with reduced milling time and milling speed. Importance of

metal oxides and salts was established as they help synergistically to produce high hydrogen yield. Salt additive helped in achieving a stable reaction rate for hydrogen fuel cell use. It was also established from the analysis that they were embedded in the outer layer and possibly within the surface of the softer aluminium particles. When reacted with water, Al particles were dissolved leaving behind salts gates created by a local aggressive electrolyte from the Cl^- ions, through which water was able to reach the surface/core of Al metal particle. The combination of CaO and CuO was found to be ideal for hydrogen generation from both economical and efficiency point of view. PO employment encouraged a favourable reaction due to the chemical and physical properties of the different salts, and their combination enabling Al activation.

4.2 Section B Effect upon hydrogen generation due to the varied solutions

In section A, active particle synthesis was described and evaluated by reacting the synthesised product with deionised water. Section B will focus on the effect of water quality and different aqueous solutions on the hydrogen generation. Relevant parameters will be analysed for the aluminium–water reaction including the effects of agitation, particle loading, initial temperature and pH. As the raw material for the reaction was synthesised in-house, it was decided to independently explore its performance in terms of its potential to generate hydrogen under different conditions.

4.2.1 Effect of agitation

Agitation is the process of stirring or mixing. It can improve the miscibility of phases and facilitate heat transfer. A study was undertaken to measure the effect of the agitation speed on the reaction kinetics. Agitation speeds of 0, 600, 700 and 1100 rpm were employed. In Figure 4-34, it can be seen that agitation speed had a noticeable effect on the reaction kinetics. The best outcome was achieved when using 700 rpm followed by 600 rpm and 1100 rpm. Corresponding to hydrogen yields of 85 %, 62 % and 60 % of 10000 sec reaction time, respectively.

As in section A, the reaction temperature was monitored to give an indication of its progress. As it is an exothermic reaction, higher temperatures would indicate more reaction is taking place and hence higher volumes of H_2 are being generated. The reaction temperature as a function of time is plotted in Figure 4-34b. It can be seen that all three agitation speeds followed the same temperature increase trend. One can see in Figure 4-34b, that after ~2000 sec the exothermic reaction temperatures had peaked in the reactor presumably because of a change in the pH. It can be said that agitation speed and temperature of the solution are critical for the reaction efficiency and volume of hydrogen gas generation.

This was verified when the non-agitated sample (0 rpm) exhibited significant slower hydrogen generation rate than the samples which were subjected to agitation. Additionally, the yield from non-agitated was only 21 % of a total (260

ml) possible from 0.3 g loading of activated aluminium. It was also observed that without agitation the temperature does not increase.

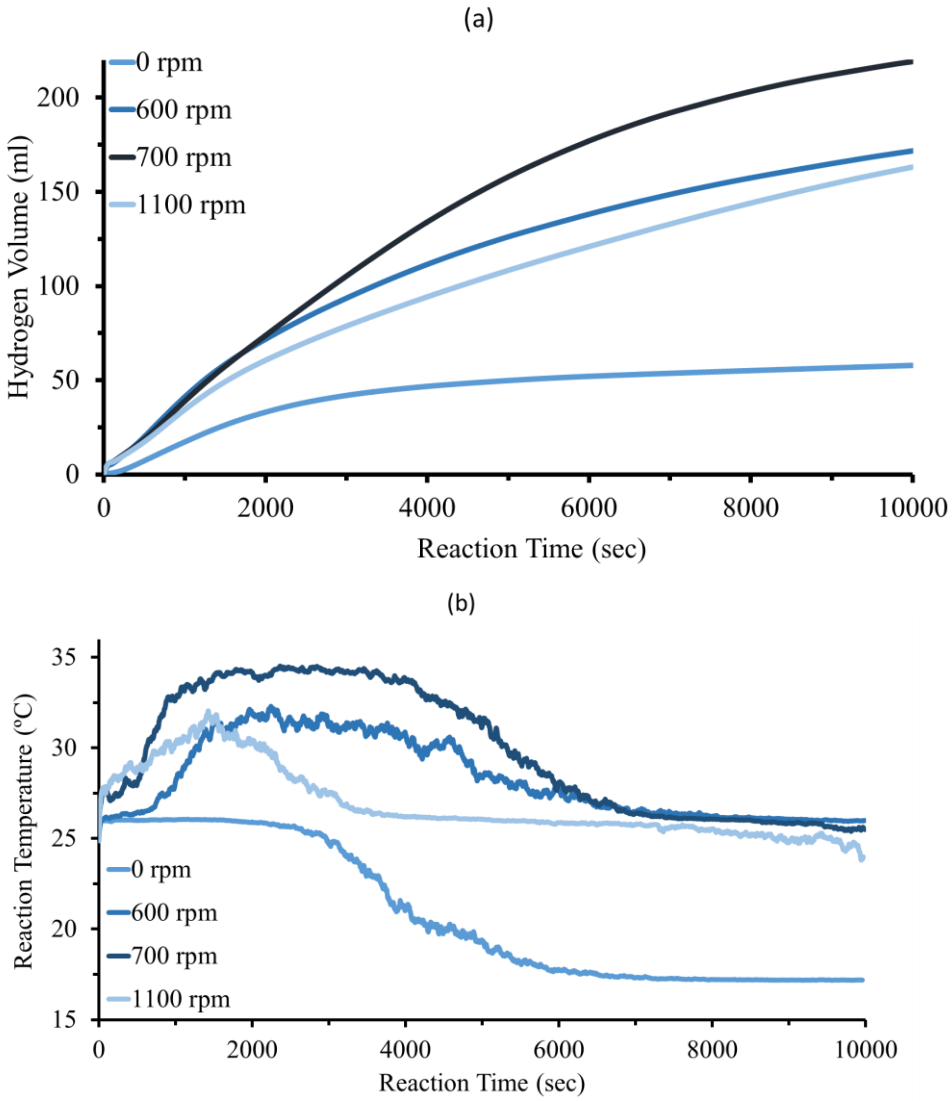

Figure 4-35: a) Volume of hydrogen gas generated using different agitation speeds of 0, 600, 700 and 1100 rpm and b) corresponding reactor fluid temperature.

The plausible reason that temperature of the reaction decreasing can be associated with the presence of the salts in the system and lack of mixing. Since there was no agitation taking place resulting in less mass transfer to occur and due to that reason, this particular reaction was not dynamic. However, the reaction did take place indicating a certain amount of aluminium hydroxide layer would have been produced on the active sites on the surface of metal particles thus blocking continuation of the process. The temperature increase is linked with the exothermic

nature of reaction since no kinetic reaction or reduced reaction was taking place it resulted in no heat being generated. Additionally, salts absorb heat during the time when no kinetics were taking place. The salts were adsorbing the heat of the water and reducing the temperature.

Heat generated from the reaction increases the temperature of the fluid in which reaction was taking place. During the reaction, aluminium hydroxide $Al(OH)_3$ is formed and its formation is influenced by the pH as suggested by Prodromou *et al.* [146]. The pH can be affected by the formation of OH^- ion from $Ca(OH)_2$ dissociation. This dissociation reaction is exothermic and which also depends on the temperature, i.e. decreases with increased temperature. The equation describing the reaction is:

$$Ca(OH)_2\ (aq) \rightleftharpoons Ca^{2+} + 2OH^- \quad \Delta H_r = -16.64\ kJ/mol \qquad (4.7)$$

According to the Le Chatelier's principle [147], for an exothermic reaction an increase in temperature results in a shift of equilibrium to the left. Therefore, one can assume that as the temperature is increased, fewer OH^- are formed from $Ca(OH)_2$ reducing the pH of the solution, i.e. making it more acidic. This has a direct effect on the crystal structure (or even crystallisation) of $Al(OH)_3$ that is formed in the $Al+H_2O$ reaction. The different structures of aluminium hydroxide, e.g. α-$Al(OH)_3$, β-$Al(OH)_3$ and γ-$Al(OH)_3$ have different densities and porosities [148]. If, for example, the most porous hydroxide layer, i.e. γ-$Al(OH)_3$ is favoured, it would permit increased mass diffusion (H_2O and H_2) than the more densely packed layer, i.e. α-$Al(OH)_3$. Therefore, it is concluded that the depending on which type of layer of $Al(OH)_3$ is produced, the effect of agitation will be different. For example, removal would be more efficient if γ-$Al(OH)_3$ layer is formed compared to when α layer is produced.

It was unexpected to see that the highest agitation speed of 1100 rpm performed inferior to lower speeds of 700 rpm and 600 rpm for hydrogen generation. It is possible that at 1100 rpm higher turbulence occurred inside the reacting mixture, compared to lower speeds stated above, adversely impacting the reaction rate. Here it is perhaps useful to compare with the temperature plot in Figure 4-34b and relate it to heat transfer effect. With higher agitation speeds, the velocity of the reactor

vessel fluid increases and an increased corrosive heat transfer will occur towards the colder outer surroundings of the reactor vessel. This reduces the local temperature and hence the reaction rate. It was found that 700 rpm provides the best agitation solution for the reaction. It must be reminded that the reactor vessel was well insulated with polystyrene street to avoid any heat loss during the reaction.

Additionally, the improved hydrogen generation when agitation was employed compared to when it was not carried out can also be explained by sedimentation (settling). When the powder is added to the reactor vessel, it settles at the bottom, causing the particles to sit on top of each other. This reduces the necessary mass transfer of water through the salt gates and the formed hydrogen to escape as bubbles towards the hydrogen gas flow meter. Hydrogen bubbles are released when they build up a certain pressure and will diffuse out. The principle of the H_2 formation and the gas discharge is shown in Figure 4-35.

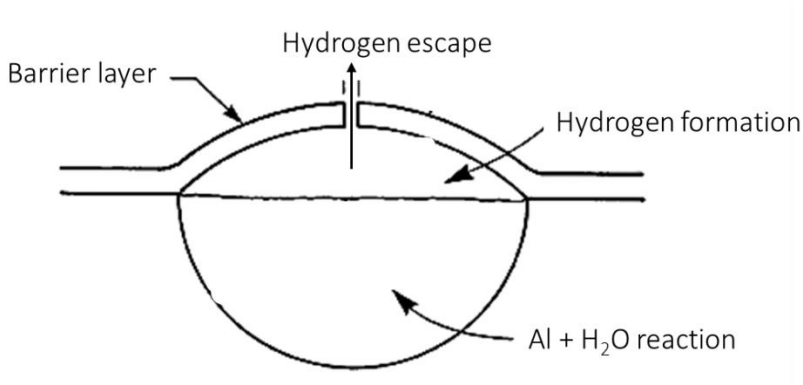

Figure 4-36: Principle of hydrogen bubble formation inside the Al particle covered with Al/AlO(OH)/Al(OH)$_3$ barrier layer.

From the above, it can be concluded that agitation is essential for hydrogen generation. It promotes the shedding of porous hydroxyl layers, in particular, the formed γ-Boehmite, thereby helping the necessary mass diffusion to occur. On the other hand, it was found that high agitation speed speeds (> 700 rpm) are detrimental for reaction as it leads to a reduction of temperature due to improved corrosive heat transfer towards the colder surrounding.

4.2.2 Effect of particle loading

Based on the agitation study and the observed mass transfer effect, it was decided to investigate the particle loading in the reactor vessel. As the reaction is exothermic, it can be argued that, if a small amount of water were to be added to 0.3 g of activated aluminium, it would lead to a sudden increase in the reaction temperature. On the other hand, a surplus amount of water, due to its heat capacity would assist in controlling the reactor vessels temperature. The effect of loading of Al was studied by using three different loadings of 0.3 g, 0.5 g and 0.7 g and adding 9 ml water corresponding to mass concentrations of 0.03 g/ml, 0.05 g/ml and 0.07 g/ml, respectively. The powder composition was kept the same as before, i.e. Al 65 wt %, MO 25 wt % and PO 10 wt %. Only a 40 µm Al particle size was used for comparison purposes.

The results obtained from the experiments were normalised to the weight of aluminium (gram) in each batch. Normalisation was carried out for 0.3 g of powder which helped to determine the actual volume of hydrogen (ml) produced from the reaction. From the Figure 4-36, it can be seen that all three loadings followed the same trend but, 0.03 g/ml produced the highest volume of hydrogen from the three concentrations compared. This was confirmed after reproducible results were obtained upon repeating.

It can be seen in Figure 4-36a, that there is a lag time for hydrogen formation when the experiment was conducted for the maximum loading of 0.7 g (0.07 g/ml). On the other hand, in Figure 4-36b, no such lag time is observed as the reaction temperature rose to 35 ºC from 25 ºC within 5 sec of the reaction.

$$Al + 3H_2O \rightarrow Al(OH)_3 + 1.5H_2, \qquad \Delta H_r = -280 \text{ kJ/mol} \qquad (4.15)$$

As shown in Figure 4-36b, it can be concluded that hydrogen gas is formed instantly as evidenced by a rapid increase in temperature (indicating exothermic reaction) recorded by the thermocouple, despite hydrogen gas, not been registered on the GFM. The observed lag time of 0.7 g (0.07 g/ml) loading can be explained with the help of Figure 4-37.

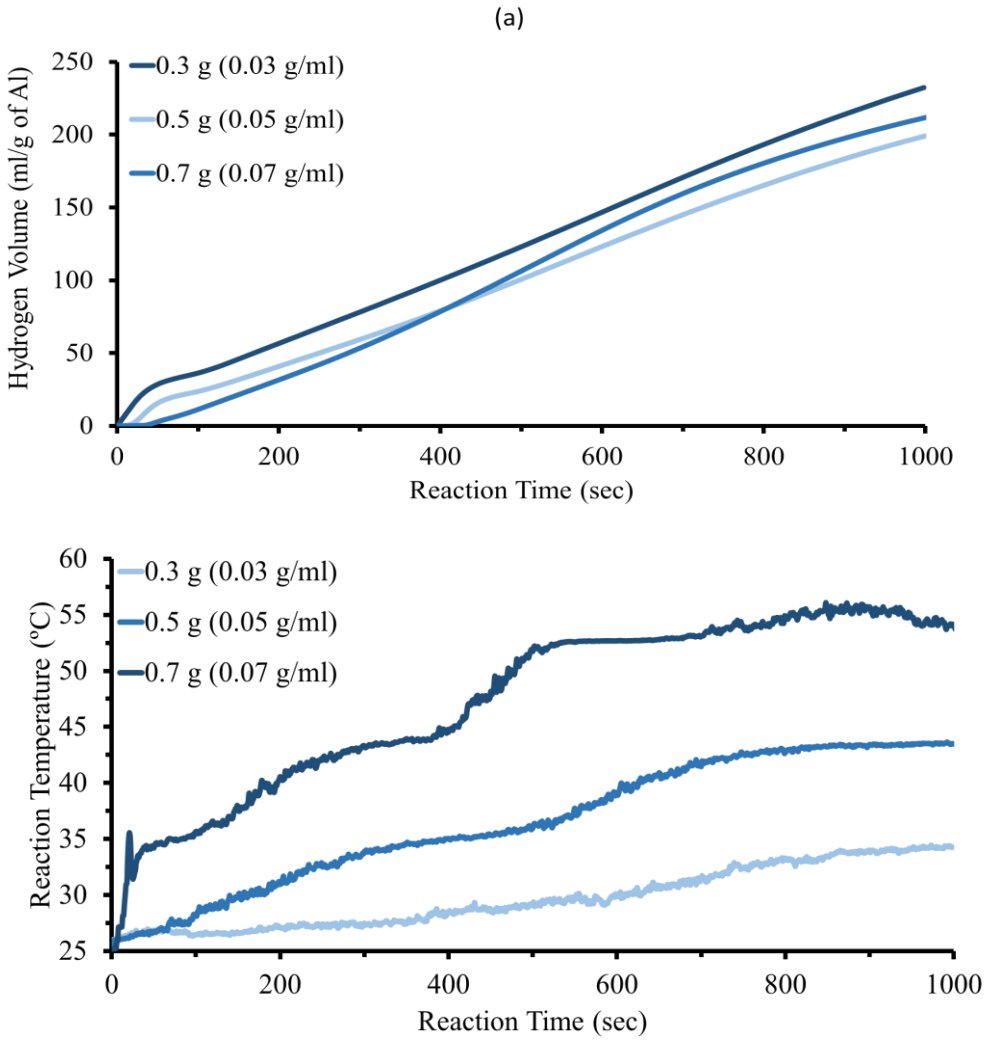

Figure 4-37: Loading effect on a) hydrogen generation and b) reaction vessel temperature, using 0.3 g, 0.5 g and 0.7 g particle loading in 9 ml water.

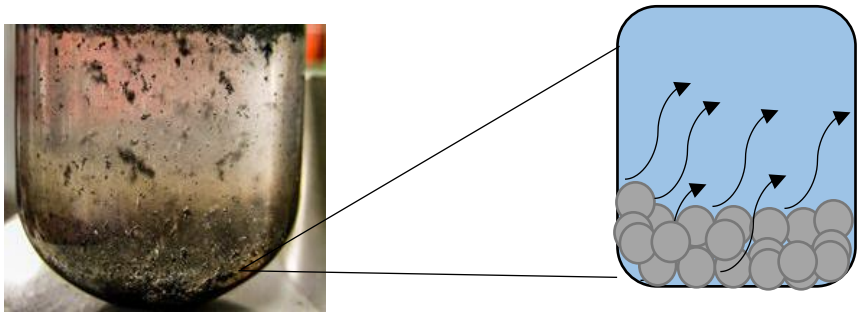

Figure 4-38: Diffusion pathway of the formed hydrogen gas. Schematic shows clarification of the pathway from sediment particles.

As stated in earlier discussions, the effect of sedimentation on the particles may prevent formed hydrogen gas to diffuse away from particles. A higher loading of the particles can hinder this further and will manifest in lag time. Another

observation made for 0.7g (0.07 g/ml), was that the reaction generated a higher temperature, which rose gradually from 25 ºC up to 55 ºC in 1000 sec. This can help to explain why more hydrogen is formed in shorter time, see Figure 4-36. From this study, it becomes apparent that using the correct ratio of powder to water for the reaction is important. Rosenband *et al.* have suggested that loading is an important factor for an H_2 generation [40]. Therefore, an experiment was carried out to gauge the optimum ratio of powder to water. Although higher reactor temperatures improve the reaction rate, higher water to powder loading ratio brings an increased control of access heat formation.

For further investigations, (results not shown in Figure 4-36), loading of activated aluminium was kept at 0.3 g, but only 2 ml of deionised water (0.15 g/ml) was added to the powder. This experiment was conducted to inspect what occurs when water ratio is kept close to the stoichiometric ratio. As soon as water came into contact with the activated aluminium, a sudden spike in the temperature inside reactor vessel was recorded. The temperature of water reached 91 °C from room temperature within the first few sec of the reaction. Also, with increased temperature, a surge of water vapour or hydrogen gas was given off, GFM was unable to record the flow rate and presented out of range error followed by an abrupt halt in the reaction. An explanation for this intense reaction (which abruptly stopped) and heat generation observed despite theoretically the same amount of exothermic heat would be released according to equation 4-15, that at this accelerated temperature rise, water will evaporate or even boil off too rapidly. If the reactor vessel is connected *in-situ* with a fuel cell, then the possible generated water vapours could cause damage to PEM membrane.

It can be concluded from this investigation that using excess water not only provides the benefit of cooling the reactor vessel, but also helps to control of the reaction kinetics. Except for the 0.15 g/ml particle loading, the 0.03, 0.05 and 0.07 g/ml provided similar hydrogen yield per gram Al but at different time scale.

4.2.3 Effect of initial reaction temperature

Results reported in the previous section showed that an increase in temperature during the reaction improves the hydrogen generation and the overall hydrogen yield on a shorter timescale. Therefore, the initial reaction temperature was varied to determine whether it has any influence on the overall reaction and hydrogen yield. The results of this experiment are plotted in Figure 4-38. One can see that when an initial temperature of the water was 25 ºC and activated aluminium was reacted with it, the reaction between them was rapid. A steep slope can be viewed in the Figure 4-38 indicating a higher rate of hydrogen formation, but the rate slows down after 100 sec. Interestingly, the rates of the reaction from the other runs with 32 °C and 45 °C initial water temperatures were slower than 25 °C before 100 sec but increased afterwards.

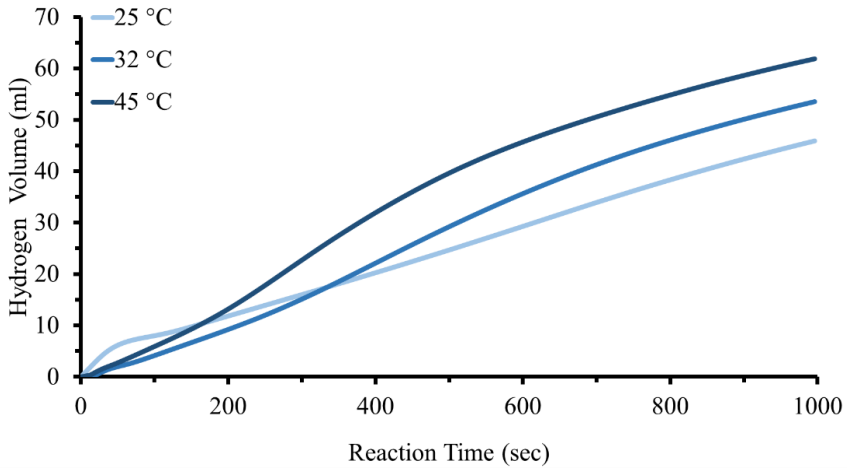

Figure 4-39: Effect of initial reaction temperature of the water during hydrogen generation during 1000 sec reaction.

The effect of initial reaction temperature has already been studied by a number of groups [52,75,93]. Chen et *al*. in 2013 pointed out that there is a correlation between the solubility of additives (salt and metal oxide additives) and temperature of the solution [93]. Haynes *et al.* suggested that any temperature change of the solution would affect the solubility of salt and metal oxides if they are present in that solution [149]. For example, CaO is a metal oxide and it forms $Ca(OH)_2$. Its solubility would decrease with increasing temperature [93]. Therefore, a lower temperature could release more OH^- ions into the solution originating from the CaO milling additive, which is beneficial for the hydrogen formation.

For salt additives such as metal halides, the dependence is more complex. This is because a small change in temperature does not influence NaCl solubility while KCl solubility increases slightly. Both these salts are dissolving endothermic, i.e. absorb heat energy from the water. On the other hand, the solubility of $CaCl_2$ increases by two times as the temperature rises from 25 °C and 45 °C [149].

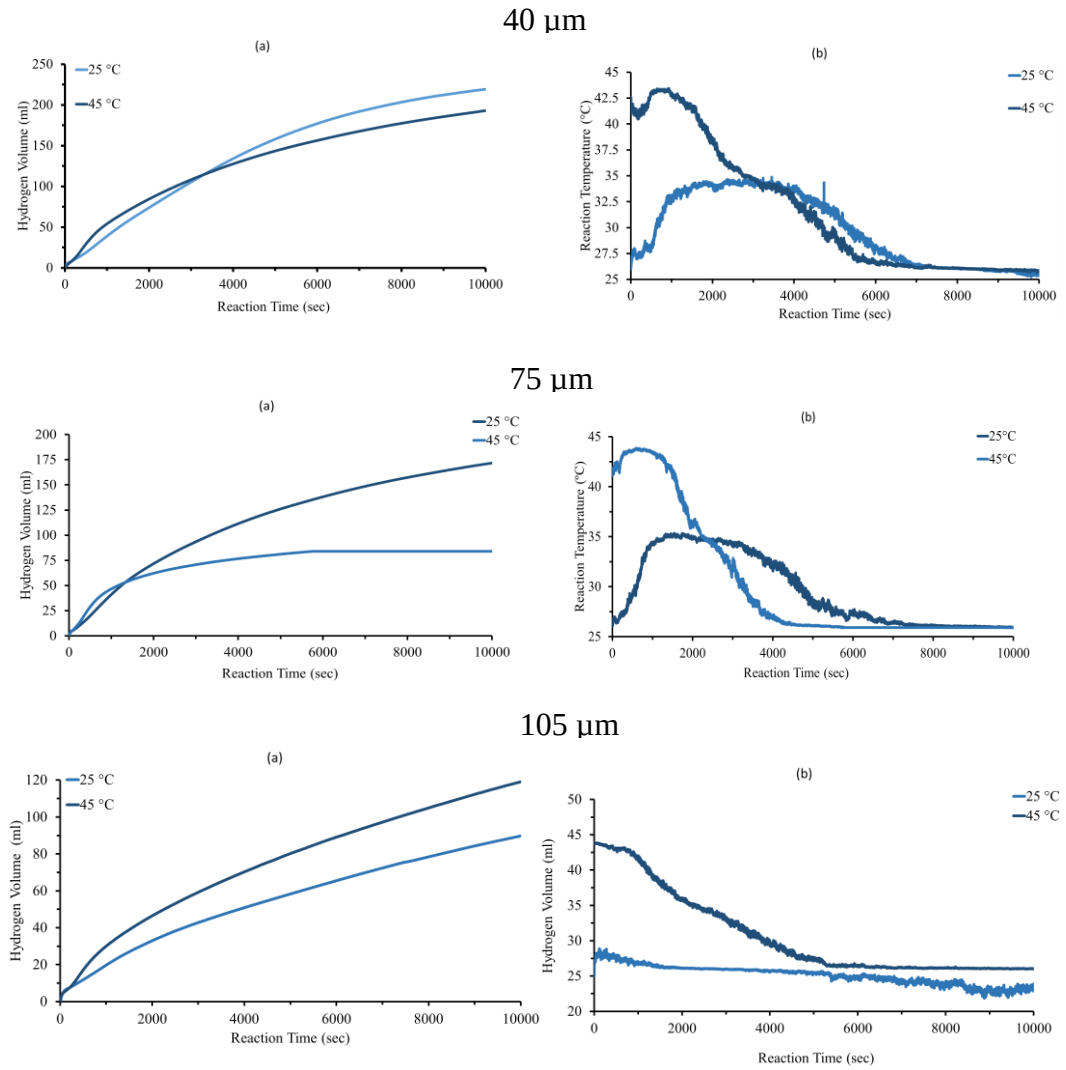

Figure 4-40: a) Effect of initial reaction temperature on hydrogen generation during 10000 sec reaction. b) Temperature profile as the reaction happens. The first row is showing 40 µm, second row 75 µm and last 105 µm Al particles.

The effect of initial temperature was also explored for different particle sizes. Although, in section A it was established that using 40 µm provides a better yield but for this study, Al particle sizes of 75 µm and 105 µm were also selected. It was conducted to observe their response to the initial temperature change and the

temperatures chosen for this study were 25 °C and 45 °C. Figure 4-39, presents the results obtained from the investigation.

As the Figure 4-6 shows that when 40 µm Al particles were reacted with deionised water at the initial temperature of 45 °C, hydrogen generated after 3000 sec was marginally more than when water temperature was 25 °C. However, the yield of the reaction (> 10000 sec) for the case of 25 °C water was 85 %, but 73 % of water at 45 °C.

This result indicated that the initial temperature of 45 °C was not suitable for the reaction. When Al particles of 75 µm average size were independently subjected to these temperatures, a similar trend to that seen for particles of 40 µm size was observed. The results of this reaction are shown in Figure 4-39b. It can be seen that initially the reaction rate is faster with a temperature of 45 °C, but reaches a plateau after approximately 1700 sec. In contrast, when the temperature was 25 °C, the reaction starts gradually and continues on until the measurement is stopped (> 10000 sec). At the end of the reaction, the yields that were recorded were 66 % for 25 °C and 28 % for 45 °C water. On the contrary, when Al 105 µm was reacted with water, a real improvement at 45 °C was observed from the start until the end of the reaction, see Figure 4-39c. Yields from after 10000 sec was 46 % at 45 ºC and only 35 % when reacted at an initial water temperature of 25 ºC.

It can be concluded that lower temperature helps in achieving a higher reaction rate and hydrogen yield. The variation in hydrogen production with initial temperature can be associated with both the gain of energy by particles to overcome the activation energy of the Al + H_2O reaction and from the variation of additives (salts and metal oxide) solubility. Increase in temperature improves the rate of reaction as supports by many studies but it also affects the solubility [17,95]. It is suggested by Chen *et al.* 2013 where they reported that temperature of 30 ºC was favourable during their research. It can be said that this study provided an understanding and importance of the solubility of CaO and salts as milling additives. The type of surface-bound aluminium hydroxide formed during the reaction can also be influenced by pH and temperature [79]; amorphous α-$Al(OH)_3$→ β-$Al(OH)_3$ → γ-$Al(OH)_3$.

With regards to the larger particle size, after milling when it was presented in water, the metal oxide layers and salts on the surface of the particle would dissolve. However, due to the insufficient surface area, it may not get enough coverage of CaO during the milling. Therefore, less of $Ca(OH)_2$ dissociation would take place. It is a possibility that high temperature would not influence $Ca(OH)_2$ dissociation, since little quantity of CaO is coating the Al particle. On the other hand, the solubility of $CaCl_2$ would increase, which will aid in the hydrolysis reaction. At the same time due to less coverage of $Ca(OH)_2$, the pH would also be affected, which will consequently produce more porous $Al(OH)_3$ which would help in the continuation of the reaction.

4.2.4 Effect of pH on activated aluminium

As it has been mentioned already, one of the several factors that can also influence the reaction is pH. Therefore, the effect of pH on the hydrogen yield and reaction was studied by varying the pH (pH 3 to 11) of water by adding either NaOH or HCl. Since NaOH and HCl will be used for this study, it was decided that 75 µm particles will be employed. It was understood that 75 µm reaction rate will be slower than 40 µm particles which will help would prevent a runaway reaction. Therefore, 75 µm sized recycled Al particles were milled together with 25 wt % CuO/CaO and 10 wt % PO salt additives. Milling programme 1a with speeds of 260 rpm was used. 0.3 g of activated aluminium with 9 ml of water with an initial temperature of the water at 25 ºC and agitation speed at 700 rpm.

It can be seen from the Figures 4-40 and Figure 4-41, that pH clearly has an effect on the production of hydrogen. In Figure 4-40a, the results of experiments using solutions with different alkaline strength, i.e. pH 9 and pH 11 are compared with deionised water (pH 7). It was seen that the solution containing pH 11 produced on average 20 ml of hydrogen gas in about 1000 sec, whereas the solution of pH 9 produced approximately half the amount of hydrogen.

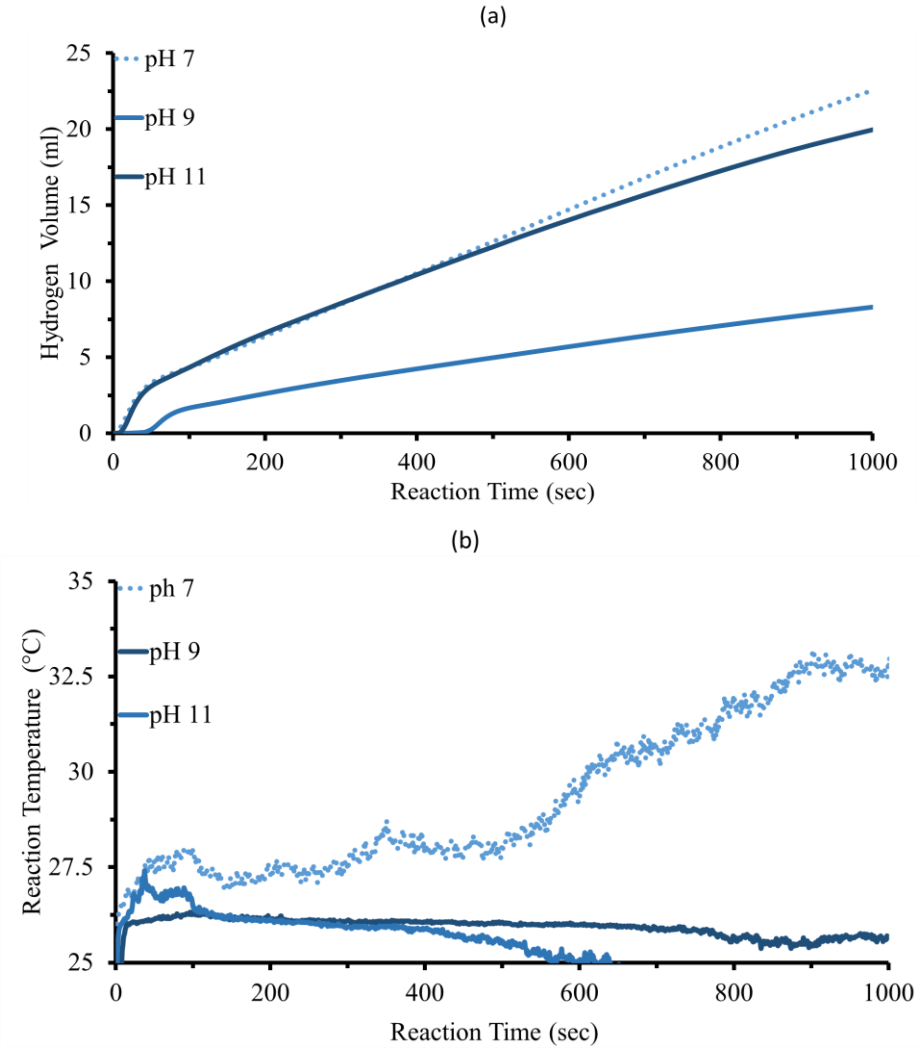

Figure 4-41: a) pH effect on the hydrogen formation using NaOH as an alkaline and b) Temperature reaction.

Similarly, acidic solutions with pH 3 and 5 were also compared with water in a separate experiment and the results are displayed in Figure 4-41a. It can be seen that very acidic solution produces a higher yield than when the solution is only slightly acidic (pH 5). The yield was found to be again high when the solution was neutral. In both cases, when the pH was closest to the neutral value, i.e. pH 5 (acid solution) and pH 9 (alkaline solution), not only was the hydrogen yield relatively poor but also a lag time of 50-100 sec was observed before the onset of reaction.

To explain this observation, it is important to recognise that aluminium is a metal whose oxides or hydroxides are amphoteric. An amphoteric species is capable of reacting with both acidic and alkali solutions. Under normal circumstances,

aluminium own its own does not react with water due to an impermeable protective layer of aluminium oxide as mentioned earlier.

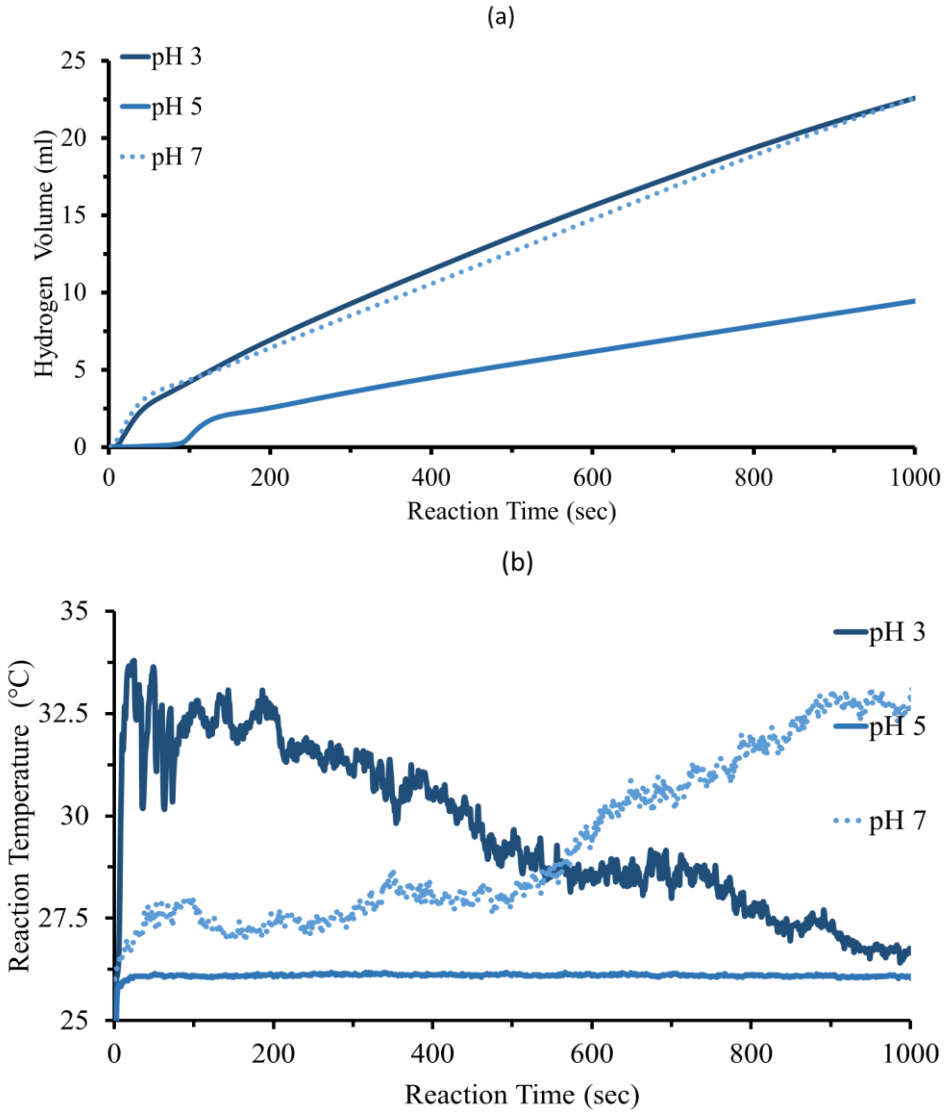

Figure 4-42: a) pH effect on the hydrogen formation using HCl as an acid agent and b) Temperature reaction.

However, as additives are also present together with aluminium in the reacting mixture, a deviation from its inert nature is expected, especially when pH, temperature or any other parameter is changed. The effect of alkalinity can be understood by recalling from section A, that when CaO additive was added into water, it dissociates and forms $Ca(OH)_2$ and the concentration of OH^- and hence the pH increased as a result. In the same fashion, the addition of NaOH in water will release OH^- ions raising the pH of the solution. There may, however, also be other

reactions that can occur in the presence of NaOH. For example, salt gates on the surface of particles and the variation of additives such as (MO+PO) can lead to different reactions with NaOH. To take an example, Sodium hydroxide, NaOH can react with Al/Al_2O_3 in the following way:

$$Al + NaOH + H_2O \rightarrow NaAlO_2 + 1.5H_2 \quad (4.16)$$

Or

$$Al_2O_3 + 2NaOH + 3H_2O \rightarrow 2NaAl(OH)_4 \quad (4.17)$$

where the latter reaction can be described by the formed $Al(OH)_3$ outer layer reacting with the NaOH as:

$$Al(OH)_3 + NaOH \rightarrow NaAl(OH)_4 \quad (4.18)$$

Formed $NaAl(OH)_4$ dissociate to aluminates, $Al(OH)_4^-$ and Na^+ as;

$$2Al + 6H_2O \rightarrow 2Al(OH)_3 + 3H_2 \quad (4.1)$$

$$Al(OH)_3 + NaOH \rightarrow Na^+ + Al(OH)_4^- \quad (4.19)$$

This means that adding NaOH helps to dissolve the Al/ $Al(OH)_3$. Whereas for the metal oxide additive CaO the reaction with NaOH is:

$$CaO + 2NaOH \rightarrow Ca(OH)_2 + Na_2O \quad (4.20)$$

, where Na_2O rapidly reacts with water as:

$$Na_2O + H_2O \rightarrow 2NaOH + O_2 \quad (4.21)$$

At high pH, $Ca(OH)_2$ dissociates to OH^- ions and makes the solution more alkaline which helps corrosion of Al layer and thus in an H_2 generation. pH 9 reaction temperature was declining faster unlike pH 11 (seen clearer in the temperature plot). Here it is important to revise the equilibrium equation 4.7, with an equilibrium constant of $K= 5.0 \times 10^6 = [Ca^{2+}] [OH^-]^2$, meaning that if more OH^- is added, the reaction will reverse until a point where $Ca(OH)_2$ would precipitate from solution. To sum up, the NaOH addition will reduce the previous benefits which have been demonstrated by the CaO milling additive. With regards to the CuO, which is not soluble in water may react with NaOH as follows:

$$CuO + NaOH \rightarrow CuOH + NaO \quad (4.22)$$

The reaction of CuO with NaOH is pH and temperature dependent, as described by Palmer and Benezeth in the study of solubility of copper oxides in water [150]. With regards to the salts present in the activated aluminium, they may also be affected

by the presence of NaOH. For example, $CaCl_2$ salt NaOH may react in a high concentration of NaOH as:

$$CaCl_2 + 2NaOH \rightarrow Ca(OH)_2 + 2NaCl \quad (4.23)$$

On the contrary, KCl and NaCl salts solubility is compromised in the presence of NaOH. This would affect the corrosion of Al surface and passive oxide layer Al_2O_3. If this were to happen then a significant lag time should be expected (pH 9) see Figure 4-40a. Therefore, it can be concluded that reaction with NaOH can generate hydrogen gas. To account for the observation made with an acidic solution, one can say that, when CaO is presented in deionised water, irrespective of the pH, it produces OH^- ions and will work to neutralise the acid (HCl). The amount of neutralisation would depend on the wt % of MO (CaO: 12.5 %) in the mixture. This hypothesis could possibly be used to explain the difference in hydrogen yields pH of 3 and pH 5 when activated aluminium was reacted. Under highly acidic conditions, aluminium can react to undergo the following reaction to produce H_2:

$$2Al + 6HCl \rightarrow 2AlCl_3 + 3H_2 \quad (4.24)$$

The formed aluminium chloride, $AlCl_3$ salt will dissociate in water as:

$$AlCl_3 \rightarrow Al^{3+} + 3Cl^- \quad (4.25)$$

Water molecules would rapidly attract Al^{+3} to form a complex (hydrated Al^{3+} ion) as proposed by Greenwood *et al.*[133]:

$$AlCl_3(s) + H_2O \rightarrow [Al(H_2O)_6]^{3+}(aq) + 3Cl^-(aq) \quad (4.26)$$

The formation of $AlCl_3$ can thus be seen as beneficial because it dissociates into Cl^- ions which improve the conductivity of the solution and promoting corrosion as was explained in earlier chapters. Moreover, if $Al(OH)_3$ is present then HCl will also react with it in the following manner:

$$Al(OH)_3 + 3HCl \rightarrow AlCl_3 + 3H_2O \quad (4.27)$$

This reaction again favours H_2 formation for the same reasons mentioned above. Therefore, the temperature increase observed in Figure 4-41b for reactions with HCl can be attributed to the above reactions. In addition, HCl can also react with metal oxides, CaO and CuO that are present in the mixture to produce $CaCl_2$ and $CuCl_2$, respectively as:

$$CuO + 2HCl \rightarrow CuCl_2 + H_2O \quad (4.28)$$

$$CaO + 2HCl \rightarrow CaCl_2 + H_2O \quad (4.29)$$

The above reaction with HCl dissolved in water is highly exothermic and will happen more vigorously when the pH is lower (more acidic conditions). This and the synergy effect can help to explain why HCl at pH 3 produces more H_2 and leads to high-temperature jump than a solution with pH 5.

As stated in the literature review that aluminium metal is covered with the thin layer of the oxide layer approximately 50 µm, which prevents it from reacting with water. However, when aluminium metal is presented in water containing corrosive chemicals which can affect the pH of the liquid. The metal comes into contact with an oxidising environment, such as water which means the "salt-gates" will very soon be re-oxidised again. These can the partially dissolve the oxide layer resulting in creating tiny pores from where water is able to penetrate through the oxide layer and reach the surface which seen also in these types of hydrogen reactions investigated here.

The physical-chemical stability of the aluminium oxide film determines the corrosion resistance and therefore seen from the reactivity of the aluminium particles. This stability is dependent upon the pH value since the oxide film is stable within the pH range of about 4 to 8.

Far below (pH 3) and well above neutral pH (pH 11) instability of the barrier oxide layer is most pronounced. Example of oxide breakdown would be; acid leads to the dissolution of the Al_2O_3 and yields Al^{3+} ions whereas an alkaline dissolution of the alumina may lead to the formation of $Al(OH)_4^-$ ions as a result of the dissolution. At a low pH such as in pH 3, the most dominant effect observed will be breakdown of the oxide barrier layer but also the oxide milling additives, whereas, in medium-low pH of 5, the added HCl will act as a buffer solution and neutralise the OH- ions released from the $Ca(OH)_2$. On the contrary, in very high pH such as in pH 11, the dominant reaction is a breakdown of oxide barrier layer and oxide additives but also have an effect on the $Al(OH)_x$ formations. At the less pH 9, the dissociation of oxide barrier layer is less and the dissolved OH ions from NaOH will affect the dissolution of $Ca(OH)_2$ in a negative way.

The reaction in aqueous solution (seen as corrosion of Al) involves oxidation (anodic reaction) of the Al and reduction (cathodic reaction) of a species in solution

(here water), with consequent electron transfer between the two reactants. See both half reactions below;

Oxidation (anodic reaction) $Al \rightarrow Al^{3+} + 3e^-$ (4.30)

Reduction (cathodic reaction) $H^+ + e^- \rightarrow \frac{1}{2} H_2$ (4.31)

The exposed Al metal undergoes intense oxidation if aggressive ions are present (such as Cl^-), resulting in potentially galvanic cells corrosion to take place, however, the chances of this happening depends on the presence of another metal (like reduced CuO to Cu invested in this Thesis). Further to elaborate on the point Figure 4-44, a Pourbaix diagram can be used [134]. The figure explains how aluminium behaves under different pH conditions, going from acid to alkaline can be seen.

From Figure 4-43, one can see that how different pHs effect the corrosion at two different extremes. The passivation region shown in the diagram is the region where aluminium oxide is formed.

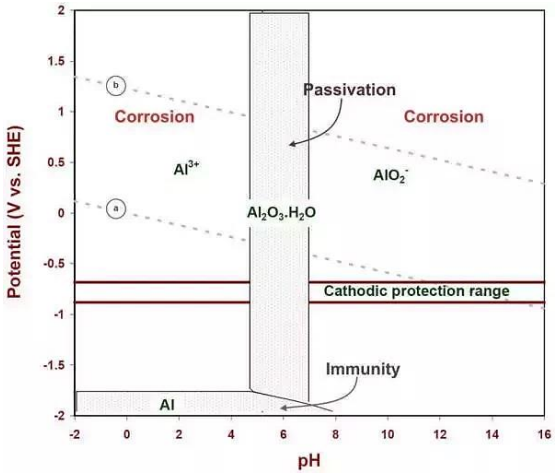

Figure 4-43: The Pourbaix diagram for corrosion of Aluminium at different pH [134].

To future understand in a separate experiment, it was decided to mill $CaCl_2$ together with Al and 25 wt % metal oxides with MO with the composition of the salt being 10 wt %. The aim of this experiment was to observe the effect on hydrogen production under variable pH conditions

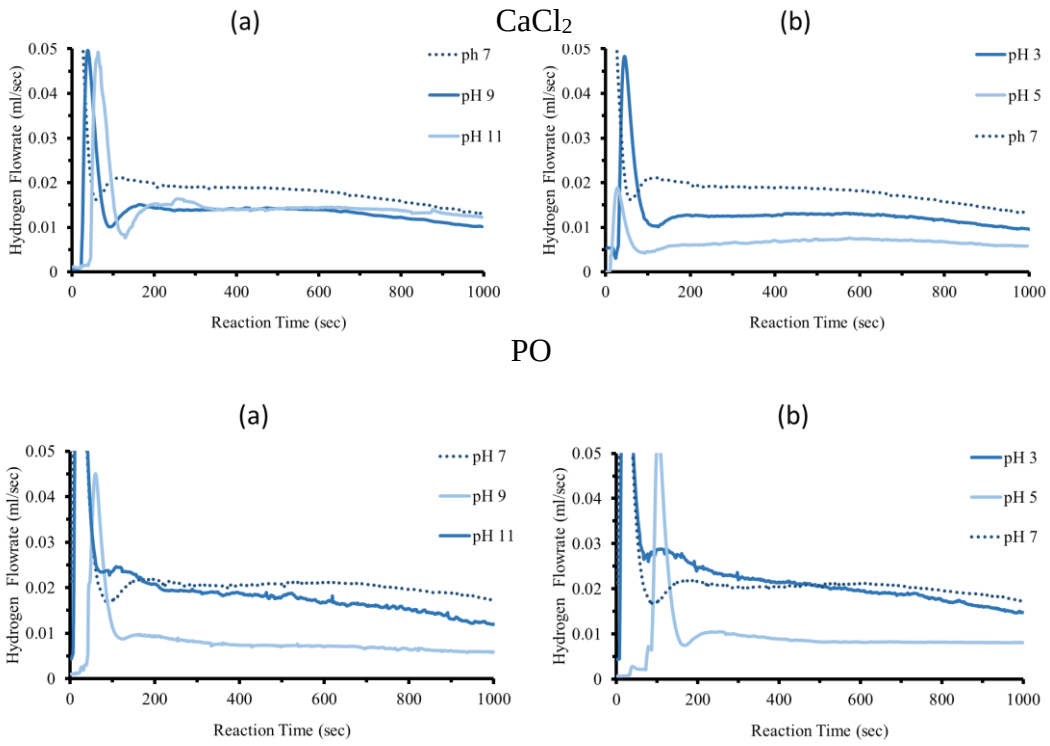

Figure 4-44: Hydrogen flow rate comparison between powder batches with different salt addition and exposed to different pH (NaOH and HCl solutions).

The results of the study are presented in Figure 4-42. Four plots are displayed: for acid or alkaline reaction of $CaCl_2$ and PO salt. The result from reaction with deionised water (denoted pH 7) is also displayed for comparison without going into any detail regarding the reaction mechanisms here in this thesis because they are beyond the scope of this research. However, it is clear to see from the plots the variations in the flow rate of hydrogen with respect to the pH in cases of metal oxide and the chloride salt. Furthermore, $CaCl_2$ is more sensitive to change in pH when the solution is acidic (pH < 7). Sodium hydroxide mostly reacts with metal oxide additive and not with $CaCl_2$. However, it has to be stated that purity of hydrogen gas can be jeopardised if solutions containing NaOH and HCl are reacted with activated aluminium. Therefore, if the reactor vessel is in situ with the fuel cell, the gas must pass through a stripper or adsorbed which can remove if any other contaminants from hydrogen gas.

4.2.5 Effect of water quality on activated aluminium

A study was conducted to mimic the more realistic operating conditions of the on-demand fuel cell. Water quality is one of the most important factors which can influence the hydrogen generation process. It must be recognised that deionised water may not be available readily or be cost-effective. Therefore, the following segment shows the results from the reaction of aluminium with different solutions. These include deionised water, tap water, sucrose solution, ethanol solution, antifreeze solution and lastly urea solution. As per the previous investigation, the 75 µm particle size batch was used again. It was again employed as a precaution to control the rate of reaction if any undesired gas is formed and the focus was to compare the different water types. Al was milled with additives 25 wt % CuO/CaO and 10 wt % PO salt mix using Milling Programme 1a (260 rpm). The initial temperature was kept at 25 ºC and agitation speed at 700 rpm.

4.2.5.1 Domestic water

Initially, domestic tap water was collected from two different locations, i.e. from East London and South London as this contained the highest amount of calcium carbonate and tested for performance towards hydrogen generation. Their results were compared with deionised water as shown in Figure 4-43. One can see that hydrogen formation from tap water was considerably slower than of when activated aluminium was reacted with deionised water. At the same time, it was noticed that water from East London was liberating more hydrogen than water than from South London, though the difference is only 5 ml. In 1000 sec reaction time the deionised water produced 35 ml H_2 gas at a higher rate of reaction. Whereas, the two tap water samples showed a 100 sec lag time and only generated an average of 20 ml H_2 in 1000 sec. As has been stated previously, the reaction of hydrogen is exothermic and will result in heat release. Monitoring the change in temperature can help identify when the reaction is starting. In Figure 4-43b, that in case of deionised water, the temperature starts to increase from the start, but not in the case of tap water from two regions in London, in agreement with the observed hydrogen evolution plots. This observation will be explained shortly, but it is understood from this study that

deionised water is a better choice than tap water for hydrogen generation in 1000 sec reaction.

Indeed, similar findings have been reported already by many researchers and a rationale has been given that due to dissolved ions in tap water, side reactions can take place before the hydrogen generation reaction can occur which can cause a lag and also affect the overall yield [80,92,103]. In order to test this theory for our study, samples from tap water were analysed using ion chromatography. Recall, that ion chromatography can separate and detect traces of ions in a given sample. The concentrations of ions in parts per million (ppm) detected in tap water from two regions in London are tabulated in Table 4-5. Referring to Table 4-5, one can see that there is little difference in the amount of dissolved ions between the two tap water samples. However, higher Ca^{2+} ions concentration was detected in tap water sample from East London. This is due to the typically high level of $CaCO_3$ and $MgCO_3$ found in some UK waters. The ICP-MS analysis only detected the dissolved metal ions and did not find any carbonate, CO_3^{-2}. It can be said that if in case of high concentrations of calcium carbonate, $CaCO_3$ and magnesium carbonate, $MgCO_3$ in tap water, a possible reaction between the formed hydrogen gas (produced via Al and water reaction) and $CaCO_3$ or $MgCO_3$ can occur to give $Ca(HCO_3)_2$ or $Mg(HCO_3)_2$.

Table 4-5: ICP-MS analysis of East and South London tap water.

Cations (ppm)							
Location	**Na^+**	**K^+**	**Ca^{2+}**	**Mg^{2+}**	**Zn^{2+}**	**Cu^+**	**Sr^{2+}**
East London	24.29	3.25	99.47	7.29	0.00	0.06	0.43
South London	23.39	4.89	69.67	6.05	0.01	0.03	0.32

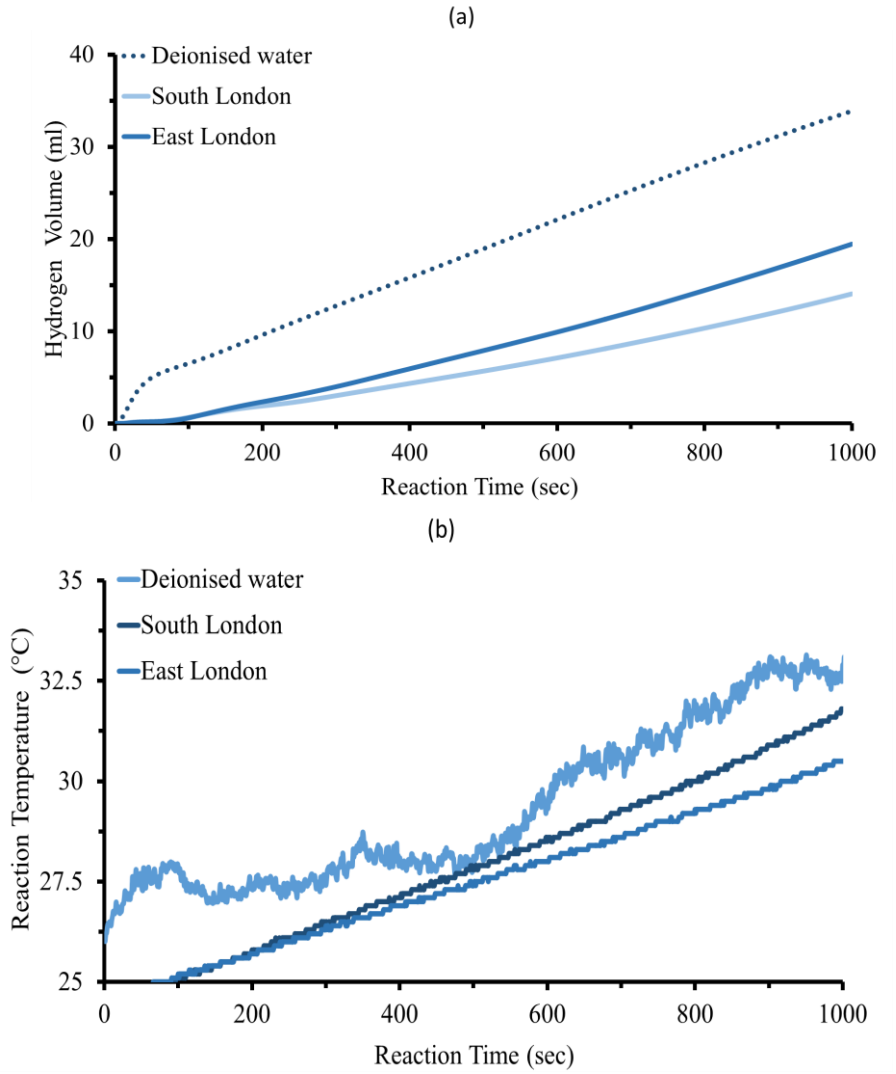

Figure 4-45: Domestic tap water and deionised water comparison on the effect on the hydrogen generation.

Calcium Carbonate, $CaCO_3$ reacts with H_2 as shown in the equation below. In this scenario, the liberated hydrogen would be consumed in the stated reaction and therefore, GFM would not record any H_2 amount.

$$2CaCO_3 + H_2 \rightarrow 2Ca(HCO_3)_2 \quad (4.31)$$

It is likely that no such reaction took place. It was suggested by Wang *et al.* that Al_2O_3 layer is not very soluble in tap water as compared to deionised water as tap water contain dissolved minerals. This could also be used to explain the reduction in hydrogen yield and reaction rate from tap water. Some reports in the literature are present in which reaction yields from sea water have been shown to be higher than from deionised water [40,107].

4.2.5.2 Effect of OH group containing solutions

In chapter 2, ethanol, ethylene glycol, and urea from urine and sucrose solution were identified as potential candidates for the portable hydrogen generation device. A common feature amongst them is the presence of OH group in their chemical structure. The results of measuring the generation of hydrogen from these sources are reported and discussed in this section.

The said chemicals can be found in wastewater and their concentration can vary depending on the location from where wastewater is collected. For example, in close vicinity to the dairy industry, a significant amount of sucrose as well as ethanol (conventional solvent), may be found in the wastewater. Similarly, antifreeze concentration in wastewater would be higher close to an automobile industry. These chemicals are of interest because hydrogen could be liberated from their reaction with activated aluminium. These stated solutions were prepared at the university, for more information see chapter 3. First wastewater type to examine was ethanol in water. In Figure 4-44, the results of hydrogen formation reactions with different concentrations of ethanol solutions are displayed. One can see that regardless of the concentration, ethanol solutions were able to produce hydrogen gas. With the highest concentration of 0.68 M, 25 ml of hydrogen gas was liberated in a 1000 sec reaction. The trend observed in the figure favours higher concentrations of ethanol solution for an efficient reaction. However, when compared with deionised water, it was 10 ml less. An independent test was also performed where pure ethanol was reacted with activated aluminium and no reaction was observed. It was observed that heat was given off in the reaction as indicated by the temperature rise.

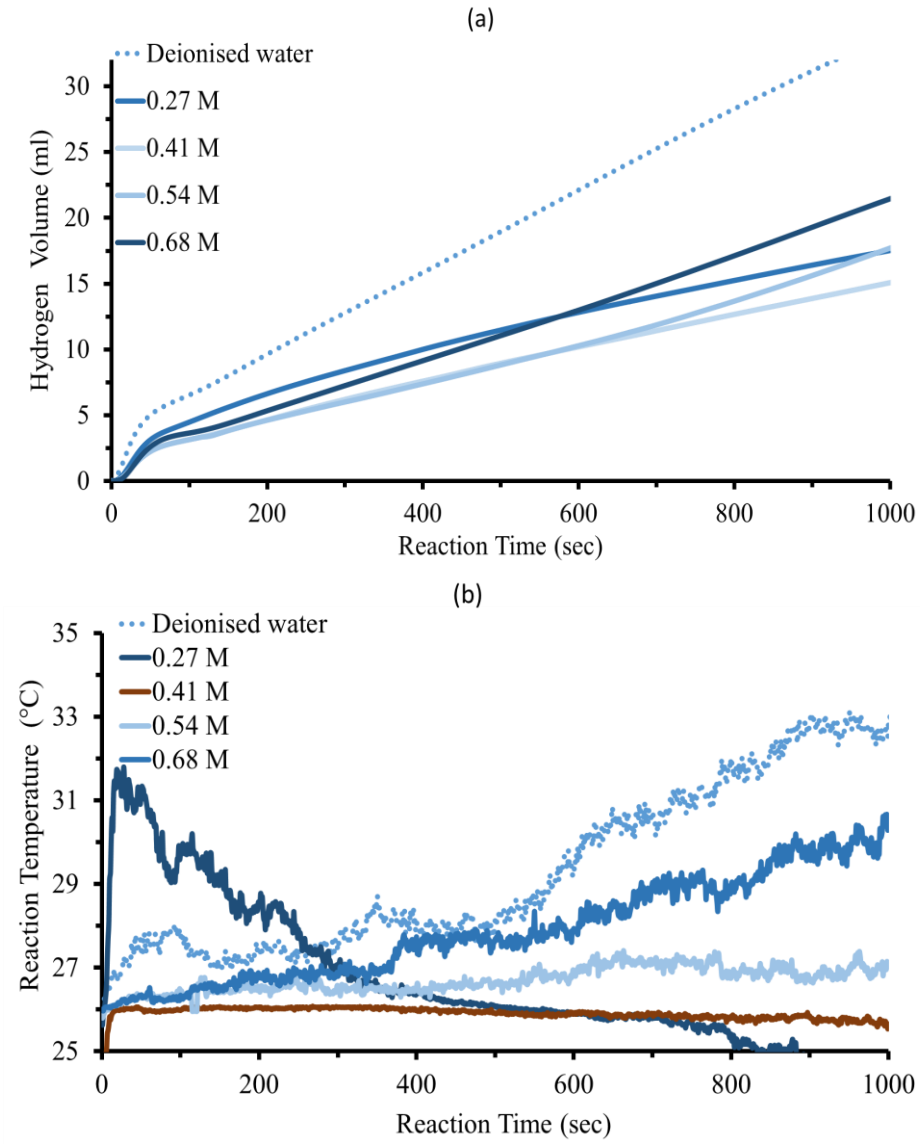

Figure 4-46: Hydrogen production using a range of 0.27-0.68 M ethanol solution when reacted with activated aluminium.

In order to account for the reaction behaviour observed here with the hydrogen gas liberation, different possible reactions of ethanol in the mixture that can take place need to be discussed. Firstly, some of the ethanol molecules in the presence of metal Al can react as shown below:

$$Al + C_2H_5OH \rightarrow Al(OC_2H_5)_3 \quad (4.32)$$

This reaction is possible because Al is milled which exposes the reactive surface. The product of the reaction is aluminium-triethoxide, $C_6H_{15}AlO_3$ which decomposes into aluminium hydroxide and ethanol only. This reaction, therefore,

does not contribute to hydrogen production. Aside from that, at room temperature, this reaction is not very favourable. Ethanol also can, under certain conditions, act as a weak acid. If this is considered as a possibility, then it will simply react with OH^- ions formed from the following reaction:

$$CaO + H_2O \rightarrow Ca(OH)_2 \rightarrow Ca^{2+} / OH^- \quad (4.6)$$

Lastly, it was observed that pure ethanol did not produce hydrogen and only diluted solutions gave off a measurable amount. This indicates that the water contents in diluted solutions may have been playing a role. Grosjean *et al.* reported a similar observation when their milled sample of Mg and MgH_2 was reacted with ethanol solutions. They also reported that increasing the concentration of ethanol in water helped improve H_2 formation. The authors also reasoned that the presence of water in the mixture solution might modify the acido-basicity of ethanol. While this assertion requires a more thorough investigation, one can discard the possibility of the Al and ethanol reaction contributing to hydrogen production and conclude that diluted ethanol solutions are able to produce hydrogen gas from their reaction with our prepared powder [96].

Next, ethylene glycol (antifreeze) was reacted with aluminium. Again, solutions of different concentrations were prepared for this investigation. Moreover, commercially available antifreeze *(Q8 antifreeze)* was also obtained to compare its performance to the prepared solutions. One can see in Figure 4-45a, increasing concentration of ethylene glycol in deionised water up to 0.77 M appears to improve the hydrogen formation. In contrast, commercial antifreeze produces the least amount of H_2. A temperature rise was observed in all cases indicates the exothermic reaction took place. Moreover, with a higher concentration of ethylene glycol the rise was higher, but the commercial (denoted as industrial in the plot) antifreeze solution produced the largest initial temperature jump.

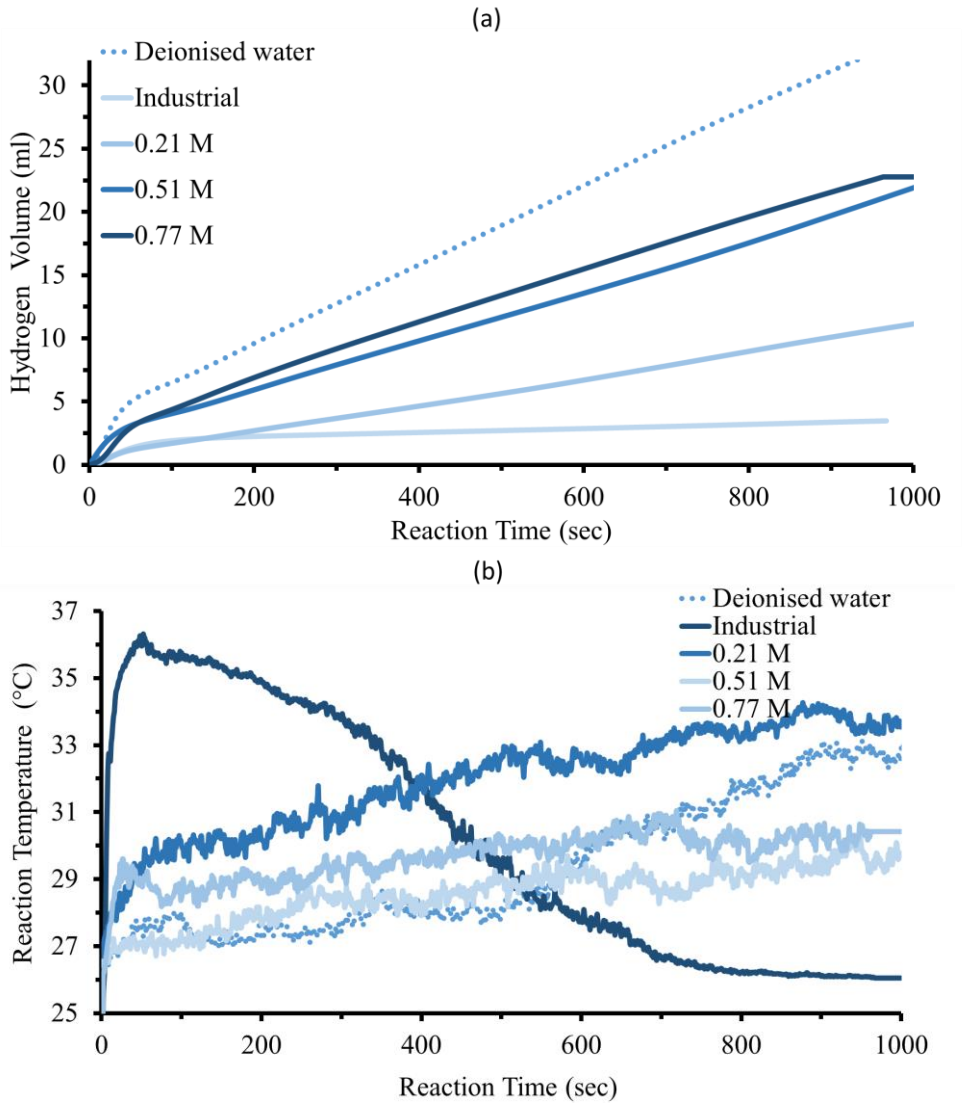

Figure 4-47: Hydrogen production using 0.21-0.77 M ethylene glycol solution compared with industrial anti-freeze when reacted with activated aluminium.

Commercial antifreeze contains the highest content of ethylene glycol (> 90 % according to the product specification) and from the trend observed from prepared solutions, it can be said that it plays a role in the exothermic reaction. The reason why hydrogen production is not very high for this chemical is due to the presence of inhibitors such as propylene glycol and oxidation prevention agents which make up the rest of 10 wt %. As antifreeze is used to protect engines from corrosion and rust despite initially a fast reaction due to the inhibition of corrosion of Al the reaction does not continue.

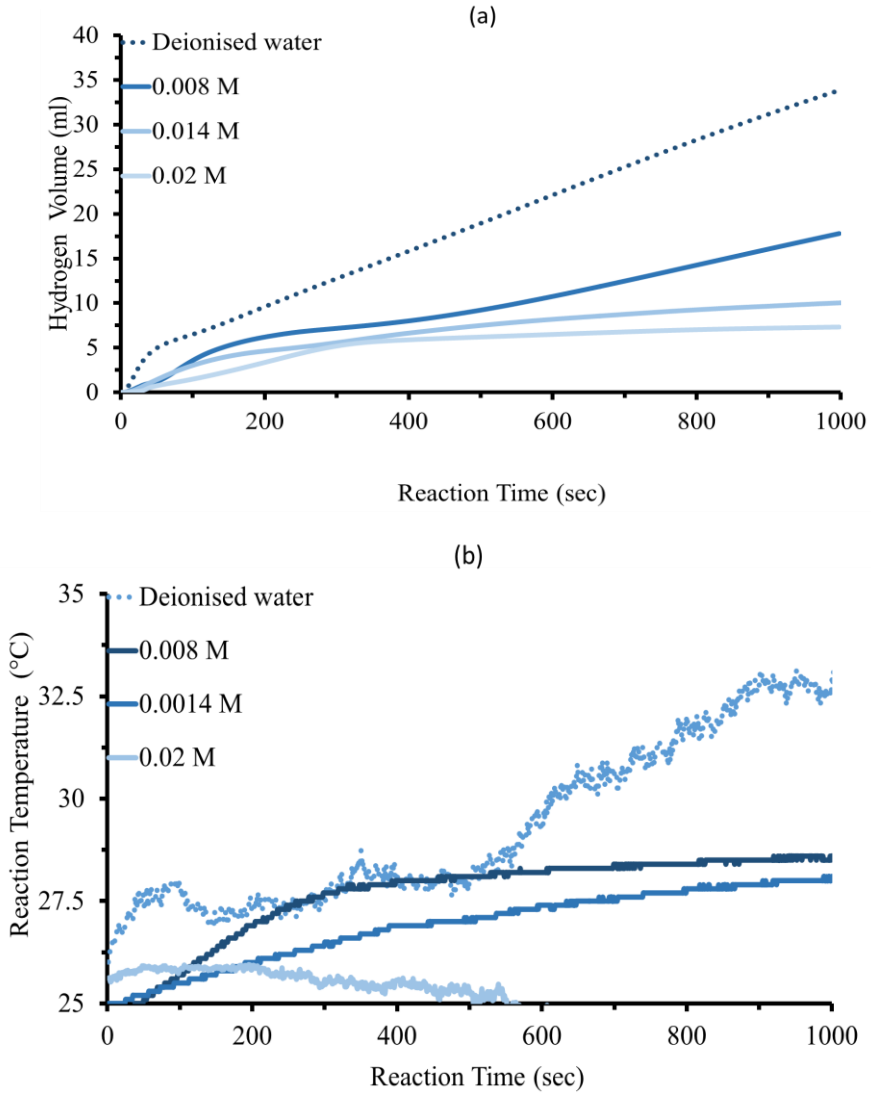

Figure 4-48: Hydrogen produced using 0.008-0.020 M sucrose solution when reacted with activated aluminium.

Lastly, sucrose solutions were also reacted with activated aluminium to assess their ability to generate hydrogen. Solutions of concentrations ranging from 0.008 mol to 0.02 mol were used for this study. Higher concentrations than this were avoided. This is because sucrose has larger molecular structure relative to water and it was reasoned that more molecules of sucrose in reaction mixture could block the access of water molecules reaching the surface for the reaction. The results of reactions are plotted in Figure 4-46 and show that while sucrose reaction with aluminium releases H_2, the volume of the gas decreases as the concentration of solution increases.

This is not a surprise as when the concentration becomes high, the channels for water to the reach the reactive surface become increasingly blocked and thus the amount of production goes down [151]. One way to describe the reaction between OH^- containing groups and Al is shown in the equation below:

$$Al + ROH \rightarrow Al(OR)_+ H_2 \quad (4.33)$$

, where ROH corresponds to species containing OH groups. However, this reaction is, in fact, slow particularly at these temperatures. Therefore, it can be disregarded. A better explanation of why the activated aluminium reaction with ROH took place to produce H_2 could be as follows.

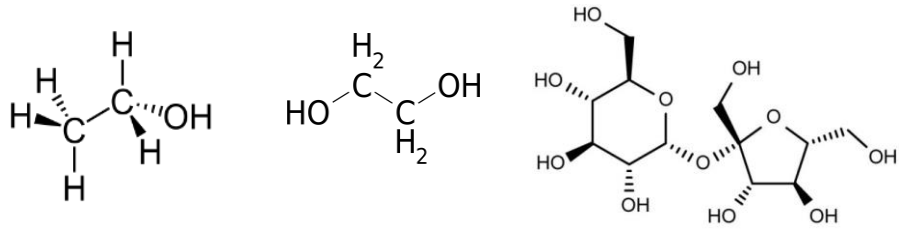

Ethanol Ethylene-glycol Sucrose

Figure 4-49: Molecular structures of ethanol, ethylene glycol and sucrose [44]**.**

If one looks at the chemical formulas of ethanol, ethylene glycol and sucrose (see Figure 4-47, for a reminder of their structures) they all contain OH groups. When these compounds are mixed in water they completely or partially get submerged forming *H- bonds* with the water molecules which form due to fluctuating charges creating transient dipoles. When activated aluminium particles are presented in the solutions, water is attracted towards to aluminium particles due to polarity effect, thus breaking these *H-bonds* with alcohol specimen to give of H_2.

With regards to the synthesis of Al particles, it shall be remembered from section A, that PO (*potash*), the in-house salt additive, helps in creating salt gates on the surface of Al particles during milling. When activated aluminium is reacted with these solutions, the additives including PO dissociate into the solutions releasing a large amount of Cl^- ions and damaging the passive oxide layer, Al_2O_3.This allows the embedded salts to dissolve creating salts gates and permitting species in solutions to access the surface of Al particles. Milling also affects the Al particles

and create grain boundaries, which can have contributed towards the corrosion sites of the Al particles, consequently helping the formation of H_2 gas [26].

4.2.5.3 Urea solution

For the final investigation, a series urea solution was prepared at the university. As was mentioned previously, urea solution is of particular interest because it is the main by-product of human urine and 97 wt % is water. There is a plentiful supply of it and so it is a potential replacement for water to be used in the fuel cell. The level of urea found in wastewater is typically in the range of 1-10 mg/L [152,153]. Therefore, to mimic real-life scenario, different concentrations of 0.15, 0.10 and 0.05 M of urea solutions were prepared with deionised water, refer to chapter 3 for more details. As one can see from the Figure 4-49a, that all of the urea solutions were able to generate H_2 when reacted with activated aluminium at 25 °C.

As shown in Figure 4-49a, the highest concentration of urea, i.e. 0.15 M liberated 43 ml of H_2 in a 1000 sec reaction. It exceeded the amount of H_2 given off by deionised water by approximately 10 ml. These results are very encouraging for use in the fuel cell for the formation of H_2. To explain the reaction of urea solution with aluminium, the following hypothesis is suggested. As stated in chapter 3, the urea solutions were prepared following the guidelines provided by Putnam [132]. All the additives including urea powder and salts, including NaCl and KCl, were added into deionised water. When more concentrated solutions were prepared a number of salts, i.e. NaCl and KCl were added to deionised water were also increased. Due to the high concentration of salts present in more concentrated solutions, the number of Cl^- ions must also be high. This increase of Cl^- ions in the solution in addition to what milling additives would release into the solution would create a high electrolytic solution synergy promoting electro-conductivity in reactions such as corrosion.

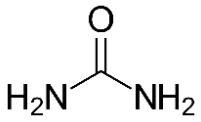

Figure 4-50: Chemical formula of urea [44]**.**

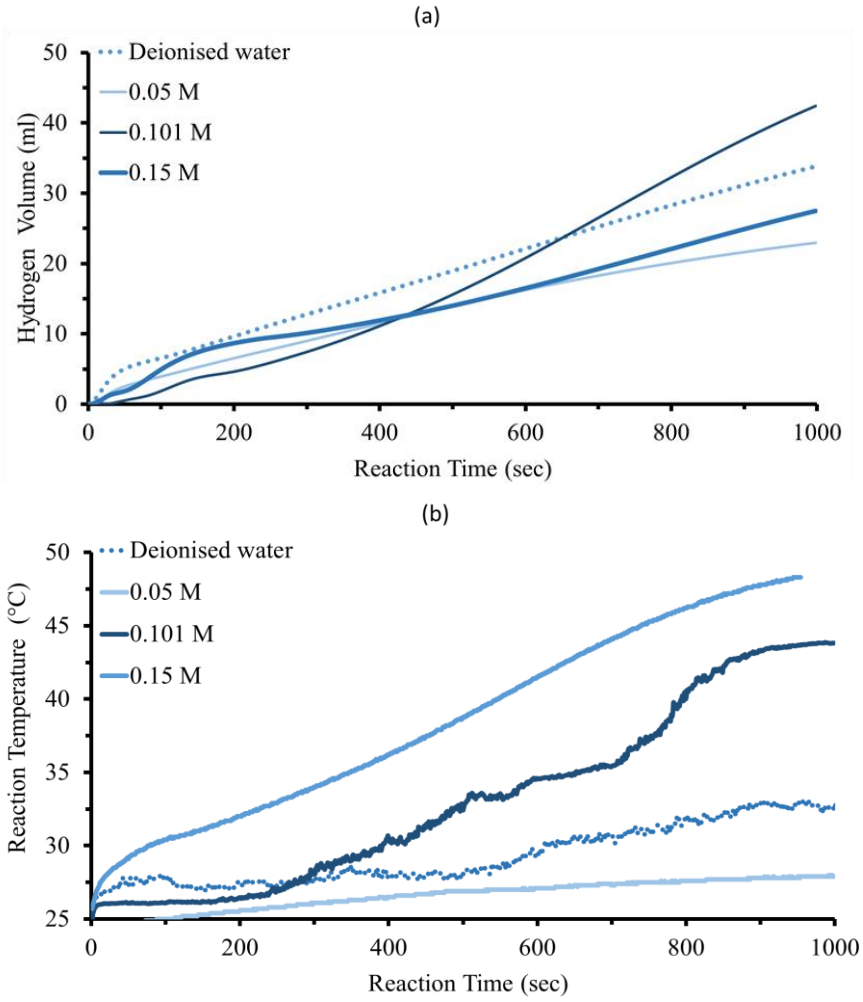

Figure 4-51: Hydrogen production using 0.05 - 0.15 M urea solution when reacted with activated aluminium.

This argument was also made by Elitzur *et al*. where the author reported that when they used urea solution and reacted their sample with deionised water and seawater, they observed an increase in the reaction rate and yield of H_2 [116]. Therefore, it can be concluded that increased salt content wt % in solution was likely an important the major factor in liberating more H_2. In this work, the attention was mainly given to assessing the performance of the said solutions to produce hydrogen. The rationale for the observed behaviour of each solution was given by reference to literature when possible or a hypothesis was presented. It must be said that the detailed investigation of various mechanisms via which different species react with aluminium was beyond the scope of this thesis.

4.2.6 Gas Analysis

The on-demand hydrogen technology must be both economically attractive and safe. Therefore, it is important to ensure that no unwanted or potentially harmful products or gases are produced inside the portable cell from the reaction which can compromise the fuel cell itself or be dangerous to the consumer. This is especially important in this particular case because the water for the reaction can come from various sources (as is the aim to use the fuel cell in many places).

Should the water contain contaminants, harmful gases may be produced when reacted with activated aluminium. The measurement reported thus far have been mainly sensitive to the production of H_2 as the GFM was calibrated for H_2. This, unfortunately, does not guarantee that H_2 is solely produced in the reaction. In order to properly analyse the contents of the evolved gas, gas chromatography was carried out. The principal gas chromatography as described in chapter 3. Hydrogen gas produced from the various solutions including deionised water, ethanol solution, ethylene glycol solution (antifreeze), sucrose solution and with urea solution (mimicking urine) was collected and investigated separately.

The results of the analysis are presented in Table 4-7 and Figure 4-51. However, for full GC results see appendix. Only the readings of retention time (in min) and full peak widths at half maximum (FWHM) for each of the 5 reactions are listed in Table 4-6. One can see that that the retention times obtained for the gas evolved from the reactions agree well with those from the standards. Allowing for a small difference of ± 5 sec this indicates that the gas measured from the reaction is indeed pure hydrogen. Moreover, FWHM values are not very different from each of the solutions. It should be mentioned that analysis of the gas also produced peaks from oxygen, nitrogen and argon in all cases.

Table 4-6: GC Retention times and peak width.

Reaction run sample	Retention time (min)	FWHM (min)
Deionised water*	1.52	0.017
Deionised water	1.54	0.025
Ethylene glycol solution	1.49	0.020
Ethanol solution	1.43	0.018
Sucrose solution	1.43	0.018
Urea solution	1.40	0.020
Standard Gases		
Hydrogen (Al+NaOH) *	1.79	0.022
Hydrogen (99 %)	1.51	0.027
Nitrogen	3.36	0.030
Oxygen	2.00	0.033
Carbon Dioxide	2.88	0.034
Argon	1.89	0.038

Please note *Column temperature setting at 35 °C.

The reason for their presence is due to the insufficient purging of the gas syringe, so traces of nitrogen and oxygen from air remained inside. Ideally, the reactor should be connected directly to the GC, thus avoiding the need to transport the gas in a vessel like a syringe and introducing traces of 'impurities'. However, as was mentioned earlier this was not possible in this case due to locality issues. But, based on this study, one can say with confidence that H_2 was released even when various complex molecules and ions were mixed with deionised water. Moreover, no harmful gases which can damage the fuel cell were detected from this investigation. Nevertheless, it is recommended that gases produced from other than the deionised water must pass through a stripper or absorber prior to being fed into a fuel cell.

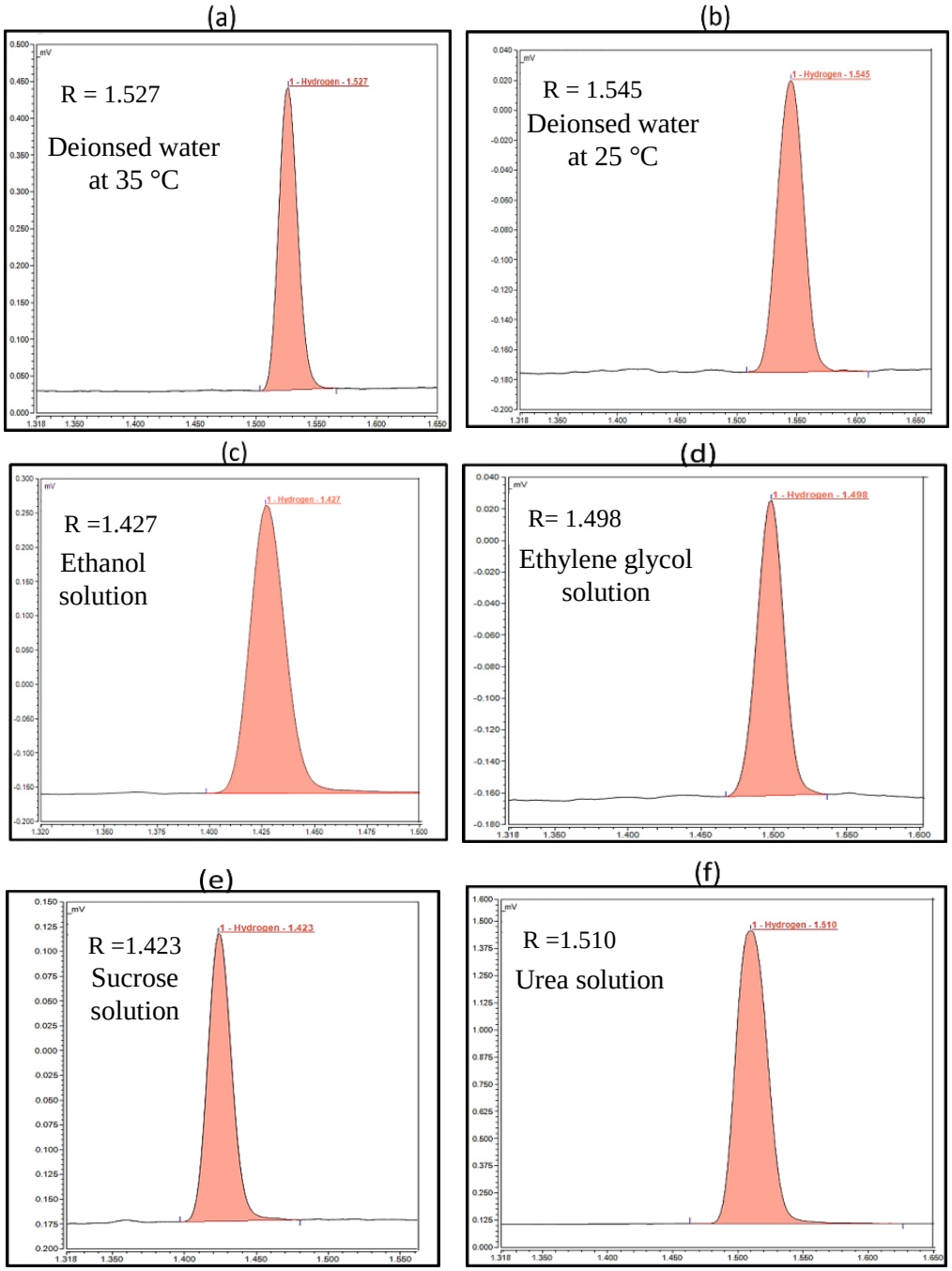

Figure 4-52: Hydrogen gas peaks generated when different solutions were analysed with GC, a) deionised water (35 °C), b) deionised water, c) Ethanol, d) Ethylene glycol, e) Sucrose and f) Urea.

4.2.6.1 Evidence for hydrogen gas formation

- To further confirm that only hydrogen gas was liberated in the reactions and that the peaks of atmospheric gases in the GC did not come from the produced gas, a dry run was performed using a gastight syringe to analyse the air present in the room where GC was stationed. Analysis of the results obtained from the dry run (not reported here) showed that no hydrogen peak was discovered. Peaks of oxygen, argon and nitrogen were detected. Moreover, the retention time of these atmospheric gases also matched that of air signatures recorded during the H_2 gas analysis.
- Activated aluminium was subjected to SEM analysis before and after reaction with deionised water. After the reaction had finished, a significant shrinkage of Al particles was observed indicating that the particles had indeed have reacted with water, in the following reaction,

$$2Al + 6H_2O \rightarrow 2Al(OH)_3 + 3H_2 \quad (4.1)$$

- A further analysis was carried out on the reacted aluminium particles using XRD to verify the by-product $Al(OH)_3$ presence. The results displayed in Figure 4-33, that confirmed $Al(OH)_3$ was produced in different forms, i.e. Gibbsite, Bayerite and Nordstrandite. Formation of these morphologies $Al(OH)_3$ is only possible if the reaction between activated particles and deionised water takes place showed in temperature plots.
- Hydrogen formation reaction is exothermic and all the reaction runs produced a significant amount of heat.
- Finally, the last analysis was conducted in a fume cupboard to avoid any unfortunate circumstances. The produced hydrogen gas was collected in the inverted column and popped. At first, the gas was not ignited. However, when a little amount of argon was mixed in the glass column carefully. This time when gas was ignited, it popped with a high pitch sound chipping the glass column.

4.2.7 Conclusion of Section B Effect upon hydrogen generation due to the varied solutions

Based on the findings from section B, it was discovered that activated aluminium particles require constant agitation at 700 rpm for achieving desirable hydrogen yield. However, if agitation speed is high, then it would reduce the possible hydrogen yield. Loading also plays a curial role in achieving desirable hydrogen yield. Increased loading of activated aluminium does not help to achieve high yield due to smothering. Starting temperature can influence the overall yield. Al particle size of 40 µm and 75 µm when employed produced lower yield compared to 105 µm, as starting temperature increase was found to be favourable for the largest particle size.

When pH of the solution is changed and activated aluminium is reacted with a solution containing either acid or alkali, it will produce hydrogen, however, an absorber or stripper must be used before the gas is sent into the fuel cell. In this research work, it was shown that wastewater could potentially be used as a source of hydrogen gas. Urea solution proved to be the best alternative as compared to wastewater tested. However, the gas may require treatment before it can be used in a fuel cell. Gas analysis was carried out on the gases given off when activated aluminium was reacted with simulated wastewater containing, ethanol, sucrose, urea and antifreeze (ethylene glycol). From the GC results, contaminants gases were detected which could potentially damage the fuel cell membrane.

4.3 Section C Economical evaluation of the research

This section presents the final instalment of the results and discussion chapter. It will highlight the importance of the overall hydrogen economics for this research work. It will include; the cost of raw material, particle processing, balanced against the hydrogen produced. The notion of this research project was to present a convenient and cost-effective process for preparing the reactive powders for an on-demand hydrogen generation aimed at fuel cells. Currently, there is no established market for on-demand hydrogen technology for fuel cells. The most common on-demand hydrogen is found in the automobile sector, where produced hydrogen is mixed with fuel in the combustion engine to reduce the fuel cost and CO_2 emissions.

These on-demand hydrogen generators produce H_2 through electrolysis process driven by the car battery. Although it is an intriguing idea to improve the mileage on the vehicle, nevertheless it is not very efficient and requires the engine to be constantly running in order to generate hydrogen. In other words, fossil fuel is still consumed during the process does contribute to greenhouse gases. Currently, there are a few portable power units based on fuel cell technology on the market, but all of them depend on hydrogen gas which needs to be fed via compressed hydrogen cartridges or cylinders. As stated, the on-demand hydrogen technology from this research work is aimed at power-producing fuel cells working off the grid and in rural areas. This would, therefore, mean that the transport and storage cost of the hydrogen can be eliminated.

This research work provides an alternative approach to the options available in the market. The concept is provided where the hydrogen generation works *in-situ* with the fuel cell, removing the need for any external hydrogen supply. The core and the main driving force for this research work are based on the aluminium and water reaction. However, aluminium metal needs to be *activated* before it can react with water efficiently in ambient conditions, i.e. atmospheric pressure and standard temperatures 25 °C. This is because aluminium forms barrier layers of Al_2O_3 when exposed to air, which prevents the water from reacting with the surface of the metal. Thus no reaction takes place when aluminium is reacted with water without the use

of any catalyst such as KOH or NaOH. For more information consent the Chapter 2.

4.3.1 Proposed milling protocols

After reviewing different possible techniques in the literature review, which can damage the aluminium barrier layer. It was decided that reactive milling would be employed for the research. However, for keeping the economics commercially attractive and to achieve desirable activation, special attention was given to the processing cost as well as additives which would be used to synthesise Al metal particles.

Aluminium particles would be milled in the presence of metal oxides and *potash*, PO and called (MO+PO), which provide a comprehensive balance of inexpensive and non-corrosive raw materials. Although selected raw materials would keep the overall cost down, the reactive milling technique itself is energy intensive, meaning a considerable amount of electricity may be consumed. The high processing cost of this technology is not mainstream in the commercial industry, although it is extensively used for research purposes. The electricity consumption can jeopardise the purpose of this technique which is to keep the process cost-effective. However, it is suggested by authors of [53,54,88,93,94,109,140] that in milling process electricity consumption can be altered by varying the functional parameters. The parameters include; milling speed, the duration of milling, ball to powder ratio, loading of powder and lastly it also depends on the type of ingredients being used during the milling.

Researchers mentioned above claimed that their samples produced higher hydrogen yield when they milled their samples for an extended period of time or at high milling speeds. In order to avoid the similar obstacles discussed, distinctive and tailored milling programmes were designed for this research. To record the energy usage of the milling machine during the processing of the metal particles, an energy reader (13 A plug-in energy saving monitor, Maplin) was connected to the milling machine. This energy meter provided the energy usage of different milling programmes which was used to calculate the processing costs. One can see from

Figure 4-51 that there is a significant difference in energy consumption between Milling Programme 1a and 1b, with the speeds of 260 rpm and 520 rpm, respectively. Likewise, Milling Programme 1a and 2 (different break times) also have a significant difference with regards to energy consumption. After Milling Programme 1a, 1b and 2 consumed 0.29 kWh, 0.72 kWh 0.55 kWh, respectively.

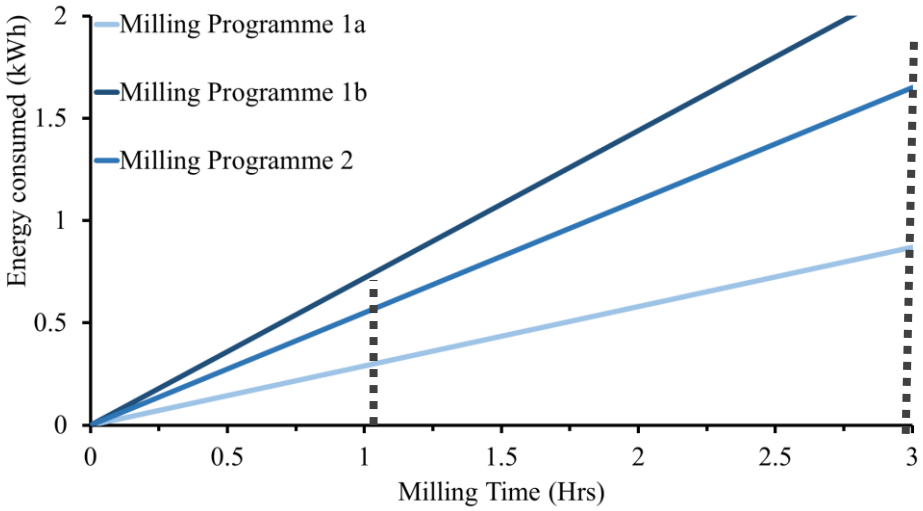

Figure 4-53: Energy consumption for three different milling programmes using device Retsch PM 100. The dotted line marks the active milling time used.

Synthesised samples produced from these three milling programmes were compared in section A. Where it was seen that Milling Programme 1a, produced a higher quality of the synthesised powder. When reacted with deionised water at 25 °C it produced approximately 85 % hydrogen yield in 3 hrs. Whereas powders synthesised using Milling Programme 2 and Milling Programme 1b were compared, they produced hydrogen yield of 34 % and 5 %, respectively when reacted with deionised water. It was established from this investigation that milling for an extended period of time or at high speed is not necessary nor even justifiable when activation of particles can be achieved with lower energy investment.

Throughout this research work, milling was carried out for 1 hr and 40 min (100 min) out of which the actual milling time when break times were deducted was only 66 min, as shown in Table 4-8. It is important to point out the fact that milling for the shorter period of time still provided encouraging hydrogen yield results thus further reaffirms the claim that milling for long duration does not help.

One can see from the Table 4-8, Milling Programme 1a and 1b both milled for just 66 min whereas Milling Programme 2 milled for 92 min. As stated earlier, that powder prepared from Milling Programme 2 had a reduced H_2 yield as compared to powder prepared from Milling Programme 1a. However, It could be argued that powder prepared from milling for an extended period of time, i.e. 2.4 hrs can provide a faster reaction rate and possibly marginally higher yield as compared to the powder which was prepared by milling for 1.1 hrs. It is essential that the hydrogen production rate is stable, this because hydrogen reactor vessel would be connected to fuel cell *in-situ* and damage the fuel cell if there is no flow controller present.

Table 4-7: Milling Programmes and their respective power consumption.

Name of programme	Milling Programme 1a	Milling Programme 1b	Milling Programme 2
Total time of milling	1 hr 40 min	1 hr 40 min	1 hr 40 min
Mass of powder	3 g	3 g	3 g
Actual processing time	66 min	66 min	92 min
Actual power consumed	0.29 kWh	0.72 kWh	0.55 kWh
Cost of processing	£ 0.02	£ 0.08	£ 0.06

From Figure 4-4, it can be seen that powder prepared from 2.4 hrs milling, does not exhibit a stable reaction when it is reacted with deionised water as compared to powder prepared from 1.1 hrs milling. As stated above that fuel cell requires a

constant and stable flow rate of H_2 gas to operate; therefore, powder prepared from 2.4 hrs milling might not be suitable.

4.3.2 Cost estimation

It was imperative that during the economic evaluation industrial scale aluminium activation process should be considered as well as the small scale (Laboratory). Since the powder activation process would be at the industrial level and all the raw material would be purchased in bulk, therefore, the overall activation process would be cost effective as compared to a university laboratory condition. Furthermore, the benefactor company is based in the United States. Therefore, a cost evaluation for the US market would also be provided.

With regards to the electricity utility, Milling Programme 1a would cost approximately £ 0.02 for activating 3 g of powder (mixture) at the university. This estimation was calculated in compliance with academic electricity rates of £ 0.09 per kWh and climate change levy of £ 0.005 [154].

Table 4-8: Raw material used for the activation of aluminium.

Material used	Amount (kg)	Cost (£)
$CaCl_2$	0.0009	£ 0.07
KCl	0.0009	£ 0.05
NaCl	0.0012	£ 0.03
CaO	0.0037	£ 0.67
CuO	0.0037	£ 0.40
Al	0.0195	£ 2.77
Total amount	0.0299	£ 3.98

It is important to state here that 3 g of powder contained 65 wt %, 25 wt % and 10 wt % of (Al, MO and PO), respectively. Based on the weight percentage of all the ingredients in 3 g of powder, it would cost £ 3.98 collectively, based on the quotation from Fisher Chemicals [141]. Using 3 g of activated aluminium

(recycled) powder is reacted in water at 25 °C see Table 4-8, it is capable of generating 2600 ml or 2.6 l of H_2 for approximately £ 4.00 at a university laboratory if the raw materials are acquired from Fisher Chemicals.

The presented cost also accounts the electricity consumed by electric stirrer/agitator and the cost of water consumed during the reaction. The overall cost of the suggested process is noticeably high even though the cost of raw material and the processes were carefully taken into consideration. The high cost of the overall process at the university can be justified as industrial tariffs and cost of raw material purchased in bulk amount will be considerably cheaper than used for academic purposes.

4.3.2.1 Forecasting large scale

This research work is aimed at proposing a milling protocol which would be employed in the activation of Al used for industrial purpose. Although the cost of production is presented here is for a research university scale activation. Some information would be taken and extrapolated to forecast the economics of the process. When a process is upscaled, the cost of raw material and electricity does not increase in linear rate. However, for this research estimation purposes cost of electricity for milling 3 g of powder was linearly increased based on the used planetary milling device.

It was calculated that to produce 1 kg or 11000 litres of hydrogen gas; it would require 12.70 kg of activated aluminium. Based on the data from Alibaba for all the raw materials and if they are brought in in the UK, it will account for only £ 5.71 ~ £ 6 [155]. Whereas, the electricity usage would account for £ 68 per kg or £ 0.006 per litre. This estimation was drafted using the electricity rates used by medium scale industry in the UK. This cost estimation would be accurate assuming if 100 % efficiency of H_2 is to be achieved. However, during the research work, when the 40 µm aluminium particle was employed, hydrogen yield attained was 85-92 %. Based on the yield taken into account, it would cost approximately £ 80 per kg H_2. It has to be remembered again that this forecast estimate is based on energy consumed if a number of Planetary Ball Mill PM 100 RETSCH were to be employed.

This does not represent the actual cost linked with the upscaling process, as the larger scale process would not follow a linear trend. However, still assuming the cost for the USA using Planetary Ball Mill PM 100 RETSCH, the estimate would be $ 90 per kg or $ 0.008 of hydrogen gas. This cost will be reduced if the large-scale miller is employed. Below, Table 4-9 shows the cost comparison for both UK and USA large scale in their respective currencies.

Table 4-9: Projected large-scale cost.

Scale / Location	United Kingdom (London)	United States (Cleveland, OH*)
Cost of raw material	£ 6	£ 7
Energy cost (medium scale)	£ 0.050 kWh	$ 0.067 kWh
Climate levy	£ 0.005 kWh	N/A
Energy usage based on Retsch PM-100	1226 kWh	1226 kWh
Cost of processing	£ 68.49	$ 83.00
Total cost per kg (100 % yield)	£ 74.22	$ 90.00
Total cost per litre	£ 0.006	$ 0.008

4.3.3 Conclusion for Section C Economical evaluation of the research

The proposed milling protocol presented and utilised throughout this research studies has considerably less energy investment than to methods presented in the literature. As stated at the beginning of section A, high speeds or longer milling times were employed by serval authors [18,26,41,45,54,66,80,134-136], including Tousi *et al.* for achieving high flow rates of hydrogen and its yield. They also attempted to mill a rare earth metal and an expensive LMP (low melting point metal) together with aluminium and succeeded in producing hydrogen, albeit at a much higher cost than this work. These factors, which include power consumption and usage of raw materials, contribute towards an increase in the overall cost of hydrogen production, whereas, as mentioned already, this thesis work aimed to

circumvent that and demonstrated an efficient use of resources to produce high yields of hydrogen (over 85 %).

The above point could be elaborated as a comparison was drawn between the work presented here against that of Tousi and co-workers [104] for the consumption of energy and the yield of hydrogen gas. Tousi and co-workers milled aluminium and potassium chloride (*potash*) at 200 rpm for 7 hrs and immersed the resulting mixture in water at 80 °C. The authors reported a yield of (> 90 %) for hydrogen after a reaction time of 4500 sec [72]. Whereas, Wang *et al.* [80] also prepared aluminium with calcium oxide and potassium chloride, but also used gallium as LMP and moreover, milled the mixture for 8 hrs at 360 rpm. Afterwards, the powder was introduced into 60 °C water to generate hydrogen whose yield, Wang claimed to be roughly 68 % in 4500 sec. This research work showed the achievable yield of hydrogen to be 61 % in 4500 sec when the prepared mixture was milled for 1.1 hrs at 260 rpm and added to 25 °C water and 80 % when milled for 2.4 hrs.

Table 4-10: Comparison of saving of energy, yield and reaction conditions.

	Tousi 2013	**Wang 2014**	**This research**
Processing time (hrs)	7 hrs	8 hrs	1.1 hrs
Milling speeds (rpm)	200 rpm	360 rpm	260 rpm
Temperature of water (°C)	80 °C	60 °C	25 °C
Yield (%) (after 4500 sec)	90 %	68 %	61 %
Temperature of water (°C)	25 °C	25 °C	25 °C
Yield (%) (after 4500 sec)	N/A	29 %	61 %

Although, Tousi and Wang's high hydrogen yields suggests rather due to reactor design factors. that their prepared powders were more reactive in water than ours. However, it is important to emphasise that hydrogen yields from their work may have been higher due to the longer milling time which would have provided their powder with better mixing and would have reduced their powder particle size. In

addition, both Tousi and Wang reacted their prepared samples in water at high temperatures, i.e. 80 °C and 60 °C, respectively. Wang reported that with water at 25 °C, the hydrogen produced after 4500 sec was substantially lower (29 % yield). This comparison provided an insight that not only there is cost saving in the proposed technique, but the quality of powder synthesised using Milling Programme 1a achieved a high reaction yield.

4.4 Chapter 4 Conclusion

A number of the different experiments were conducted in this chapter including the particle process effect on the hydrogen generation. The importance of the milling additives and their subsequent importance in the hydrogen production are described in detail. Furthermore, it is clarified how the choice of aluminium metal, type of milling additive (salt and oxides) and composition plays an important role in the final processed particle. For the optimal composition, it was found that a shorter milling programmes duration and lower milling speed produced promising hydrogen yield.

To the best knowledge of the author, no research has examined and described the details of the milling additives effect. In particularly when either combining two metal oxides additives or combining salt additives which in both cases appeared to create a synergy effect on the hydrogen yield. It was identified that using both CaO-CuO metal oxides over one, does have a significant effect on the hydrogen production, similarly as the in-house salt mix (PO) improved the hydrogen reaction considerably explained both by the physical and chemical effects on metal aluminium particles. Furthermore, the starting metal particle size effect proved to be sensitive to the milling programme conditions and the additive choice.

The 40 μm recycled Al particles provided the best hydrogen yield compared to larger particle sizes which were described by a larger surface area to get integrated with the chosen milling additives (CaO/CuO + PO). The best chosen starting temperature of the water was 25 °C due to a balance of less heat energy input needed and the achieved amount of hydrogen. Higher temperatures such a 45 °C of could provide high hydrogen yield but would have the disadvantage of added heat energy

need, which would not be feasible in a portable on-demand hydrogen generation/fuel cell device.

For real-life scenarios, the activated particles were tested on various types of water as deionised water would not be obtainable nor cost-effective for users. It is in detail described the effect of different dissolved ions and molecules in a wide range of water types, on both the reaction with Al and with the milling additives. The choice of water types was estimated for availability in real life scenarios. As the types of water varied greatly from the ideal deionised water it was important to assure the purity of the hydrogen gas was high and acceptable for a fuel cell. From the typical waster waters, which would possibly produce a less pure H_2 gas, it was found in GC gas analysis that only hydrogen was produced and no inferior gases. However, for device development, it is suggested that a post- gas treatment is required.

Additionally, the activated powder might have some disadvantages associated with itself because it would be used in generator *in-situ* with a fuel cell. A considerable amount of controls system needs to be installed for controlling the temperature of the gas, flow rate, moisture content and purity of hydrogen gas before intake for the fuel cell. Controlling these parameters is very necessary for the fuel cell to operate at its maximum efficiency. However, there are also a few external factors which need attention such as keeping the activated powder in a sealed bag containing an inert gas (such as argon) and no moisture content must be present in it. Any leakage of the bag would result in contamination of the activated powder thus making it defective or less efficient.

One of the major factors which can affect the fuel cell operation is the rate of hydrogen production and it must meet the demand of the fuel cell intake. Therefore, it is necessary that generator and controls are built for the fuel cell requirements. Taking an example from the fuel cell available from the iHOD USA [6], one of the fuel cells produces 15 W power, for estimation purposes, it is assumed that it produces 12 W electricity. Based on these statistics the fuel cell would potentially require 261 ml/min of hydrogen gas to work in optimum condition. During this research work, only 0.3 g of powder was used for the hydrogen and it delivered 260

ml in approximately 3hrs, therefore, it would not be suitable to be used directly for the fuel cell. However, some parameters have adjusted according to the need and to advance the process, such recommendations are, i.e. limiting the water content in the reaction to increase the reaction rate, as discussed earlier. Once all the necessary enhancements are made, this would then assure the activated powder prepared during this research would be adequate for the purpose.

Overall cost evaluation was estimated for particle processing and hydrogen generation for both small laboratory scale and larger. It was estimated that it would cost around £ 4 per 260 ml H_2 at laboratory small scale, while up-scaled it would cost around £ 70 per 1 kg (11,000 L) of H_2 (£ 0.06 per litre hydrogen) if the same type of high-speed ball milling machine was to be employed.

In order to make the process more sustainable for both commercial and environmental perspective, the by-product can be recycled. It was confirmed through XRD of the reacted powder see Figure 4-33, that considerable amount of aluminium hydroxide is present in different morphologies, to read more about the types and how do they differ please refer to chapter 2. The by-product, $Al(OH)_3$ can be used for various purposes, i.e. it can be used to recover any Al metal using a Bayer process [44,115,147], although that is an expensive route a good recovery ratio is possible. It can also be used in paper and pharmaceutical industry; therefore, it can be proposed that either the aluminium hydroxide is used for recycling the aluminium or it is sold to the relevant industry, it is a commodity and contains protentional to still bring revenue and in an eco-friendly manner.

It was concluded that by a thoroughly investigated milling protocols (milling conditions and additives) resulted in a reduced energy investment for an optimised activated aluminium particle able to produce high hydrogen yield in ambient conditions. Furthermore, it shows that the processed particles were able to produce high hydrogen yield when used in cheap and available types of wastewaters such as urea.

Chapter 5 Conclusion and future works

5.1 Overview

In this thesis, the activation of aluminium particles was investigated using reactive ball milling. The goal was to find optimised parameters for ball milling which would deliver improved activation of Al powder, as well as reduce the energy investment into the process. Activated powder from reactive milling would be used for generation of hydrogen gas. It was discovered that the elected method of synthesising the Al particles, i.e. reactive ball milling was an ideal method. Once the processing method was completed the quality of activation was adequate for the prepared powder to be reacted with water. Activated aluminium powder was able to produce a high yield of hydrogen gas in an exothermic reaction without the aid of any external heat or catalysts. This type of activation is both efficient and has good commercial value.

According to authors of Dutta *et al.*, activation via milling statistically seems more reasonable and environmentally friendly option than other processing techniques. However, a drawback of reactive milling is that it consumes a considerable amount of energy [10] and is expensive. Aluminium was milled together with two different types of metal oxides (CaO and CuO) and a prepared in-house salt. After a number of trials, a protocol was developed which was named as “Milling Programme 1a”. It provided both the comprehensive activation as well as a cost-effective solution to be used for hydrogen generation. The Milling Programme 1a was used with different milling periods and different particles sizes of Al powder. It was observed that milling for a longer period was better for hydrogen generation at the same time the processing cost also increases. The additives (MO+PO) were also deemed to have played a vital role in the reactive milling process. EDX and SEM confirmed that the morphologies of Al particles changed after the reactive milling process. This is because (MO+PO) was pressed on the surface of Al due to the collision of milling balls as a result of centrifugal force generated during the milling process.

Metal particles regardless of their sizes before milling showed surface damage after milling. These defects and role of additives on the surface permitted water to interact with Al particles thus allowing faster corrosion and production of hydrogen. Smaller size metal particles, i.e. 40 µm, when milled using Milling Programme 1a, produced a high H_2 yield of 85 % in 10000 sec at ambient conditions due to the larger surface area. After reactive milling process, Al particles can still produce hydrogen with water at different initial temperatures. However, it was observed that larger particles, i.e. 105 µm, was unable to produce an appreciatable yield at 25 °C. It was also noted that hydrogen yield decreases with the increase of temperature. Furthermore, agitation is necessary for achieving higher yield and without agitation yield is only 34 %. Furthermore, pH of water has effect nevertheless the pH 7 performed as good as extreme acid or alkali solutions due to the presence of CaO and CuO as additives. Research work also presented the production of hydrogen gas when wastewater is used especially when urea water was employed.

Table 5-1: Comparison of by-products and advantages

	Product made	**KOH**	**NaOH**
Hazardous material	No	Yes	Yes
By – products	$Al(OH)_3$	$K[Al(OH)_4]$	$NAAl(OH)_4$
Usage in the industry	Pharmaceutical	Dying agent	Water softener
Corrosive	Marginally	Intensely	Intensely
Have to keep in inert gas	Yes	Yes (solution)	Yes (solution)
Can it react with air	Yes	Yes	Yes

5.2 Future works

- Fuel cell should be *in-situ* with the H_2 reactor to analyse any device complications.
- The hydrogen process capability should be conducted on a larger scale and if possible using a CSTR hydrogen reactor to observe if there are any adjustments required.
- Implementation of process control for up-scaled hydrogen process to improve efficiency.
- Milling larger quantities of activated particles should be investigated as planetary mills are not aimed at larger process scales
- Development of a full kinetic model of the reaction which would support process design and process simulation.
- Investigation of the exothermic heat generated from the reaction and if it can be harnessed and reused.
- Recovering the Al from the $Al(OH)_3$ product development so the metal can be used again.
- More alternative available water sources should be investigated such as rainwater and seawater.
- Lifetime analysis should be conducted for the particle processing it would help to better understand the economics of the process.

5.3 Closing remarks

From this research, it was established that Al particle size of 40 µm, when milled with two metal oxides, i.e. CaO and CuO and in-house at 260 rpm for 1.1 hrs, produces a high-quality synthesised powder. When this powder is reacted at 25 °C with water or urea solution, it produces hydrogen at high quality and at a study rate with a yield of hydrogen up to 85 % in 3 hrs of reaction time. This process of synthesising Al particles can further be applicable on the larger industrial scale as well.

Appendix

Errors and uncertainty

In the course of this research work, the data were collected using instruments such as a digital gas flow meter and thermocouple were connected to a digital data collector (Pico Meter 2204). All these instruments have associated uncertainties in measurement. For example, the total uncertainty of the measurement from the GFM-17 can be as high as 2.5 % depending on the temperature of hydrogen gas. More specifically, it was observed that when inverted column produced 240 ml of hydrogen gas, the flowmeter was displaying 235 ml which indicate that a difference of ± 2 % should be expected when comparing the flow meter reading and the GFM-17. In light of this fact, the measurements were repeated, where possible, in order to estimate the error. As an example, refer to Figure 4-19 in Chapter 4 (Section A), which shows the production of hydrogen gas against time from a sample (Al+MO). The measurement was repeated twice and the result is presented in Figure 6-1 together with the error bars.

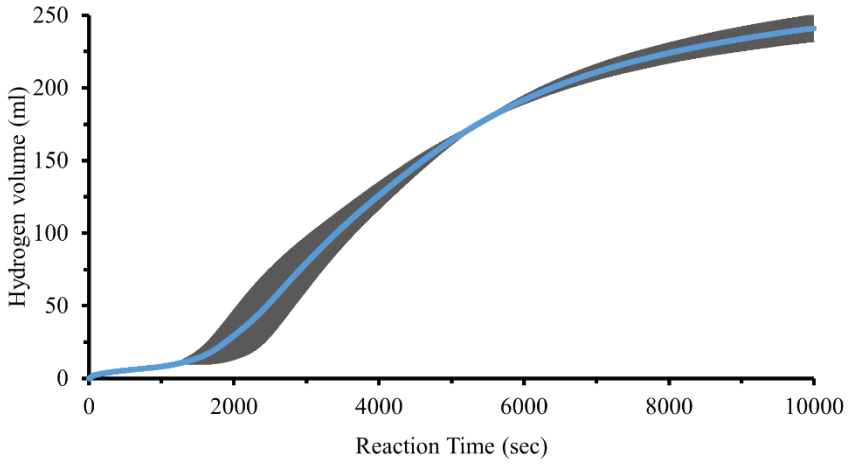

Figure 6-5-1: Two different reaction runs showing error bars calculated standard deviation at every 1 sec interval.

One can see in Figure 6-1 that uncertainty in measurements was relatively low at the beginning of the reaction. As the hydrogen reaction proceeds, the uncertainty grew in terms of measurements. However, the difference between the two experiments was marginal and is depicted by the error bars. Due to the high density

of data points (collected every second), the error bars forms a dark background. In order to show the extent of deviation from the mean values, a few data points were selected and their errors calculated as tabulated in Table 6-1 and plotted in Figure 6-2. The errors were calculated following the procedure presented by Pipes [156]. The error bars were taken as the standard error of the mean as follows:

$$s = \frac{\sigma}{\sqrt{n}}$$

, where symbol σ is the sample standard deviation and n is the number of trails. The standard deviation was calculated by using the following formula:

$$\sigma = \sqrt{\frac{1}{n-1}\sum_{i=1}^{n}(V_i - \mu)^2}$$

, where V_i is the volume produced, n is the total number of repeated measurements and μ is the mean of the sample given by:

$$\mu = \frac{1}{n}\sum_{i=1}^{n} n_i$$

Table 6-2: Interval reading of the full reaction.

Time (1000 sec)	Run 1 (Hydrogen volume ml)	Run 2 (Hydrogen volume ml)	Average of Run 1+2	Standard Deviation
1	7	8	7.5	0.71
2	40	17	28.5	16.26
3	9	67	38	41.01
4	131	119	125	8.49
5	165	162	163.5	2.12
6	189	193	191	2.83
7	207	214	210.5	4.95
8	219	228	223.5	6.36
9	227	239	233	8.49
10	234	247	240.5	9.19

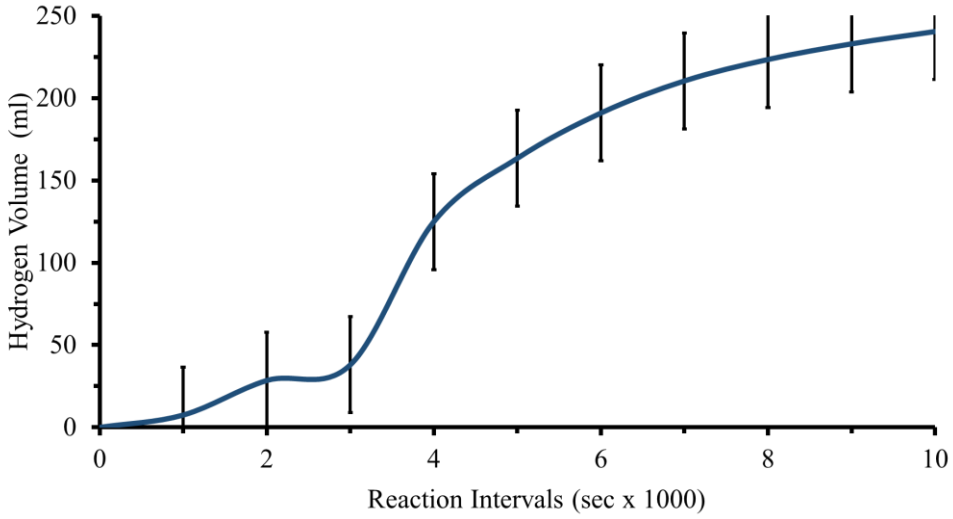

Figure 5-2: Error bars calculated standard deviation at every 1000 sec.

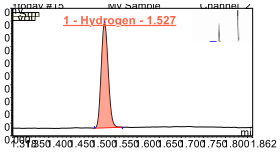

Figure 5-3: Hydrogen pecks from the gas produced from deionised water while peaks of Nitrogen and Oxygen can be seen in the right-hand side box.

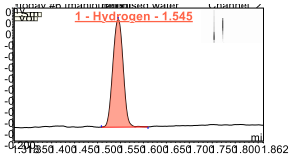

Figure 5-4: Hydrogen pecks from the gas produced from ethanol while peaks of Nitrogen and Oxygen can be seen in the right-hand side box.

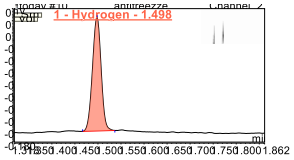

Figure 5-5: Hydrogen pecks from the gas produced from ethanol while peaks of Nitrogen and Oxygen can be seen in the right-hand side box.

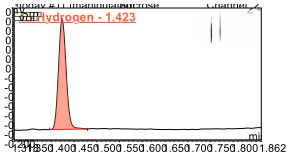

Figure 5-6: Hydrogen pecks from the gas produced from sucrose while peaks of Nitrogen and Oxygen can be seen in the right-hand side box.

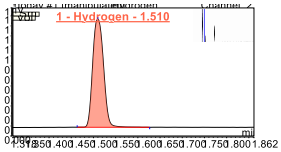

Figure 5-7: Hydrogen pecks from the gas produced from urea while peaks of Nitrogen and Oxygen can be seen in the right-hand side box.

Reference List

[1] M. Ni, M.K.H. Leung, K. Sumathy, D.Y.C. Leung, Potential of renewable hydrogen production for energy supply in Hong Kong, Int J Hydrogen Energy. 31 (2006) 1401-1412.

[2] A.H. Awad, T.N. Veziroğlu, Hydrogen versus synthetic fossil fuels, Int J Hydrogen Energy. 9 (1984) 355-366.

[3] S. Kotay, D. Das, Biohydrogen as a renewable energy resource Prospects and potentials, Int J Hydrogen Energy. 33 (2008) 258-263.

[4] K. Urbaniec, M. Markowski, A. Budek, Studies on the energy demand of two-stage fermentative hydrogen production from biomass in a factory equipped with the fuel-cell-based power plant, Int J Hydrogen Energy. 39 (2014) 7468-7475.

[5] J.W. Fergus, Recent developments in cathode materials for lithium ion batteries, J. Power Sources. 195 (2010) 939-954.

[6] iHOD USA, Homepage, (2017). [Online]. 2017. [Accessed Aug 2017]. Available from: http://ihod.com/the-fuel-of-the-future/

[7] Johnson Matthey Fuel Cell Today (FCT), PEMFC, [Online]. (2017). [Accessed Arp 2017]. Available from: http://www.fuelcelltoday.com/technologies/pemfc

[8] The Global CCS Institute, Industrial hydrogen and synfuel production and use, [Online] (2016). [Accessed Arp 2017]. Available from: https://hub.globalccsinstitute.com/publications/ccs-roadmap-industry-high-purity-co2-sources-sectoral-assessment-%E2%80%93-final-draft-report-1

[9] HFP Secretariat, European Hydrogen & Fuel Cell Technology Platform Deployment Strategy, Report [Online]. (2005). [Accessed Arp 2017]. Available from:

http://www.fch.europa.eu/sites/default/files/documents/hfp_ds_report_aug2005.pdf

[10] S. Dutta, A review of the production, storage of hydrogen and its utilization as an energy resource, Journal of Industrial and Engineering Chemistry. 20 (2014) 1148-1156.

[11] A. Leon, Hydrogen Technology: Mobile and Portable Applications (Green Energy and Technology), 1st ed., Springer Science & Business Media, Germany, 2008.

[12] A. Contreras, F. Posso, Technical and Financial Study of the Development in Venezuela of the Hydrogen Energy System, Renewable Energy. 36 (2011) 3114-3123.

[13] J. Petrovic, G. Thomas, Reaction of Aluminum with Water to Produce Hydrogen, Report to US Department for Energy (2010). [Accessed Arp 2017]. Available from: https://www1.eere.energy.gov/hydrogenandfuelcells/pdfs/aluminium_water_hydrogen.pdf

[14] UK H2Mobility, The development of hydrogen production capacities over time in the roadmap. [Online]. (2014). [Accessed Arp 2017]. Available from: http://www.itm-power.com/wp-content/uploads/2013/02/UK-H2Mobility-Synopsis-of-Phase-1-Results-Feb-2013.pdf

[15] T. Meyer, A. Alstrum, M. Brennaman, Chemical approaches to artificial photosynthesis, Accounts of Chemical Research. 5 (1989) 6802-27.

[16] M. Ozaki, S. Tomura, R. Ohmura, Y.H. Mori, Comparative study of large-scale hydrogen storage technologies: Is hydrate-based storage at advantage over existing technologies? Int J Hydrogen Energy. 39 (2014) 3327-3341.

[17] S. Tousi S., J.A. Szpunar, Modification of the shrinking core model for hydrogen generation by reaction of aluminium particles with water, Int J Hydrogen Energy. 41 (2016) 87-93.

[18] S. Tousi S., J.A. Szpunar, Role of Ball Milling of Aluminum Powders in Promotion of Aluminum-Water Reaction to Generate Hydrogen, Metallurgical and Materials Transactions. 1 (2014) 247–256.

[19] A.V. Ilyukhina, O.V. Kravchenko, B.M. Bulychev, E.I. Shkolnikov, Mechanochemical activation of aluminium with gallams for hydrogen evolution from water, Int J Hydrogen Energy. 35 (2010) 1905-1910.

[20] K. Nath, D. Das, Improvement of fermentative hydrogen production: various approaches. Applied Microbiology and Biotechnology. 65 (2004) 520-9.

[21] T. Drennen, J. Rosthal, Pathways to a Hydrogen Future, 1st ed., Elservier, USA, 2007.

[22] X. Qi, C. Gao, Z. Zhang, S. Chen, B. Li, S. Wei, Production and characterization of hollow glass microspheres with high diffusivity for hydrogen storage, Int J Hydrogen Energy. 37 (2012) 1518-1530.

[23] K. Mazloomi, C. Gomes, Hydrogen as an energy carrier: Prospects and challenges, Renewable and Sustainable Energy Reviews. 16 (2012) 3024-3033.

[24] T. Raissi, D. Block, Hydrogen: Automotive Fuel of the Future, International Energy Agency Implementing Agreement on Advanced Motor Fuels. Automotive Fuels Information Service. 2 (2004) 43.

[25] L. Klebanoff, Hydrogen Storage Technology: Materials and Applications, 1st ed., CRC Press, USA, 2012.

[26] Z. Zhao, X. Chen, M. Hao, Hydrogen generation by splitting water with Al–Ca alloy, Energy. 36 (2011) 2782-2787.

[27] P. Marcus, Corrosion Mechanisms in Theory and Practice, 3rd ed., CRC Press, USA, 2011.

[28] G. Totten, S. MacKenzie, Handbook of Aluminum: Volume 2: Alloy Production and Materials Manufacturing, (2003) 736.

[29] D.A. Johnson, Metals and Chemical Change, Royal Society of Chemistry, volume 1, 2002.

[30] P. Leckner, Ludwig's Applied Process Design for Chemical and Petrochemical Plants Volume 1, By A. Kayode Coker, Chemical Engineering. 115 (2008) 8-9.

[31] Y. Yavor, S. Goroshin, J.M. Bergthorson, D.L. Frost, R. Stowe, S. Ringuette, Enhanced hydrogen generation from aluminium–water reactions, Int J Hydrogen Energy. 38 (2013) 14992-15002.

[32] Y. Yavor, S. Goroshin, J.M. Bergthorson, D.L. Frost, the Comparative reactivity of industrial metal powders with water for hydrogen production, Int J Hydrogen Energy. 40 (2015) 1026-1036.

[33] C.P. Sharma, Engineering Materials: Properties and Applications of Metals and Alloys, PHI Learning Pvt. Ltd. 1st ed, 2003.

[34] V.I. Kirillov, A.N. Vastrebov, Magnesium alloy for hydrogen production. US Patent US5494538 A (1996).

[35] S. Yu, J. Uan, T. Hsu, Effects of concentrations of NaCl and organic acid on the generation of hydrogen from magnesium metal scrap, Int J Hydrogen Energy. 37 (2012) 3033-3040.

[36] H. Grosjean, M. Zidoune, L. Roué, Y. Huot, Hydrogen production via hydrolysis reaction from ball-milled Mg-based materials, Int J Hydrogen Energy. 31 (2006) 109-119.

[37] M. Liu, D.S. Shih, C. Parish, A. Atrens, The ignition temperature of Mg alloys WE43, AZ31 and AZ91, Corrosion Science. 54 (2012) 139-142.

[38] S. Narayana, A. Kumar, E. Shafirovich, Conversion of aluminium foil to powders that react and burn with water, Combust. Flame. 161 (2014) 322-331.

[39] A.V. Parmuzina, O.V. Kravchenko, Activation of aluminium metal to evolve hydrogen from water, Int J Hydrogen Energy. 33 (2008) 3073-3076.

[40] V. Rosenband, A. Gany, Application of activated aluminium powder for generation of hydrogen from water, Int J Hydrogen Energy. 35 (2010) 10898-10904.

[41] S. Tousi S., J.A. Szpunar, Effect of ball size on the steady state of aluminium powder and efficiency of impacts during milling, Powder Technol. 284 (2015) 149-158.

[42] M. Fan, L. Sun, F. Xu, Feasibility Study of Hydrogen Production for Micro Fuel Cell from Activated Al–In Mixture in Water, Energy. 35 (2010) 1333-1337.

[43] M. Reijalt, Hydrogen and fuel cell education in Europe: from when? And where? To here! And now! J. Clean. Prod. 18, Supplement 1 (2010) S112-S117.

[44] J. Kent, Kent and Riegel's Handbook of Industrial Chemistry and Biotechnology, 11st ed (2007) 1875.

[45] M. Fan, D. Mei, D. Chen, C. Li, K. Shu, Portable hydrogen generation from activated Al-Li–Bi alloys in water, Renewable Energy. 36 (2011) 3061-3067.

[46] X. Huang, T. Gao, X. Pan, D. Wei, C. Li, L. Qin, Y. Huang, A Review: Feasibility of Hydrogen Generation from the Reaction between Aluminium and Water for Fuel Cell Applications, J. Power Sources. 229 (2013) 133-140.

[47] HORDESKI F, Alternative fuels the future of hydrogen, 2nd ed., CRC Press, USA, 2008.

[48] Y. Liu, X. Wang, H. Liu, Z. Dong, S. Li, H. Ge, M. Yan, Improved hydrogen generation from the hydrolysis of aluminium ball milled with a hydride, Energy. 72 (2014) 421-426.

[49] M. Bareiß, Printed array of thin-dielectric metal-oxide-metal (MOM) tunnelling diodes, Journal of Applied Physics. 110 (2011) 316.

[50] D.S. Sundaram, V. Yang, Y. Huang, G.A. Risha, R.A. Yetter, Effects of particle size and pressure on combustion of nano-aluminium particles and liquid water, Combust. Flame. 160 (2013) 2251-2259.

[51] J.E. Hatch, Aluminum: Properties and Physical Metallurgy, 2nd ed., ASM International, USA, 1984.

[52] H.Z. Wang, D.Y.C. Leung, M.K.H. Leung, M. Ni, A review on hydrogen production using aluminium and aluminium alloys, Renew. Sust. Energy. Rev. 13 (2009) 845-853.

[53] S. Kahtan, T.N. Haider, N.I. Siti, Study of the feasibility of producing Al–Ni intermetallic compounds by mechanical alloying, The Physics of Metals and Metallography. 117 (2016) 795–804.

[54] M. Ramezani, T. Neitzert, Mechanical Milling of Aluminium Powder Using Planetary Ball Milling Process, Journal of Achievement in Materials and Manufacturing Engineering. 55 (2012) 790-798.

[55] C. Suryanarayana, Mechanical Alloying and Milling, 1st ed., Marcel Dekker, USA, 2003.

[56] P.R. Soni, Mechanical Alloying: Fundamentals and Applications, 1st ed., Cambridge International Science Publishing, United Kingdom, 1998.

[57] C. Suryanarayana, Mechanical alloying and milling, Progress in Materials Science. 46 (2001) 1-184.

[58] M. Fan, F. Xu, L. Sun, J. Zhao, T. Jiang, W. Li, Hydrolysis of ball milling Al-Bi–hydride and Al-Bi–salt mixture for hydrogen generation, J. Alloys Compounds. 460 (2008) 125-129.

[59] J. Huot, D.B. Ravnsbæk, J. Zhang, F. Cuevas, M. Latroche, T.R. Jensen, Mechanochemical synthesis of hydrogen storage materials, Progress in Materials Science. 58 (2013) 30-75.

[60] F. Burmeister, A. Kwade, Process Engineering With Planetary Ball Mills, Chem. Soc. Rev. 42 (2013) 7660-7667.

[61] L. Takacs, S. McHenry, Temperature of the Milling Balls in Shaker and Planetary Mills, Journal of Materials Science. 41 (2006) 5246–5249.

[62] T.P. Yadav, O.N. Srivastava, Synthesis of nanocrystalline cerium oxide by high energy ball milling, Ceram. Int. 38 (2012) 5783-5789.

[63] L. Budd, R. Ibberson, l.W. Marshall, S. Parsons, The Effect Of Temperature And Pressure On The Crystal Structure Of Piperidine, Chemistry Central Journal. 9 (2015).

[64] M.Q. Fan, S. Liu, L. Sun, F. Xu, S. Wang, J. Zhang, D. Mei, F. Huang, Q. Zhang, Synergistic Hydrogen Generation from Al Alloy and Solid-State $NabH_4$ Activated By $COCl_2$ in Water for Portable Fuel Cell, International Journal of Hydrogen Energy. 37 (2012) 4571-4579.

[65] H. Abdoli, M. Ghanbari, S. Baghshahi, Thermal stability of nanostructured aluminium powder synthesized by high-energy milling, Materials Science and Engineering: A. 528 (2011) 6702-6707.

[66] S. Siebeck, D. Nestler, Influence of Milling Atmosphere on the High-Energy Ball-Milling Process of Producing Particle-Reinforced Aluminum Matrix Composite, in M. Fathi (Ed.), Integration of Practice-Oriented Knowledge Technology: Trends and Prospective, 1st ed., Springer Berlin Heidelberg, 2013, pp. 315-321.

[67] S. Tousi S., J.A. Szpunar, R. Yazdani R, E. Salahi, I. Mobasherpour, Production of Al–20 wt.% Al2O3 composite powder using high energy milling, Powder Technol. 192 (2009) 346-351.

[68] Y.F. Zhang, L. Lu, S.M. Yap, Prediction of the amount of PCA for mechanical milling, Journal of Materials Processing Technology. 89 (1999) 260-265.

[69] S. Elitzur, V. Rosenband, A. Gany, Study of hydrogen production and storage based on aluminium–water reaction, Int J Hydrogen Energy. 39 (2014) 6328-6334.

[70] Sharma P., Sharma S., Khanduja D., On the Use of Ball Milling for the Production of Ceramic Powders, - Materials and Manufacturing Processes. 30 (2015) 1370-1370-1376.

[71] P.H. Kumar, A. Srivastava, V. Kumar, P. Kumar, V.K. Singh, Effect of High-Energy Ball Milling and Silica Fume Addition in BaCO -Al O. Part I: Formation of Cementing Phases, J Am Ceram Soc. 97 (2014) 3755; 3755.

[72] S. Tousi S., J.A. Szpunar, Effect of structural evolution of aluminium powder during ball milling on hydrogen generation in aluminium-water reaction, Int J Hydrogen Energy. 38 (2013) 795-806.

[73] M. Ghadimi, A. Shokuhfar, H.R. Rostami, M. Ghaffari, Effects of milling and annealing on the formation and structural characterization of nanocrystalline intermetallic compounds from Ni–Ti elemental powders, Mater Lett. 80 (2012) 181-183.

[74] C. Wang, T. Yang, Y. Liu, J. Ruan, S. Yang, X. Liu, Hydrogen generation by the hydrolysis of magnesium–aluminium–iron material in aqueous solutions, Int J Hydrogen Energy. 39 (2014) 10843-10852.

[75] P. Dupiano, D. Stamatis, E.L. Dreizin, Hydrogen production by reacting water with mechanically milled composite aluminium-metal oxide powders, Int J Hydrogen Energy. 36 (2011) 4781-4791.

[76] A. Wagih, Mechanical properties of Al-Mg/Al2O3 nanocomposite powder produced by mechanical alloying, Advanced Powder Technology. 26 (2015) 253-258.

[77] B. Alinejad, K. Mahmoodi, A Novel Method for Generating Hydrogen By Hydrolysis Of Highly Activated Aluminium Nanoparticles In Pure Water, Int J Hydrogen Energy. 34 (2009) 7934-7938.

[78] J. Skrovan, A. Alfantazi, T. Troczynski, Enhancing aluminium corrosion in water, Journal of Materials Science. 39 (2009) 1695-1702.

[79] A.S. Lozhkomoev, E. Glazkova, O.V. Bakina, M.I. Lerner, I. Gutman, E. Gutmanas, S. Kazantsev, S.G. Psakhie, Synthesis of core-shell AlOOH hollow nanospheres by reacting Al nanoparticles with water, Nanotechnology. 27 (2016) 205603.

[80] H. Wang, J. Lu, S.J. Dong, Y. Chang, Y.G. Fu, Preparation and Hydrolysis of Aluminum-Based Composites for Hydrogen Production in Pure Water, Materials Transactions. 55 (2014) 892; 892.

[81] R. Demichelis, Y. Noël, P. Ugliengo, C.M. Zicovich-Wilson, R. Dovesi, Physico-chemical features of aluminum hydroxides as modeled with the hybrid B3LYP functional and localized basis functions, The Journal of Physical Chemistry C. 115 (2011) 13107-13134.

[82] CRYSTAL - Theoretical Chemistry Group, MOLDRAW features and a series of Python script, (2017). [Online]. 2017. [Accessed Aug 2017]. Available from: http://www.crystal.unito.it/prtfreq/jmol.html.

[83] K. Hart, The formation of films on aluminium immersed in water, Transactions of the Faraday Society. 53 (1957) 1020-1027.

[84] J. Farndon, Aluminum, 1st ed. Benchmark Books, 2001.

[85] M. Fan, F. Xu, L. Sun, Studies on hydrogen generation characteristics of hydrolysis of the ball milling Al-based materials in pure water, Int J Hydrogen Energy. 32 (2007) 2809-2815.

[86] J.M. Woodall, J.T. Ziebarth, C.R. Allen, D.M. Sherman, J. Jeon, G. Choi, Recent Results on Splitting Water with Aluminum Alloys, in Anonymous Materials Innovations in an Emerging Hydrogen Economy, John Wiley & Sons, Inc., 2009; 2008, pp. 119-127.

[87] J.M. Woodall, J. Ziebarth, C.R. Allen, The science and technology of Al-Ga alloys as a material for energy storage, transport and splitting water, (2007).

[88] M.Q. Fan, L.X. Sun, F. Xu, Hydrogen production for micro-fuel-cell from activated Al–Sn–Zn–X (X: hydride or halide) mixture in water, Renewable Energy. 36 (2011) 519-524.

[89] W. Wang, D.M. Chen, K. Yang, Investigation on microstructure and hydrogen generation performance of Al-rich alloys, Int J Hydrogen Energy. 35 (2010) 12011-12019.

[90] A.C.D. Chaklader, Hydrogen generation from water split reaction, WO2002014213 A2 (2003).

[91] A.C.D. Chaklader, Hydrogen generation from water split reaction, US patent US6440385 B1 (2002).

[92] H. Wang, H. Chung, H. Teng, G. Cao, Generation of hydrogen from aluminium and water Effect of metal oxide nanocrystals and water quality, Int J Hydrogen Energy. 36 (2011) 15136-15144.

[93] X. Chen, Z. Zhao, M. Hao, D. Wang, Research of hydrogen generation by the reaction of Al-based materials with water, J. Power Sources. 222 (2013) 188-195.

[94] Y. Liu, X. Wang, H. Liu, Z. Dong, S. Li, H. Ge, M. Yan, Effect of salts addition on the hydrogen generation of Al–LiH composite elaborated by ball milling, Energy. 89 (2015) 907-913.

[95] S. Tousi S., J.A. Szpunar, Effect of addition of water-soluble salts on the hydrogen generation of aluminium in reaction with hot water, J. Alloys Compounds. 679 (2016) 364-374.

[96] M. Grosjean, M. Zidoune, J. Huot, L. Roué, Hydrogen generation via alcoholysis reaction using ball-milled Mg-based materials, International Journal of Hydrogen Energy. 31 (2006) 1159-1163.

[97] W. Li, T. Cochell, A. Manthiram, Activation of Aluminum as an Effective Reducing Agent by Pitting Corrosion for Wet-chemical Synthesis, 3 (2013).

[98] L. Meng, Improved Hydrogen Sorption Kinetics in Wet Ball Milled mg Hydride, 1st ed., julich, Germany, 2011.

[99] M. Zhao, X. Yang, T.L. Church, A.T. Harris, 'Corrigendum to "Interaction between a bimetallic Ni-Co catalyst and micrometre-sized CaO for enhanced H2 production during cellulose decomposition, Int J Hydrogen Energy. 37 (2012) 1853.

[100] Y.J. Chai, Y.M. Dong, H.X. Meng, Y.Y. Jia, J. Shen, Y.M. Huang, N. Wang, Hydrogen generation by aluminium corrosion in cobalt (II) chloride and nickel (II) chloride aqueous solution, Exergy, An International Journal; 68 (2014) 204-209.

[101] H. Zou, S. Chen, Z. Zhao, W. Lin, Hydrogen production by hydrolysis of aluminium, J. Alloys Compounds. 578 (2013) 380-384.

[102] M. Zou, R. Yang, X. Guo, H. Huang, J. He, P. Zhang, The preparation of Mg-based hydro-reactive materials and their reactive properties in sea water, International Journal of Hydrogen Energy. 36 (2011) 6478-6483.

[103] W. Gai, Z. Deng, Effect of Trace Species in Water on the Reaction of Al with Water, J. Power Sources. 245 (2014) 721-729.

[104] S. Tousi S., J.A. Szpunar, Mechanism of Corrosion of Activated Aluminum Particles by Hot Water, Electrochim. Acta. 127 (2014) 95-105.

[105] H. Gutbier, K. Hohne, Process for the generation of hydrogen, U.S. Patent 3,932,600 (1976).

[106] M. Huang, L. Ouyang, J. Ye, J. Liu, X. Yao, H. Wang, H. Shao, M. Zhu, Hydrogen generation via hydrolysis of magnesium with seawater using Mo, MoO 2, MoO 3 and MoS 2 as catalysts, Journal of Materials Chemistry A. 5 (2017) 8566-8575.

[107] G. Ma, H. Dai, D. Zhuang, H. Xia, P. Wang, Controlled hydrogen generation by reaction of aluminium/sodium hydroxide/sodium stannate solid mixture with water, Int J Hydrogen Energy. 37 (2012) 5811-5816.

[108] W. Gai, W. Liu, Z. Deng, J. Zhou, Reaction of Al powder with water for hydrogen generation under ambient condition, Int J Hydrogen Energy. 37 (2012) 13132-13140.

[109] W. Gai, C. Fang, Z. Deng, Hydrogen Generation by the Reaction of Al with Water Using Oxides as Catalysts, Inc. J. Energy Res. 38 (2014) 918-925.

[110] H. Nie, M. Schoenitz, Kinetcis of Aluminum-water split Reaction. International Journal of Hydrogen Energy. (2012) 11035-45.

[111] E.E. Stansbury, R.A. Buchanan, Fundamentals of Electrochemical Corrosion, 1st ed ASM International, 2000.

[112] R. Davis, Corrosion of Aluminum and Aluminum Alloys, 1st ed (1999) 313.

[113] T. Tayeh, A.S. Awad, M. Nakhl, M. Zakhour, J.-. Silvain, J.-. Bobet, Production of hydrogen from magnesium hydrides hydrolysis, Int J Hydrogen Energy. 39 (2014) 3109-3117.

[114] K. Samir, Anaerobic Biotechnology for Bioenergy Production: Principles and Applications, (2008) 320.

[115] J. McMurry, Fundamentals of Organic Chemistry, 7th ed., Cengage Learning, 2010.

[116] S. Elitzur, V. Rosenband, A. Gany, Urine and aluminium as a source of hydrogen and clean energy, International Journal of Hydrogen Energy. 41 (2016) 11909-11913.

[117] B. Boggs, R. King, G. Botte, Urea electrolysis: direct hydrogen production from urine, Chem. Commun. (2009) 4859-4861.

[118] R. Galli, The Relationship Between Energy Intensity and Income Levels: Forecasting Long Term Energy Demand in Asian Emerging Countries, The Energy Journal. 19 (1998) 85-105.

[119] M. Walsh, Global trends in motor vehicle pollution control: a 2011 update. Part 3, Silniki Spalinowe. 50 (2011) 98-103.

[120] R. Lowes, Heat, Incumbency and Transformations-Overview, 2015. (2017). [Online]. 2017. [Accessed Aug 2017]. Available from: http://geography.exeter.ac.uk/research/groups/energypolicy/research/hit/.

[121] J. Lu, J. Hossain, Vehicle-to-Grid: Linking Electric Vehicles to the Smart Grid, The Institution of Engineering and Technology, 2015.

[122] I. Dincer, C. Zamfirescu, Sustainable hydrogen production options and the role of IAHE, Int J Hydrogen Energy. 37 (2012) 16266-16286.

[123] C.H. Zheng, C.E. Oh, Y.I. Park, S.W. Cha, Fuel economy evaluation of fuel cell hybrid vehicles based on equivalent fuel consumption, Int J Hydrogen Energy. 37 (2012) 1790-1796.

[124] M. Klell, Storage of hydrogen in the pure form, Handbook of hydrogen storage: new materials for future energy storage. 1st ed. (2010)

[125] U. Bossel, B. Eliasson, Energy and the hydrogen economy, Methanol Institute Report, Arlington, VA. (2003).

[126] ITM POWER, Final Results for the Year to 30 April 2017, (2017). [Online]. 2017. [Accessed Aug 2017]. Available from: http://www.itm-power.com/news-item/final-results-for-the-year-to-30-april-2017.

[127] C. Hammond, C. Hammond, Basics of Crystallography and Diffraction, Oxford University Press; 4th ed, 2001.

[128] O. Krivanek, T. Aoki, P. Batson, P. Crozier, N. Dellby, R. Egerton, T. Lovejoy, P. Rez, Vibrational spectroscopy in the electron microscope, (2014).

[129] Thames Water, Hardness, (2017). [Online]. 2017. [Accessed April 2017]. Available from: https://www.thameswater.co.uk/Help-and-Advice/Water-Quality/Check-the-water-quality-in-your-area.

[130] H.E. Taylor, Inductively Coupled Plasma-Mass Spectrometry: Practices and Techniques, Academic Press, 2001.

[131] Sheffield Hallam University, Gas chromatography, (2017). [Online]. 2017. [Accessed April 2017]. Available from: https://teaching.shu.ac.uk/hwb/chemistry/tutorials/chrom/gaschrm.html.

[132] D.F. Putnam, Composition and concentrative properties of human urine. NASA Report (1971).

[133] N.N. Greenwood, A. Earnshaw, Chemistry of the Elements, Butterworth-Heinemann; 2 ed., 2012.

[134] Y. Liu, X. Wang, H. Liu, Z. Dong, S. Li, H. Ge, M. Yan, Improved hydrogen generation from the hydrolysis of aluminium ball milled with a hydride, Energy. 72 (2014) 421-426.

[135] Y. Jia, J. Shen, H. Meng, Y. Dong, Y. Chai, N. Wang, Hydrogen generation using a ball-milled Al/Ni/NaCl mixture, J. Alloys Compounds. 588 (2014) 259-264.

[136] S. Liu, M. Fan, C. Wang, Y. Huang, D. Chen, L. Bai, K. Shu, Hydrogen generation by hydrolysis of Al-Li–Bi–NaCl mixture with pure water, Int J Hydrogen Energy. 37 (2012) 1014-1020.

[137] H. Gasan, O.N. Celik, N. Aydinbeyli, Y.M. Yaman, Effect of V, Nb, Ti and graphite additions on the hydrogen desorption temperature of magnesium hydride, Int J Hydrogen Energy. 37 (2012) 1912-1918.

[138] B.D. Stojanovic, A.Z. Simoes, C.O. Paiva-Santos, C. Jovalekic, V.V. Mitic, J.A. Varela, Mechanochemical synthesis of barium titanate, Journal of the European Ceramic Society. 25 (2005) 1985-1989.

[139] M.-. Grosjean, M. Zidoune, L. Roué, Hydrogen production from highly corroding Mg-based materials elaborated by ball milling, J. Alloys Compounds. 404–406 (2005) 712-715.

[140] X. Chen, Z. Zhao, X. Liu, M. Hao, A. Chen, Z. Tang, Hydrogen generation by the hydrolysis reaction of ball-milled aluminium–lithium alloys, Journal of Power Sources. 254 (2014) 345-352.

[141] Fisher Chemcials, Catalog, (2017). [Online]. 2017. [Accessed April 2017]. Available from: https://www.fishersci.co.uk/gb/en/home.html

[142] Z. Zhao, X. Chen, M. Hao, Hydrogen generation by splitting water with Al–Ca alloy, Energy. 36 (2011) 2782-2787.

[143] M. Basualdo, D. Feroldi, R. Outbib, PEM fuel cells with bio-ethanol processor systems, Springer. 10 (2011) 978-971.

[144] K. Mutombo, M. Toit, Mechanical properties of 5083 aluminium welds after manual and automatic pulsed gas metal arc welding using an E5356 filter, Trans Tech Publications. 654 (2011) 2560-2563.

[145] S. Shih, C. Ho, Y. Song, J. Lin, Kinetics of the reaction of Ca (OH) 2 with CO2 at low temperature, Ind Eng Chem Res. 38 (1999) 1316-1322.

[146] K. Prodromou, A. Pavlatou-Ve, Formation of aluminium hydroxides as influenced by aluminium salts and bases, Clays Clay Miner. 43 (1995) 111-115.

[147] E. Wood, Organic chemistry: By Marye Anne Fox and James K Whitesell. pp 870. Jones and Bartlett, Boston and London, 1994.£ 21.95 ISBN 0-86720-207-6, Biochemistry and Molecular Biology Education. 23 (1995) 44-44.

[148] L. Samain, A. Jaworski, M. Edén, D.M. Ladd, D. Seo, F. Javier Garcia-Garcia, U. Häussermann, Structural analysis of highly porous γ-Al2O3, Journal of Solid State Chemistry. 217 (2014) 1-8.

[149] W.M. Haynes, CRC Handbook of Chemistry and Physics, CRC Press, .1st ed, 2014.

[150] D.A. Palmer, P. Bénézeth, J. Simonson, Solubility of copper oxides in water and steam, (2004) 491-496.

[151] H.A. Tajmir-Riahi, Sucrose interaction with alkaline earth metal ions. Synthesis, spectroscopic and structural characterization of sucrose adducts with the Mg(II) and Ca(, Journal of Inorganic Biochemistry. 31 (1987) 255-265.

[152] K. Rittstieg, K. Robra, W. Somitsch, Aerobic treatment of a concentrated urea wastewater with simultaneous stripping of ammonia, Appl. Microbiol. Biotechnol. 56 (2001) 820-825.

[153] W.W. Eckenfelder, L.K. Cecil, Applications of New Concepts of Physical-Chemical Wastewater Treatment: Vanderbilt University, Nashville, Tennessee September 18-22, 1972, Elsevier, 2013.

[154] Gov UK, Prices of fuels purchased by manufacturing industry in Great Britain (p/kWh), (2016).

[155] Ali Baba, Cataloge, (2017). [Online]. 2017. [Accessed April 2017]. Available from: https://www.alibaba.com/

[156] L. Pipes, Harvill. Lawrence, Applied Mathematics for Engineers and Physicists:, 3rd ed., Dover Publications, USA, 2014.